Kinetic theory of self-gravitating systems

Jean-Baptiste Fouvry[1]

[1] *Institut d'Astrophysique de Paris;* fouvry@iap.fr

Version compiled on December 12, 2019

1 Introduction

The main goal of these lectures is to illustrate how tools from kinetic theory, can be extended to self-gravitating stellar systems, and more generically to systems driven by long-range interactions (Campa et al., 2009). A comprehensive introduction to stellar dynamics can be found in Binney & Tremaine (2008). Previous lectures from James Binney can also be found under the link[1].

Let us first note some of the key differences between a self-gravitating system and an electrostatic plasma:

- There are no charges for gravity, which makes the associated force systematically attractive, in direct opposition with the repulsive electrostatic force for particles with the same sign of charge. This is the key reason why self-gravitating systems can develop instabilities on their largest scale, and why they can also strongly amplify perturbations on these large scales.

[1] http://www-thphys.physics.ox.ac.uk/people/JamesBinney/kt.pdf

- As a consequence, self-gravitating systems are globally inhomogeneous, contrary to plasmas which are inhomogeneous only on scales smaller than the Debye length $\lambda_{\rm D}$. As a result, to describe the long-term dynamics of self-gravitating systems, one has to carefully account for the fact that the mean potential satisfies $\Phi(\mathbf{x}) \neq 0$, defining a complex orbital structure. Even in the absence of any perturbations and fluctuations, stars follow intricate orbital motions.
- In a solid or a liquid, the forces acting on a particle is typically dominated by the contribution from its close neighbours. Particles are submitted to violent and short-lived accelerations separated with longer periods during which they move with nearly constant velocities. Similarly, in an electrostatic plasma, forces are dominated by the contributions from the particles within $\lambda_{\rm D}$. This is radically different in self-gravitating systems, where, since gravity cannot be screened, forces are dominated by remote particles, i.e. the force is long-range, as we briefly justify below.

Let us consider one test particle, placed at the origin of the coordinates system, and embedded within a stellar system composed of $N \gg 1$ particles (e.g., $N \simeq 10^5$ stars in a globular cluster, or $N \simeq 10^{11}$ stars in the Milky Way (MW)). On scales larger than the mean inter-particle distance, we can describe this system with a smooth density $\rho(\mathbf{x})$. The small cell at distance $|\mathbf{x}|$ from the test particle and within the solid angle $\mathrm{d}\mathbf{\Omega}$ contains a mass $\mathrm{d}M = \rho(\mathbf{x})\,|\mathbf{x}|^2\,\mathrm{d}|\mathbf{x}|\,\mathrm{d}\mathbf{\Omega}$. This cell therefore generates a gravitational force per unit mass with a magnitude given by $\mathrm{d}F = \mathrm{d}M \times G/|\mathbf{x}|^2 = G\,\rho(\mathbf{x})\,\mathrm{d}|\mathbf{x}|\,\mathrm{d}\mathbf{\Omega}$, where, importantly, one notes that the factor $|\mathbf{x}|^2$ has disappeared. As a consequence, the force on that test particle is driven by the system's smooth density profile $\rho(\mathbf{x})$, rather than by the local contributions from the nearby neighbors. As a result, the force on a given star does not, typically, vary rapidly, and each star undergoes a smooth acceleration generated by the self-gravitating system as a whole. This is the archetype of a long-range interacting system.

Self-gravitating systems, such as galaxies, are therefore complex dynamical systems that require a careful modelling to account for their key specificities and describe to their long-term evolutions, as illustrated in Fig. 1.1.

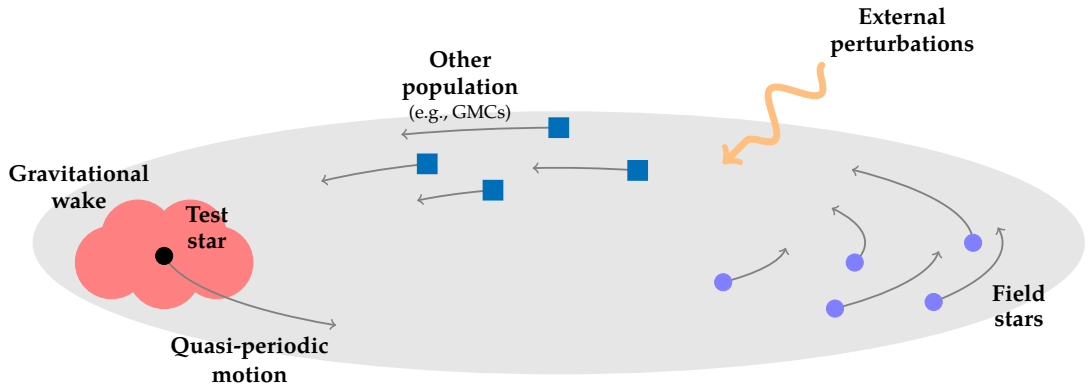

Figure 1.1: . Illustration of the different components involved in the long-term dynamics of a test star embedded in a galaxy. To describe the complex quasi-periodic motion of the test star, one has to rely on angle-action-coordinates. The galaxy being self-gravitating, any perturbation is dressed by collective effects, and therefore surrounded by a gravitational wake. The long-term orbital diffusion of the test star can finally be induced either by external perturbations (e.g., through the cosmic environment) or by internal perturbations (e.g., finite-N effects).

- Galaxies are *inhomogeneous*. Because a galaxy's mean potential is non-zero, individual stars follow intricate orbits. As a consequence, the physical phase space coordinates $(\mathbf{x}, \mathbf{v})$ are no longer appropriate to describe the mean-field motion of the stars. One has to resort to labelling the system's orbital structure. This asks for the use of the angle-action coordinates $(\boldsymbol{\theta}, \mathbf{J})$ (see Section 2).
- Galaxies are dynamically *relaxed*. Following the first few dynamical times after its formation, a self-gravitating system rapidly reaches a quasi-stationary distribution, $F(\mathbf{J}, t)$, through the processes of violent relaxation (Lynden-Bell, 1967) and phase mixing. Such a configuration is dynamically frozen for the mean-field dynamics, and can keep evolving only under the effects of perturbations. This asks for the construction and specification of a system's admissible quasi-stationary distributions and equilibria (see Section 2).
- Galaxies are *self-gravitating*. Stars evolve in the potential that they self-consistently construct. This allows the system to amplify perturbations by self-gravity, which can accelerate the galaxy's secular dynamics or even cause linear instabilities. This asks for the computation of the system's linear response theory (see Section 3.4).
- Galaxies are *resonant*. To each orbit is associated a set of orbital frequencies, $\mathbf{\Omega}(\mathbf{J})$, which characterise the star's mean-field motion. This naturally introduces a time dichotomy between the fast orbital timescale to

sweep orbits, and the slow secular timescale to distort the system's orbital structure. This asks therefore for the correct accounting of resonant contributions on secular evolutions (see Section 5).

- Galaxies are *discrete* and *perturbed*. Galaxies are composed of a finite number of constituents. As a result, finite-N effects induce internal perturbations that act as seeds to source long-term orbital distortions. This asks for the detailed accounting of the long-term effects associated with Poisson shot noise on a system's structure (see Section 5).

Any worthy attempt at quantitatively describing the long-term evolution of self-gravitating systems must necessarily account for all these defining features, as they drastically impact the system's long-term behaviour. Overall, this drives the system's secular dynamics, i.e. the long-term relaxation induced by long-range resonant couplings between the amplified perturbations undergone by the system, see Fig. 1.2. This is the dynamics

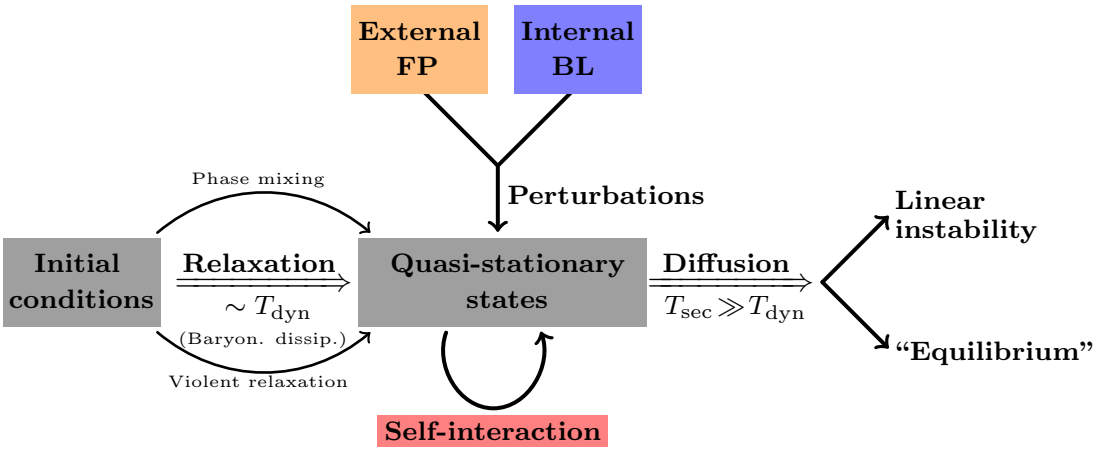

Figure 1.2: Illustration of the typical fate of a long-range interacting system, such as a galaxy. On the first few dynamical times, the galaxy's evolution is governed by collisionless Vlasov-Poisson system. As a result of violent relaxation (Lynden-Bell, 1967) and phase mixing, the galaxy reaches a quasi-stationary state, i.e. a state dynamically frozen for the smooth mean-field dynamics. Later, on much longer timescales, fluctuations present in the galaxy, amplified by self-gravity, and coupled through orbital resonances, drive an irreversible long-term distortion of the galactic orbital structure: this is the secular dynamics. These perturbations may be internal (e.g., induced by finite-N fluctuations), and captured by the inhomogeneous Balescu-Lenard equation (Heyvaerts, 2010; Chavanis, 2012), or external (e.g., passing-by perturbers), and described by the dressed Fokker-Planck equation (Binney & Lacey, 1988; Weinberg, 2001).

over which we will focus here.

1.1 Virial Theorem

As an highlight of these properties, let us first obtain an important result, the virial theorem, that connects the mass of a self-gravitating system to its extent in real and velocity space. We consider N particles of individual mass m evolving within their mutually generated gravitational potential, as dictated by the pairwise interaction $U(\mathbf{x}, \mathbf{x}') = -G/|\mathbf{x} - \mathbf{x}'|$. The system's instantaneous moment of inertia w.r.t. the origin is given by

$$I = \sum_{i=1}^{N} m\, \mathbf{x}_i^2. \tag{1.1}$$

And its second derivative is given by

$$\ddot{I} = 2\left(\sum_{i=1}^{N} m\, \mathbf{v}_i^2 + \sum_{i=1}^{N} m\, \mathbf{x}_i \cdot \frac{\mathrm{d}\mathbf{v}_i}{\mathrm{d}t} \right). \tag{1.2}$$

The last term can be computed furthermore, using the equations of motion for particle i. We write it as

$$\begin{aligned}\sum_{i=1}^{N} m\,\mathbf{x}_i \cdot \frac{\mathrm{d}\mathbf{v}_i}{\mathrm{d}t} &= -\sum_{\substack{i,j\\ i\neq j}}^{N} m^2 \mathbf{x}_i \cdot \frac{\partial U(\mathbf{x}_i,\mathbf{x}_j)}{\partial \mathbf{x}_i} \\ &= -\frac{1}{2}\sum_{\substack{i,j\\ i\neq j}}^{N} m^2\,(\mathbf{x}_i-\mathbf{x}_j)\cdot \frac{\partial U(\mathbf{x}_i,\mathbf{x}_j)}{\partial \mathbf{x}_i} \\ &= -\frac{1}{2}\sum_{\substack{i,j\\ i\neq j}}^{N} G\,m^2\,(\mathbf{x}_i-\mathbf{x}_j)\cdot \frac{(\mathbf{x}_i-\mathbf{x}_j)}{|\mathbf{x}_i-\mathbf{x}_j|^3} \\ &= \sum_{i<j}^{N} m^2\,U(\mathbf{x}_i,\mathbf{x}_j), \end{aligned} \tag{1.3}$$

where the second line was obtained by using the symmetrisation $i \leftrightarrow j$, and relying on Newton's second law of equal action and reaction. To get the last line, we finally used the fact that the gravitational interaction is a a power law, $U(\mathbf{x},\mathbf{x}')=-G/|\mathbf{x}-\mathbf{x}'|$, making the computation of the forces explicit.

Let us now assume that the system is in equilibrium, i.e. we assume that $\langle I\rangle = 0$, where $\langle\,\cdot\,\rangle$ stands for both an average over realisations. Equation (1.2) allows us then to finally obtain

$$2K + W = 0, \tag{1.4}$$

where we introduced the averaged kinetic and potential energies as

$$K = \left\langle \frac{1}{2}\sum_{i=1}^{N} m\,\mathbf{v}_i^2 \right\rangle \quad ; \quad W = \left\langle \sum_{i<j}^{N} m^2\,U(\mathbf{x}_i,\mathbf{x}_j) \right\rangle. \tag{1.5}$$

The virial theorem from Eq. (1.4) is an important result that directly connects the system total kinetic energy, i.e. the system's velocity dispersion, to the system's total potential energy, i.e. the system's physical extension.

1.2 Thermal Equilibrium

Relying on the virial theorem, let us now investigate in more details the thermodynamics of self-gravitating systems, and argue why, contrary to electrostatic plasmas with their Maxwell distributions, self-gravitating systems cannot reach their thermal equilibrium.

Let us assume that the self-gravitating system comprises N confined particles in thermal equilibrium. Assuming that the particles have no internal degrees of freedom, and that binary systems can be neglected, we can formally treat this system as a monoatomic gas, whose temperature satisfies $\frac{3}{2}Nk_{\mathrm{B}}T = K$, and its internal energy is given by $E = K + W = -K$, which is negative. The heat capacity of that system is then given by

$$C = \frac{\partial E}{\partial T} = -\frac{\partial K}{\partial T} = -\frac{3}{2}Nk_{\mathrm{B}}, \tag{1.6}$$

which is also negative. This is very problematic, as it makes it impossible for the self-gravitating system to reach a thermal equilibrium with a conventional heat bath, as such a configuration would be unstable. Indeed, let us assume that the system and heat bath were in thermal equilibrium. Then, we assume that some fluctuations $\delta E > 0$ of energy flows from the system to the heat bath. As a result, the system would heat up by the amount $\delta T = -\delta E/C > 0$. By losing energy, the system gets hotter. As a consequence, since the system is now hotter than the bath, more heat would flow from the system to the bath, and the system would get hotter and hotter, with no apparent limit. Such an argument is a first illustration of why self-gravitating systems cannot generically reach their thermal equilibrium.

Another complication associated with thermal equilibria comes from the system's unavoidable tendency of evaporating by launching particles to infinitely large radii. Assuming that the system's gravitational potential is defined so that $\Phi(r) \to 0$ for $r \to +\infty$, a star is unbounded to the system if ever its individual energy, $E = \frac{1}{2}\mathbf{v}^2 + \Phi(r)$, satisfies $E > 0$. Phrased differently, at a given location, self-gravity confines particles only up to a finite escape speed given by $v_{\mathrm{esc}}(\mathbf{x}) = \sqrt{-2\Phi(\mathbf{x})}$. This already tells us that in thermal equilibrium, the system's distribution function (DF), $F(\mathbf{x},\mathbf{v})$, would have to vanish for $v > v_{\mathrm{esc}}$, which cannot be a Maxwellian, since it is always non-zero. As a result, any form of equilibrium will always scatter stars to $v > v_{\mathrm{esc}}$, which

would then "evaporate" from the system. We can estimate the efficiency of this evaporation by computing the mean square value of $v_{\rm esc}$, as follows

$$\begin{aligned}\sigma_{\rm esc}^2 &= \frac{1}{M_{\rm tot}}\int {\rm d}\mathbf{x}\,\rho(\mathbf{x})\,v_{\rm esc}^2(\mathbf{x})\\ &= -\frac{2}{M_{\rm tot}}\int {\rm d}\mathbf{x}\,\rho(\mathbf{x})\,\Phi(\mathbf{x})\\ &= -\frac{2}{M_{\rm tot}}\int {\rm d}\mathbf{x}{\rm d}\mathbf{x}'\,U(\mathbf{x},\mathbf{x}')\,\rho(\mathbf{x})\,\rho(\mathbf{x}').\end{aligned} \tag{1.7}$$

where to get the last line, we wrote the system's potential as

$$\Phi(\mathbf{x}) = \int {\rm d}\mathbf{x}'\,U(\mathbf{x},\mathbf{x}')\,\rho(\mathbf{x}'). \tag{1.8}$$

Paying a careful attention to the over-counting of pairwise interactions, the last integral from Eq. (1.7) is equal to $2W$, so that we obtain

$$\sigma_{\rm esc}^2 = -4\frac{W}{M_{\rm tot}} = 8\frac{K}{M_{\rm tot}} = 4\sigma^2, \tag{1.9}$$

where we used the virial theorem from Eq. (1.4), and introduced the cluster's velocity dispersion as $\sigma^2 = \langle \mathbf{v}_i^2\rangle$. As a consequence, we have $\sigma_{\rm esc} = 2\sigma$, which is not far into the high-velocity tail. For the purpose of this calculation, if we assume that the system is in a thermal equilibrium with a Maxwellian distribution, so that its DF is of the form $F(\mathbf{v}) \propto {\rm e}^{-3|\mathbf{v}|^2/(2\sigma^2)}$, we can then estimate the fraction of escaping and unbound stars as

$$f_{\rm esc} = \frac{\int_{2\sigma}^{+\infty}{\rm d}v\,v^2\,{\rm e}^{-3v^2/(2\sigma^2)}}{\int_0^{+\infty}{\rm d}v\,v^2\,{\rm e}^{-3v^2/(2\sigma^2)}} = \frac{\int_{\sqrt{6}}^{+\infty}{\rm d}u\,{\rm e}^{-u^2}}{\int_0^{+\infty}{\rm d}u\,{\rm e}^{-u^2}} \simeq \frac{1}{140}. \tag{1.10}$$

If we assume that this evaporation process removes a fraction $f_{\rm esc}$ of stars every relaxation time (defined more precisely in the upcoming section), we can then compute the rate of loss by evaporation as

$$\frac{{\rm d}N}{{\rm d}t} = -\frac{f_{\rm esc}N}{t_{\rm relax}}, \tag{1.11}$$

which gives a typical time for evaporation as $t_{\rm evap} = t_{\rm relax}/f_{\rm esc} \simeq 140\times t_{\rm relax}$. This is an important conclusion, which states that owing to the absence of any thermal equilibrium, a self-gravitating system will unavoidably lose a substantial fraction of its mass over a few relaxation times. This once again emphasises the impossibility for self-gravitating system to reach any true thermal equilibrium. This is in strong opposition with electrostatic plasmas that can indeed reach their thermal Maxwellian distribution. As a result, describing the long-term evolution of a self-gravitating system asks for the the detailed description of the (incomplete) relaxation undergone by a kinetic system far from its thermal equilibrium.

1.3 Relaxation time

Let us now develop a first approximate calculation of the relaxation time, $t_{\rm relax}$, of a self-gravitating system (Binney & Tremaine, 2008; Hamilton et al., 2018). We assume that the system is of total mass $M_{\rm tot} = Nm$, and of characteristic size R. Following the virial theorem, we expect the typical internal speed within the system to be of order $\sigma = \sqrt{GM_{\rm tot}/R}$. We are interested in how the spontaneous Poisson fluctuations in the system, i.e. the unavoidable shot noise associated with the system's finite number of particles, can lead to the system's irreversible relaxation.

We consider a subregion of size $r = xR$ which undergoes some potential fluctuations. On average, this region contains the mass $M_r \simeq x^3 M_{\rm tot}$, and therefore a number of particle equal to $N_r \simeq x^3 N$. This local number of particles fluctuates as result of Poisson shot noise, with an amplitude of the order $\delta N_r \simeq N_r/\sqrt{N_r}$, so that the mass within that subregion fluctuates with the amplitude $\delta M_r = M_r/\sqrt{N_r} = x^{3/2}M_{\rm tot}/\sqrt{N}$, and this fluctuation typically lasts $\delta t = xR/\sigma$, i.e. the time for the fluctuation to flow away from that small subregion.

We now consider a test particle that is a distance yR from this subregion, and we want to compute the effects of the fluctuations of this subregion onto the test particle. Under the effect of this perturbation, the velocity of the test star will typically change by

$$\delta v = \delta F\,\delta t = \frac{G\,\delta M_r}{(yR)^2}\,\delta t = \frac{GM_{\rm tot}x^{3/2}}{(yR)^2\sqrt{N}}\,\frac{xR}{\sigma} = \frac{\sigma\,x^{5/2}}{y^2\sqrt{N}}. \tag{1.12}$$

This equation describes the local velocity kick undergone by the test star and induced by the spontaneous Poisson fluctuations in some distant subregion.

Let us now sum the contributions of these deflections from all the different subregions of size x. We assume that different contributions are statistically independent, so that we must add them in quadrature. For a fixed y, i.e. for a fixed distance to the test star, there are $\sim 4\pi(y/x)^2$ subregions of size x, and during one dynamical time of the test particle $t_{\rm d} = R/\sigma$, each subregion has undergone $t_{\rm d}/\delta t = 1/x$ independent episode of fluctuations. As a result, during one dynamical time, the overall contributions from all these subregions leads to an increase in $(\Delta v)^2$ scaling like

$$(\Delta v)^2 = 4\pi \frac{y^2}{x^3} (\delta v)^2 = 4\pi \frac{\sigma^2 x^2}{y^2 N}. \tag{1.13}$$

Keeping fixed x, the size of the perturbing subregions, we must now sum over all the distances to the test particle, i.e. we must sum over $y = x, 2x, ..., 1$. This sum is computed using an integral with ${\rm d}y = x$, and we can write

$$\sum \frac{1}{y^2} \simeq \frac{1}{x} \int_x^1 \frac{{\rm d}y}{y^2} \simeq \frac{1}{x}\left(\frac{1}{x} - 1\right) \simeq \frac{1}{x^2}. \tag{1.14}$$

As a result, within one dynamical time, the subregions of scale x lead to a change in $(\Delta v)^2$ of the order

$$(\Delta v)^2 \simeq 4\pi\sigma^2 \frac{1}{N}. \tag{1.15}$$

This is a remarkable result, as it shows that the contributions of each scale is independent of their size, i.e. independent of x. This illustrates in particular why gravity is in the complicated dynamical regime, where small and large scales fluctuations apparently contribute equally to the relaxation undergone by the system. The total change of the test particle's velocity must finally be summed over all the relavant scales x. The relevant scales of fluctuations go from the smallest one $x_{\rm min}$ and the largest one $x = 1$, and to account for them, we may multiply Eq. (1.15) by $-\ln(x_{\rm min})$, i.e. the typical number of different scales that independently source the relaxation, to obtain the overall relaxation induced by the whole cluster. The smallest scale to consider should be of the order of the inter-particle distance $x_{\rm min} \simeq 1/N^{1/3}$. The overall change of the test particle's velocity over one dynamical time is finally given by

$$\big(\Delta v\big)^2_{t_{\rm d}} \simeq \frac{4\pi\sigma^2 \ln(N)}{3N}. \tag{1.16}$$

The system's relaxation time, $t_{\rm relax}$, is then defined as the time required for these Poisson fluctuations to lead to a change in the test particle's velocity of the order of itself, i.e. the time required for $(\Delta v)^2$ to accumulate to σ^2. Following Eq. (1.16), we finally obtain

$$t_{\rm relax} \simeq \frac{0.2\, N}{\ln(N)}\, t_{\rm d}. \tag{1.17}$$

Of course, there are numerous very significant shortcomings in the present calculation. But, it still provides us with various physical enlightenings as we will now discuss.

- We note that the relaxation time scales like $\propto N t_{\rm d}$, where for most purposes the $\ln(N)$ from Eq. (1.17) can be ignored. The larger the number particles, the more one has to wait for the relaxation to happen. In the present calculation, this number comes from the fact that spontaneous Poisson fluctuations have an amplitude of the order $1/\sqrt{N}$, and since they are assumed to be de-correlated one from another, they only contribute in quadrature to the velocity kicks, leading to the observed scaling w.r.t. N. In the upcoming calculations, we will show how, owing to the system's orbital structure, "encounters" should not be treated as decorrelated, but rather as resonant and correlated.
- In Eq. (1.17), the Coulomb logarithm associated with $\ln(N)$ is a consequence of the "scale conspiracy" of the Newtonian interaction, $-G/|\mathbf{x} - \mathbf{x}'|$, that makes it so that the small number of very nearby deflections and the large number of very far-away deflections contribute equally to the budget of a test star's diffusion. This logarithm factor also illustrates our mis-handling of the contributions from very nearby particles, where our assumption of small velocity kicks does not apply anymore, as well as our mis-handling of the contributions from particles on largest scales, where the homogeneity assumption does not hold anymore as well.
- In Eq. (1.17), we note that the ratio $t_{\rm relax}/t_{\rm d}$ only depends on N the number of particles, and is completely independent of σ, a proxy for the dynamical temperature of the system. This is because we have assumed that the source of fluctuations were "bare" Poisson fluctuations, i.e. only generated by the finite number of particles. In practice, this is not correct as self-gravity, i.e. the ability of the system to amplify perturbations will "dress" the Poisson fluctuations, significantly boost their amplitude, and therefore can drastically accelerate the system's overall relaxation. This is of particular importance on the largest scales,

where the self-gravitating amplification is the most efficient. Hence, large-scale fluctuations are expected to have larger amplitude than simple Poisson fluctuations, so that rather than all scales contributing equally to the relaxation, we can expect the fluctuations on the size of the system to possibly be the dominant driver of the system's relaxation.

All these remarks will make our task of characterising in detail the relaxation of self-gravitating systems more cumbersome in two respects. First, on the system's overall scale, we cannot rely on any homogeneous assumption, and assume that the particles' unperturbed trajectories are simple straight lines, an assumption that was legitimate in electrostatic plasmas. One has to account for inhomogeneity, and the associated intricate orbital motions. Second, because of the importance of self-gravity, we will need to solve the system's linear response, to characterise the efficiency of the associated amplification of perturbations. In the coming sections, we will develop all the needed tools to make the estimation from Eq. (1.17) much more precise, reaching our final in goal in Eq. (5.2), where we will present the inhomogeneous Balescu-Lenard equation, the kinetic equation describing the spontaneous, resonant and dressed relaxation of a discrete inhomogeneous long-range interacting system.

2 Mean-field dynamics

In this section, we present the tools and methods needed to describe the mean-field dynamics of a self-gravitating system. We refer to Goldstein (1950); Arnold (1978); Binney & Tremaine (2008) for thorough presentations of Hamiltonian dynamics.

2.1 Hamiltonian dynamics

A d-dimensional system can be described by its Hamiltonian H expressed as a function of the canonical coordinates $(\mathbf{q}, \mathbf{p})$. These coordinates evolve according to Hamilton's equations

$$\frac{\mathrm{d}\mathbf{q}}{\mathrm{d}t} = \frac{\partial H}{\partial \mathbf{p}} \quad ; \quad \frac{\mathrm{d}\mathbf{p}}{\mathrm{d}t} = -\frac{\partial H}{\partial \mathbf{q}}. \tag{2.1}$$

To shorten the notations, we denote the $2d$-dimensional phase space coordinates with the $\mathbf{w} = (\mathbf{q}, \mathbf{p})$.

For two functions $F(\mathbf{w})$ and $G(\mathbf{w})$, we define their Poisson brackets as

$$\big[F(\mathbf{w}), G(\mathbf{w})\big] = \frac{\partial F}{\partial \mathbf{q}} \cdot \frac{\partial G}{\partial \mathbf{p}} - \frac{\partial F}{\partial \mathbf{p}} \cdot \frac{\partial G}{\partial \mathbf{q}}. \tag{2.2}$$

With these notations, Hamilton's equation can be written under the short form

$$\frac{\mathrm{d}\mathbf{w}}{\mathrm{d}t} = \big[\mathbf{w}, H\big]. \tag{2.3}$$

In addition, the canonical phase space coordinates satisfy the canonical commutation relations

$$\big[\mathbf{w}_p, \mathbf{w}_q\big] = \mathbf{J}_{pq} \quad \text{with} \quad \mathbf{J} = \begin{pmatrix} \mathbf{0} & \mathbf{I} \\ -\mathbf{I} & \mathbf{0} \end{pmatrix}, \tag{2.4}$$

where $\mathbf{J}$ is the $2d \times 2d$ symplectic matrix, with $\mathbf{0}$ and $\mathbf{I}$ respectively the $d \times d$ zero and identity matrices.

Because Hamiltonian dynamics describes the dynamics in phase space, it allows for generalised change of coordinates. Some phase space coordinates $\mathbf{W} = (\mathbf{Q}, \mathbf{P})$ are said to be canonical if they satisfy the canonical commutation relations, i.e. if one has

$$\big[\mathbf{W}_p, \mathbf{W}_q\big] = \mathbf{J}_{pq}. \tag{2.5}$$

Canonical coordinates satisfy many fundamental properties. An essential one is that Hamilton's equations conserve the same form. This means that one has $\dot{\mathbf{W}} = [\mathbf{W}, H]$, where the Hamiltonian is expressed as a function of these new coordinates, and the Poisson bracket also involves derivatives w.r.t. the new coordinates. We note that infinitesimal phase space volumes are also conserved by canonical transformations, so that $\mathrm{d}\mathbf{W} = \mathrm{d}\mathbf{w}$. Similarly, Poisson brackets are also conserved through canonical transformations.

2.2 Klimontovich Equation

Throughout these notes, we will generically be interested in the dynamics of a N-body system, embedded within some physical space of dimension d. We have therefore N particles at our disposal, of individual mass m

and coupled through some long-range interaction potential $U(\mathbf{x},\mathbf{x}')$. To shorten the notations, we finally denote the phase space coordinates as $\mathbf{w}=(\mathbf{x},\mathbf{v})$. At any given time, the full state of the system can be characterised by the discrete DF (also called empirical DF)

$$F_{\rm d}(\mathbf{w},t)=\sum_{i=1}^{N} m\,\delta_{\rm D}(\mathbf{w}-\mathbf{w}_i(t)), \tag{2.6}$$

where $\mathbf{w}_i(t)$ stands for the location in phase space at time t of the $i^{\rm th}$ particle. At this stage, we emphasise that if the DF $F_{\rm d}(\mathbf{w},t)$ is provided, then one knows exactly the state of the system, and the system's evolution is fully deterministic.

Let us now determine the evolution equations satisfied by this discrete DF. Taking a time derivative, we can write

$$\begin{aligned}\frac{\partial F_{\rm d}(\mathbf{w},t)}{\partial t} &= \sum_{i=1}^{N} m\frac{\partial}{\partial \mathbf{w}_i(t)}\big[\delta_{\rm D}(\mathbf{w}-\mathbf{w}_i(t))\big]\,\dot{\mathbf{w}}_i(t)\\ &= -\sum_{i=1}^{N} m\frac{\partial}{\partial \mathbf{w}}\big[\delta_{\rm D}(\mathbf{w}-\mathbf{w}_i(t))\big]\,\dot{\mathbf{w}}_i(t)\\ &= -\frac{\partial}{\partial \mathbf{w}}\cdot\Big[\sum_{i=1}^{N}\delta_{\rm D}(\mathbf{w}-\mathbf{w}_i(t))\,\dot{\mathbf{w}}_i(t)\Big]\\ &= -\frac{\partial}{\partial \mathbf{w}}\cdot\Big[\sum_{i=1}^{N} m\,\delta_{\rm D}(\mathbf{w}-\mathbf{w}_i(t))\,\mathbf{w}(t)\Big]\\ &= -\frac{\partial}{\partial \mathbf{w}}\cdot\Big[F_{\rm d}(\mathbf{w},t)\,\dot{\mathbf{w}}(t)\Big].\end{aligned} \tag{2.7}$$

To get the second line, we simply used the parity of the Dirac delta, to switch the variable w.r.t. which the derivative is computed. To get the third line, as the derivative only acts on $\mathbf{w}$, we may move all particle's phase space velocities, $\dot{\mathbf{w}}_i(t)$, within the derivative. Finally, to get the last line, we used the presence of the Dirac delta to identify the phase space location where the phase space velocity, $\dot{\mathbf{w}}$, has to be computed[1]. In that equation, the phase space velocity $\dot{\mathbf{w}}$ should therefore be interpreted as the phase space velocity that a test particle at location $\mathbf{w}$ and time t would feel. Following Eq. (2.3), it is given by

$$\dot{\mathbf{w}}=\big[\mathbf{w},H_{\rm d}\big], \tag{2.8}$$

where, in the present case, the discrete Hamiltonian is given by

$$H_{\rm d}(\mathbf{w})=\frac{|\mathbf{v}|^2}{2}+\Phi_{\rm d}(\mathbf{x},t), \tag{2.9}$$

with the discrete Hamiltonian $\Phi_{\rm d}(\mathbf{x},t)$

$$\Phi_{\rm d}(\mathbf{x},t)=\sum_{i=1}^{n} m\,U(\mathbf{x},\mathbf{x}_i(t))=\int\!{\rm d}\mathbf{w}'\,U(\mathbf{x},\mathbf{x}')\,F_{\rm d}(\mathbf{w}',t). \tag{2.10}$$

As a consequence, following Eq. (2.7), we have been able to rewrite the evolution of the discrete DF, $F_{\rm d}(\mathbf{w},t)$, as a continuity equation reading

$$\frac{\partial F_{\rm d}(\mathbf{w},t)}{\partial t}+\frac{\partial}{\partial \mathbf{w}}\cdot\big[F_{\rm d}(\mathbf{w},t)\,\dot{\mathbf{w}}\big]=0. \tag{2.11}$$

Luckily, owing to the Hamiltonian structure, this equation can be rewritten under an even simpler form. Indeed, Eq. (2.11) becomes

$$\begin{aligned}0 &= \frac{\partial F_{\rm d}}{\partial t}+\frac{\partial}{\partial \mathbf{x}}\cdot\big[F_{\rm d}\,\dot{\mathbf{x}}\big]+\frac{\partial}{\partial \mathbf{v}}\cdot\big[F_{\rm d}\,\dot{\mathbf{v}}\big]\\ &= \frac{\partial F_{\rm d}}{\partial t}+\frac{\partial F_{\rm d}}{\partial \mathbf{x}}\cdot\frac{\partial H_{\rm d}}{\partial \mathbf{v}}-\frac{\partial F_{\rm d}}{\partial \mathbf{v}}\cdot\frac{\partial H_{\rm d}}{\partial \mathbf{v}}+F_{\rm d}\left(\frac{\partial}{\partial \mathbf{x}}\cdot\frac{\partial H_{\rm d}}{\partial \mathbf{v}}-\frac{\partial}{\partial \mathbf{v}}\cdot\frac{\partial H_{\rm d}}{\partial \mathbf{x}}\right)\\ &= \frac{\partial F_{\rm d}}{\partial t}+\frac{\partial F_{\rm d}}{\partial \mathbf{x}}\cdot\frac{\partial H_{\rm d}}{\partial \mathbf{v}}-\frac{\partial F_{\rm d}}{\partial \mathbf{v}}\cdot\frac{\partial H_{\rm d}}{\partial \mathbf{x}},\end{aligned} \tag{2.12}$$

[1] A careful reader would have noted that there is a subtlety associated with how self-interactions are considered, i.e. how one should one treat contributions from $U(\mathbf{x},\mathbf{x})$. As long as one assumes that there are no self-forces, the present derivation holds.

where to get the second line, we used the canonical equations of motion, as given by Eq. (2.8), and the simplification in the third line comes from Schwarz' theorem. Looking carefully at Eq. (2.12), we note that the two last terms can identified back as a Poisson bracket. All in all, the dynamics of $F_{\rm d}(\mathbf{w},t)$ in phase space is therefore given by

$$\boxed{\frac{\partial F_{\rm d}}{\partial t} + \big[F_{\rm d}, H_{\rm d}\big] = 0.} \tag{2.13}$$

This is the Klimontovich equation (Klimontovich, 1967). It is an important result, as it highlights how the dynamics of the whole N-body can be rewritten under the (seemingly) simple form of a continuity equation in phase space, that flows through phase space according to Hamilton's equations. Of course, here the main difficulty comes from the fact that the DF, $F_{\rm d}(\mathbf{w})$, and the Hamiltonian, $H_{\rm d}(\mathbf{w})$, are highly discontinuous phase space functions, that keep track exactly of the system's instantaneous phase space distribution. As such, this equation is formally equivalent to the $2dN$ Hamilton's equations, or the dN Newton's equations. The Klimontovich equation will be our starting point to derive a kinetic theory describing the long-term evolution of self-gravitating systems.

2.3 Angle-action coordinates

As we have already emphasised in Eq. (2.5), one of the key strength of the Hamiltonian framework, is that one can perform change of phase space coordinates towards new coordinates that might be better tailored to describe the intricate orbits of particles in an inhomogeneous system.

An integral of motion $I(\mathbf{w})$ is defined to be any function of the phase space coordinates that is constant along the orbits. Moreover, it is said to be isolating if for any value in the image of I, the region of phase space reaching this value is a smooth manifold of dimension $2d-1$. For example, for a Hamiltonian independent of time, the energy constitutes an isolating integral of motion. A system is then said to be integrable if it possesses d independent integrals of motion, i.e. d integrals whose differentials are linearly independent in all points of phase space. For such integrable systems, one can then devise a set of canonical coordinates, the angle-action coordinates $(\boldsymbol{\theta},\mathbf{J})$, such that the actions are independent isolating integrals of motion, and the angles are 2π-periodic. Within these coordinates, the system's Hamiltonian H becomes independent of the angles $\boldsymbol{\theta}$, and one has $H=H(\mathbf{J})$.

In that case, Hamilton's Eq. (2.1) take the simple form

$$\frac{{\rm d}\boldsymbol{\theta}}{{\rm d}t} = \frac{\partial H}{\partial \mathbf{J}} = \boldsymbol{\Omega}(\mathbf{J}) \quad ; \quad \frac{{\rm d}\mathbf{J}}{{\rm d}t} = -\frac{\partial H}{\partial \boldsymbol{\theta}} = 0, \tag{2.14}$$

where we introduced the orbital frequencies $\boldsymbol{\Omega}(\mathbf{J})=\partial H/\partial\mathbf{J}$. In these coordinates, the orbits are then straight lines, as one has

$$\boldsymbol{\theta}(t) = \boldsymbol{\theta}_0 + \boldsymbol{\Omega}(\mathbf{J})\,t \quad ; \quad \mathbf{J}(t) = {\rm cst}. \tag{2.15}$$

In Fig. 2.1, we illustrate one example of angle-action coordinate in the case of a harmonic oscillator. From the

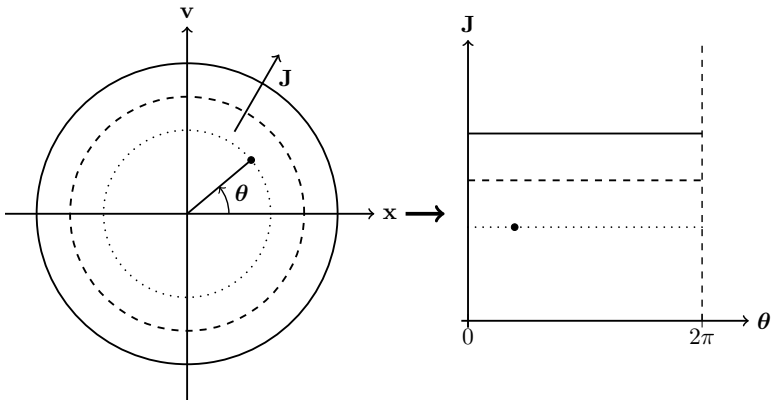

Figure 2.1: Illustration of the phase space diagram of a harmonic oscillator. Left panel: Illustration of the trajectories in the physical phase space $(\mathbf{x},\mathbf{v})$. The trajectories take the form of concentric circles along which the particle moves. Here, the action $\mathbf{J}$ should therefore be seen as a label for the circle associated with the orbit, and the angle $\boldsymbol{\theta}$ should be seen as the position along the circle. Right panel: Illustration of the same trajectories in angle-action space $(\boldsymbol{\theta},\mathbf{J})$. In these coordinates, the mean-field motions are straight lines. The action $\mathbf{J}$ is conserved, while the angle $\boldsymbol{\theta}$ evolves linearly in time with the frequency $\boldsymbol{\Omega}(\mathbf{J})=\partial H/\partial\mathbf{J}$.

unperturbed motions of Eq. (2.15), we can also already note the essential role played by the orbital frequencies,

as illustrated in Fig. 2.2. Indeed, the presence or absence of resonance condition satisfied by the orbital frequencies. If the orbital frequencies are incommensurate, so that there exists no relation of the form $\mathbf{k}\cdot\boldsymbol{\Omega}(\mathbf{J})=0$, the orbit is said to be quasi-periodic. The orbit fills in the entire available angle volume. Inversely, if the orbital frequencies satisfy a resonance condition then the orbit is resonant and does not fill in the entire available volume, as illustrated in Fig. 2.2. A Hamiltonian system is said to be degenerate if ever there exists some global

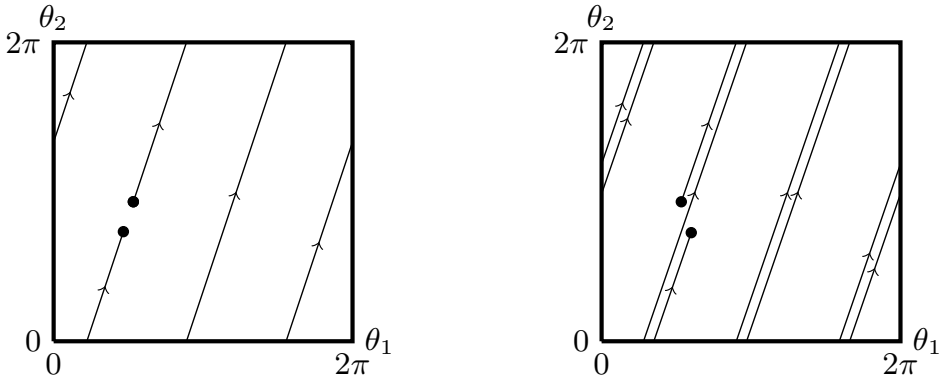

Figure 2.2: Illustration of two integrable trajectories in angle space, $\boldsymbol{\theta}=(\theta_1,\theta_2)$. An orbit is fully characterised by its action $\mathbf{J}$, while the position of the particle along its orbit is tracked by the angle $\boldsymbol{\theta}$. Along the unperturbed motion, the actions are conserved, while the angle evolve linearly in time with the frequency $\boldsymbol{\Omega}$. Left panel: Illustration of a degenerate orbit, for which there exists $\mathbf{k}\in\mathbb{Z}^2$ such that $\mathbf{k}\cdot\boldsymbol{\Omega}(\mathbf{J})=0$, i.e. the frequencies are commensurate. The orbit is then closed, periodic, and does not fill in the available angle space (e.g., see Section 7.2 for the kinetic description of degenerate galactic nuclei). Right panel: Illustration of a non-degenerate trajectory, for which the trajectory is quasiperiodic and densely covers the available angle domain.

resonance condition of the form $\forall\mathbf{J},\mathbf{k}\cdot\boldsymbol{\Omega}(\mathbf{J})=0$ satisfied by all the orbits, i.e. for all $\mathbf{J}$. Examples of degenerate systems include spherically symmetric systems, where, owing to angular momentum conservation, the orbit stays in the same orbital plane, as well as Keplerian systems, where the Keplerian motion imposed by a central mass takes the form of a closed ellipse.

Let us finally mention some additional properties of the angle-action coordinates. As angle-action coordinates are canonical, they leave the Poisson bracket invariant, so that one generically has

$$\begin{aligned}\big[F(\mathbf{w}),G(\mathbf{w})\big] &= \frac{\partial F}{\partial\mathbf{q}}\cdot\frac{\partial G}{\partial\mathbf{p}}-\frac{\partial F}{\partial\mathbf{p}}\cdot\frac{\partial G}{\partial\mathbf{q}}\\ &= \frac{\partial F}{\partial\boldsymbol{\theta}}\cdot\frac{\partial G}{\partial\mathbf{J}}-\frac{\partial F}{\partial\mathbf{J}}\cdot\frac{\partial G}{\partial\boldsymbol{\theta}}.\end{aligned}\tag{2.16}$$

As a result, angle-action coordinates also leave the infinitesimal phase space volumes invariant so that $\mathrm{d}\mathbf{w}=\mathrm{d}\mathbf{x}\mathrm{d}\mathbf{v}=\mathrm{d}\boldsymbol{\theta}\mathrm{d}\mathbf{J}$.

Angle-action coordinates are constructed such that the angles $\boldsymbol{\theta}$ are 2π-periodic. As a consequence, any phase space function can be Fourier expanded as

$$G(\mathbf{w})=G(\boldsymbol{\theta},\mathbf{J})=\sum_{\mathbf{k}}G_{\mathbf{k}}(\mathbf{J})\,\mathrm{e}^{\mathrm{i}\mathbf{k}\cdot\boldsymbol{\theta}}\quad\text{with}\quad G_{\mathbf{k}}(\mathbf{J})=\int\frac{\mathrm{d}\boldsymbol{\theta}}{(2\pi)^d}\,G(\boldsymbol{\theta},\mathbf{J})\,\mathrm{e}^{-\mathrm{i}\mathbf{k}\cdot\boldsymbol{\theta}},\tag{2.17}$$

where $\mathbf{k}\in\mathbb{Z}^d$ is a resonance vector composed of integers.

Actions are also adiabatic invariants. If H evolves on a timescale longer than the dynamical time, $t_{\mathrm{d}}\simeq 1/\Omega$, an orbit of H will evolve in such a way that $\mathbf{J}=\mathrm{cst}$.

For self-gravitating systems, an important example of integrable system are $3D$ spherically symmetric systems with a mean central potential $\Phi(r)$. An appropriate choice of action are then $\mathbf{J}=(J_r,L,L_z)$. Here, J_r is the radial action that quantifies the radial excursions. It is given by

$$J_r=\frac{1}{\pi}\int_{r_{\mathrm{p}}}^{r_{\mathrm{a}}}\mathrm{d}r\,\sqrt{2(E-\Phi(r))-L^2/r^2},\tag{2.18}$$

with E and L the energy and the norm of the angular momentum of the orbit, and $(r_{\mathrm{p}},r_{\mathrm{a}})$ its peri- and apocentre, i.e. the two roots of $v_r=\sqrt{2(E-\Phi(r))-L^2/r^2}=0$. The second action is L, the norm of the angular momentum, and the third one is L_z, the projection of the angular momentum vector along a gixen z-axis. In Fig. 2.3, we illustrate one such quasi-periodic orbit. As a conclusion, being able to construct angle-action coordinates amounts to being able to characterise in detail the orbital structure of an (integrable) inhomogeneous system.

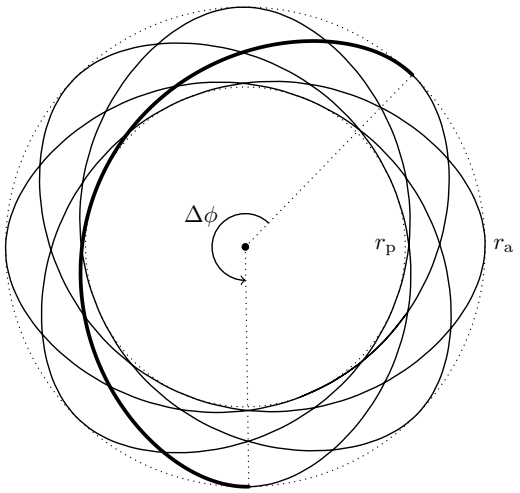

Figure 2.3: Illustration of a typical quasi-periodic orbit in a central potential, $\Phi(r)$. Such an orbit is the combination of an azimuthal oscillation at the frequency Ω_ϕ and a radial libration at the frequency Ω_r between the orbit's pericentre, $r_{\rm p}$, and apocentre, $r_{\rm a}$. In bold is highlighted the azimuthal increase $\Delta\phi = 2\pi\Omega_\phi/\Omega_r$ during one radial oscillation. For degenerate orbits, a resonance condition of the form $\mathbf{k}\cdot\boldsymbol{\Omega}(\mathbf{J})=0$ is satisfied, implying that $\Delta\phi$ is a multiple of 2π, i.e. the orbital frequencies Ω_ϕ and Ω_r are in a rational ratio. This overall leads to a closed and periodic orbit.

2.4 Mean-Field equilibrium

Having determined the evolution equation for the system, as given by the Klimontovich Eq. (2.13), and having constructed appropriate phase space coordinates to describe intricate orbital motions, as given by the angle-action coordinates $(\boldsymbol{\theta}, \mathbf{J})$, we may now construct a system's mean-field equilibrium.

Following the definition from Eq. (2.13), we introduce the system's mean DF and mean Hamiltonian as

$$F_0 = \big\langle F_{\rm d} \big\rangle \quad ; \quad H_0 = \big\langle H_{\rm d} \big\rangle, \tag{2.19}$$

where $\langle\,\cdot\,\rangle$ stands for the ensemble average over the system's realisations. Following Eq. (2.9), the mean-field Hamiltonian can generically be written as

$$H_0 = \frac{|\mathbf{v}|^2}{2} + \Phi_0(\mathbf{x},t) \quad \text{with} \quad \Phi_0(\mathbf{x},t) = \int \mathrm{d}\mathbf{w}'\, U(\mathbf{x},\mathbf{x}')\, F_0(\mathbf{w}',t), \tag{2.20}$$

where $\Phi_0(\mathbf{x},t)$ stands therefore for the system's mean-field potential.

A system is said to be in a mean-field equilibrium, equivalently said to be in a quasi-stationary state, if its mean-field DF is left unchanged by the mean-field dynamics. Following Eq. (2.13), the system is therefore in a mean-field equilibrium if it satisfies

$$\big[F_0, H_0\big] = 0. \tag{2.21}$$

If the mean-field Hamiltonian is integrable, we know that there exist some angle-action coordinates $(\boldsymbol{\theta}, \mathbf{J})$, so that $H_0 = H_0(\mathbf{J})$. The constraint from Eq. (2.21) therefore tells us that mean-field equilibria are states whose mean DF and mean Hamiltonian are of the form

$$\begin{cases} F_0 = F_0(\mathbf{J},t) \\ H_0 = H_0(\mathbf{J},t). \end{cases} \tag{2.22}$$

This is the appropriate generalisation of what was considered for electrostatic plasmas, where one assumed that $F_0 = F_0(\mathbf{v})$, since in an unperturbed homogeneous system one has $\mathbf{v} = \mathrm{cst}$. For self-gravitating systems, $\mathbf{v}$ is not an appropriate coordinate, as the actions $\mathbf{J}$ are the good labels of the system's orbital structure. Owing to this fundamental similarity, many of the formulae derived for electrostatic plasmas will naturally go over to stellar systems through the substitution $(\mathbf{x},\mathbf{v}) \mapsto (\boldsymbol{\theta},\mathbf{J})$. Deriving the kinetic theory of a self-gravitating system amounts then to deriving the long-term evolution of the system's mean orbital distribution, i.e. the long-term evolution of $F_0(\mathbf{J},t)$.

When interpreted in angle-action coordinates, the dynamics imposed by a mean-field integrable Hamiltonian is very simple. Indeed, let us consider some phase space distribution $G(\mathbf{w})$, whose dynamics is driven by

the mean-field Hamiltonian $H_0(\mathbf{J})$. Following Eq. (2.13), its evolution is governed by

$$\begin{aligned} 0 &= \frac{\partial G}{\partial t} + \big[G, H_0\big] \\ &= \frac{\partial G}{\partial t} + \boldsymbol{\Omega}(\mathbf{J}) \cdot \frac{\partial G}{\partial \boldsymbol{\theta}}, \end{aligned} \tag{2.23}$$

where we recall that the orbital frequencies are defined as $\boldsymbol{\Omega}(\mathbf{J}) = \partial H_0/\partial \mathbf{J}$. Such a flow in phase space is the one associated with phase mixing, as illustrated in Fig. 2.4. Phase mixing corresponds to the shearing in angle space

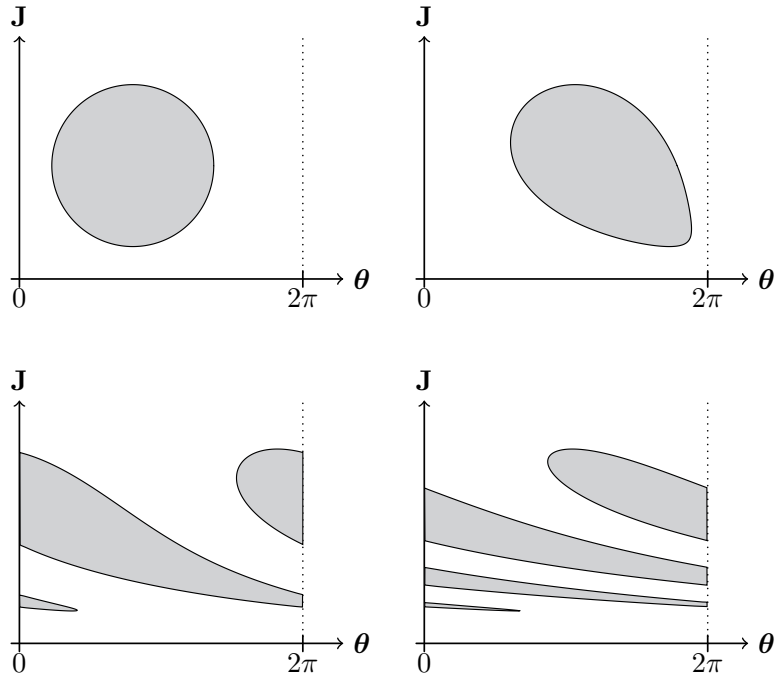

Figure 2.4: Illustration of phase mixing in angle-action space as a function of time. Here, within the angle-action coordinates, as a result of the conservation of the actions, trajectories are simple straight lines. Provided that the orbital frequencies $\boldsymbol{\Omega}(\mathbf{J})$ change with the actions, particles of different actions dephase. This leads to the appearance of ever finer structures in phase space. This is phase mixing. When coarse grained, these fine structures are washed out, and the system reaches a quasi-stationary distribution that depends only on the system's distribution of orbits. This unavoidable mixing in $\boldsymbol{\theta}$ is one the main justifications for our consideration of orbit-averaged diffusion, i.e. the construction of kinetic theories that describe the long-term dynamics of $F_0(\mathbf{J}, t)$.

associated with differences in orbital frequencies for different actions. This unavoidable dissolution of angular structures highlights again the relevance of characterising a system's long-term evolution by characterising in detail the long-term evolution of its mean-field orbital distribution $F_0(\mathbf{J}, t)$, i.e. the distribution independent of $\boldsymbol{\theta}$.

We now have at our disposal the main tools (evolution equations and angle-action coordinates) required to describe the long-term evolution of self-gravitating systems. In order to highlight the various relaxation processes undergone by these systems, we will proceed in successive stages. First, in Section 3, we will consider the dynamics of a zero-mass test particle embedded in a background fluctuating self-gravitating system. And we will characterise the properties and the orbital diffusion undergone by the test particle. In Section 4, we will then assume that that same particle is now massive, so that it perturbs the background self-gravitating system itself, and therefore undergoes an associated backreaction, that is called dynamical friction. Gluing together these two essential components, we will derive in Section 5, the main result of these notes, the so-called inhomogeneous Balescu-Lenard equation, that describes the self-consistent long-term resonant relaxation undergone by a discrete self-gravitating system. Benefiting from all the tools and techniques gathered in the previous sections, we will show in Section 6, how that same kinetic equation can also be obtained from the direct quasi-linear expansion of the Klimontovich equation. Finally, in Section 7, we will illustrate examples of these kinetic frameworks in the astrophysical context, in particular for self-gravitating galactic discs, as well as galactic nuclei, i.e. stellar clusters around supermassive black holes.

3 Orbital diffusion

As a first step towards the study of the the long-term dynamics of self-gravitating systems, let us consider the problem of the diffusion of a test particle embedded in an external "bath" of $N \gg 1$ particles. For now, we therefore assume that the particle diffusing is a zero-mass test particle, i.e. a particle that only acts as a probe of the potential generated by the bath. Such a dynamics is completely deterministic in the sense that the evolution of the test particle is fully determined by the positions and velocities, $(\mathbf{x}_i, \mathbf{v}_i)$ of the bath particles at the initial time. Yet, the intricate motions of the N bath particles, in the large N limit should rather be interpreted as a random process, which stochastically drives the long-term evolution of the test particle. As a result, the potential fluctuations induced by the background bath, which depend on the exact motion of the bath particles, will be replaced by a stochastic potential that can be characterised by its statistical correlations. Again, we emphasise that, for now, the test particle is taken to be of zero-mass, i.e. it does not induce any back-reaction onto the background bath.

Let us now specify some of the key properties of the background bath. For generality, we assume that it takes the form of a N-body system governed by a long-range pairwise interaction potential, $U(\mathbf{x}, \mathbf{x}')$, and we denote with d the dimension of the physical space. For example, in the usual gravitational case, one has $d = 3$, and $U(\mathbf{x}, \mathbf{x}') = -G/|\mathbf{x} - \mathbf{x}'|$. For simplicity, we assume that the bath is of total mass $M_{\rm tot}$, and that all the bath particles have the same individual mass $m_{\rm b} = M_{\rm tot}/N$.

The test particle is embedded in that noisy environment. The specific Hamiltonian driving the test particle's dynamics takes the generic form

$$H_{\rm t}(\mathbf{x}, \mathbf{v}) = \frac{1}{2}|\mathbf{v}|^2 + \sum_{i=1}^{N} m_{\rm b}\, U(\mathbf{x}, \mathbf{x}_i(t)), \tag{3.1}$$

where $(\mathbf{x}, \mathbf{v})$ stands for the location of the test particle in phase space, while $\mathbf{x}_i(t)$ stands for the location at time t of the $i^{\rm th}$ background bath particle. At this stage, we assume that the background is in a quasi-stationary equilibrium, so that by averaging over all the possible bath realisations, i.e. over the initial conditions of the background particles, we can introduce $\langle H_{\rm t} \rangle = |\mathbf{v}|^2/2 + \Phi_0(\mathbf{x}) = H_0(\mathbf{x}, \mathbf{v})$ as the test particle's mean Hamiltonian imposed by the mean background bath, with $\langle \cdot \rangle$ the ensemble average over the bath realisations. Following our construction of quasi-stationary equilibria, we also assume that this mean Hamiltonian is integrable, so that there exists a mapping to angle-action coordinates, $(\mathbf{x}, \mathbf{v}) \mapsto (\boldsymbol{\theta}, \mathbf{J})$, within which the mean Hamiltonian reads $H_0 = H_0(\mathbf{J})$. Even if the ensemble-averaged Hamiltonian is only a function of $\mathbf{J}$, a given bath realisation, as a result of the finite number of background particles has unavoidably some instantaneous potential fluctuations. We can therefore generically rewrite the test Hamiltonian from Eq. (3.1) as

$$H_{\rm t}(\mathbf{x}, \mathbf{v}) = H_0(\mathbf{x}, \mathbf{v}) + \delta\Phi(\mathbf{x}, t). \tag{3.2}$$

where we introduced $\delta\Phi(\mathbf{x}, t)$ as the instantaneous fluctuations generated by the bath and felt by the test particle. Owing to the angle-action mapping, we can subsequently rewrite this Hamiltonian as

$$H_{\rm t}(\boldsymbol{\theta}, \mathbf{J}) = H_0(\mathbf{J}) + \sum_{\mathbf{k}} \delta\Phi_{\mathbf{k}}(\mathbf{J}, t)\, {\rm e}^{{\rm i}\mathbf{k}\cdot\boldsymbol{\theta}} \quad \text{with} \quad \delta\Phi_{\mathbf{k}}(\mathbf{J}, t) = \int \frac{{\rm d}\boldsymbol{\theta}}{(2\pi)^d}\, \delta\Phi(\mathbf{x}[\boldsymbol{\theta}, \mathbf{J}], t)\, {\rm e}^{-{\rm i}\mathbf{k}\cdot\boldsymbol{\theta}}. \tag{3.3}$$

where we relied on the 2π-periodicity of the angles $\boldsymbol{\theta}$ to perform a Fourier transform. We recall that we assume that $\delta\Phi$ are fluctuations, so that we have $|\delta\Phi| \ll |H_0|$, and $\langle \delta\Phi \rangle = 0$.

Starting from the Hamiltonian from Eq. (3.3), and relying on the fact that $(\boldsymbol{\theta}, \mathbf{J})$ are canonical coordinates, we can immediately get the equations of motion for the test particle. They read

$$\begin{aligned} \frac{{\rm d}\boldsymbol{\theta}}{{\rm d}t} &= \frac{\partial H_{\rm t}}{\partial \mathbf{J}} = \boldsymbol{\Omega}(\mathbf{J}) + \sum_{\mathbf{k}} {\rm e}^{{\rm i}\mathbf{k}\cdot\boldsymbol{\theta}}\, \frac{\partial}{\partial \mathbf{J}} \delta\Phi_{\mathbf{k}}(\mathbf{J}, t), \\ \frac{{\rm d}\mathbf{J}}{{\rm d}t} &= -\frac{\partial H_{\rm t}}{\partial \mathbf{J}} = -{\rm i} \sum_{\mathbf{k}} \mathbf{k}\, {\rm e}^{{\rm i}\mathbf{k}\cdot\boldsymbol{\theta}}\, \delta\Phi_{\mathbf{k}}(\mathbf{J}, t), \end{aligned} \tag{3.4}$$

where we introduced $\boldsymbol{\Omega}(\mathbf{J}) = \partial H_{\rm t}/\partial \mathbf{J}$ as the mean orbital frequencies. At this stage, we note that the dynamics of $\boldsymbol{\theta}(t)$ and $\mathbf{J}(t)$ are radically different. Indeed, on the one hand, the evolution of the test particle's angle,

$\boldsymbol{\theta}(t)$, is primarily dominated by the mean-field motion that, in the absence of fluctuations, would lead to the motion $\boldsymbol{\theta}(t) = \boldsymbol{\theta}_0 + \boldsymbol{\Omega}(\mathbf{J})\, t$. On the other hand, the evolution of the test particle's action is only affected by the fluctuations, $\delta\Phi_{\mathbf{k}}(\mathbf{J}, t)$, and in the absence of fluctuations, it would lead to the motion $\mathbf{J}(t) = \mathrm{cst}$. Equations (3.4) are the starting points to characterise the long-term evolution of the test particle's action $\mathbf{J}$.

Let us now investigate the stochastic long-term dynamics undergone by the orbit of a test particle embedded in that noisy environment. At any time, the current action of the test particle is given by $\mathbf{J}(t)$, so that we can introduce the function

$$\varphi(\mathbf{J}, t) \equiv \delta_{\mathrm{D}}(\mathbf{J} - \mathbf{J}(t)), \tag{3.5}$$

as the discrete probability distribution function (PDF) describing the instantaneous location of the test particle in a given bath realisation. The main interest of such a writing is that it allows us to easily perform ensemble averages over the statistics of the test particle. Indeed, let us assume that the test particle is drawn according to some PDF, $P(\mathbf{J}, t)$, so that

$$P(\mathbf{J}, t) = \big\langle \varphi(\mathbf{J}, t) \big\rangle, \tag{3.6}$$

where, once again, $\langle \cdot \rangle$ stands for the average over the initial conditions of the background bath, as well as for the average over the initial conditions of the test particles. Rather than investigating one particular trajectory of one test particle in action space, as given by $\varphi(\mathbf{J}, t)$, our goal will be to investigate the statistical evolution of a large collection of test particles driven by different bath realisations, as given by the dynamics of $P(\mathbf{J}, t)$. Describing the mean long-term evolution of the test particle amounts then to describing the long-term evolution of the PDF, $P(\mathbf{J}, t)$.

The function $\varphi(\mathbf{J}, t)$ satisfies the continuity equation

$$\begin{aligned}
\frac{\partial \varphi(\mathbf{J}, t)}{\partial t} &= \frac{\partial}{\partial t}\big[\delta_{\mathrm{D}}(\mathbf{J} - \mathbf{J}(t))\big] \\
&= \frac{\mathrm{d}\mathbf{J}(t)}{\mathrm{d}t} \cdot \frac{\partial}{\partial \mathbf{J}(t)}\big[\delta_{\mathrm{D}}(\mathbf{J} - \mathbf{J}(t))\big] \\
&= -\frac{\mathrm{d}\mathbf{J}(t)}{\mathrm{d}t} \cdot \frac{\partial}{\partial \mathbf{J}}\big[\delta_{\mathrm{D}}(\mathbf{J} - \mathbf{J}(t))\big] \\
&= -\frac{\partial}{\partial \mathbf{J}} \cdot \big[\varphi(\mathbf{J}, t)\, \dot{\mathbf{J}}(\mathbf{J}, \boldsymbol{\theta}(t), t)\big],
\end{aligned} \tag{3.7}$$

where $\dot{bJ} = \dot{\mathbf{J}}(\boldsymbol{\theta}, \mathbf{J}, t)$ stands for the action velocity at the phase location $(\boldsymbol{\theta}, \mathbf{J})$ and time t, as imposed by Hamilton's Eq. (3.4). Using explicitly the test particle's evolution equations, we get

$$\frac{\partial \varphi(\mathbf{J}, t)}{\partial t} = \frac{\partial}{\partial \mathbf{J}} \cdot \left[\sum_{\mathbf{k}} \mathrm{i}\mathbf{k}\, \delta\Phi_{\mathbf{k}}(\mathbf{J}, t)\, \mathrm{e}^{\mathrm{i}\mathbf{k}\cdot\boldsymbol{\theta}(t)}\, \varphi(\mathbf{J}, t) \right], \tag{3.8}$$

where we recall that $(\boldsymbol{\theta}(t), \mathbf{J}(t))$ is the instantaneous location in phase space of the test particle. Now, in order to describe the statistics of the test particle, we can perform an ensemble average of that equation, to obtain

$$\frac{\partial P(\mathbf{J}, t)}{\partial t} = \frac{\partial}{\partial \mathbf{J}} \cdot \left[\sum_{\mathbf{k}} \mathrm{i}\mathbf{k} \left\langle \delta\Phi_{\mathbf{k}}(\mathbf{J}, t)\, \mathrm{e}^{\mathrm{i}\mathbf{k}\cdot\boldsymbol{\theta}(t)}\, \varphi(\mathbf{J}, t) \right\rangle \right]. \tag{3.9}$$

Further simplifications of Eq. (3.9) are challenging, as the computation of the ensemble-averaged term in its r.h.s. is not obvious. Indeed, we note that this term involves the average of a product of the noise function, $\delta\Phi_{\mathbf{k}}(\mathbf{J}, t)$, and a functional of this noise as it involves the current location $(\boldsymbol{\theta}(t), \mathbf{J}(t))$ of the test particle, whose value is governed by all the past history of the noise imposed by the bath.

To proceed forward, we need some more assumptions on the properties of the noise generated by the background particles. As they correspond to the joint contributions from N bath particles, owing to the central limit theorem, we may assume that $\delta\Phi_{\mathbf{k}}(\mathbf{J}, t)$ is a random time-stationary Gaussian noise, whose main statistical properties can be characterised by its two-point correlation functions

$$C_{\mathbf{k}\mathbf{k}'}(\mathbf{J}, \mathbf{J}', t - t') = \big\langle \delta\Phi_{\mathbf{k}}(\mathbf{J}, t)\, \delta\Phi^*_{\mathbf{k}'}(\mathbf{J}', t') \big\rangle. \tag{3.10}$$

Relying on this assumption, let us now evaluate the r.h.s. of Eq. (3.9). As shown by Eqs. (3.4), the exact trajectory of the test particle in phase space is itself a function of the stochastic noise $\delta\Phi_{\mathbf{k}}(\mathbf{J}, t)$. One should therefore interpret the r.h.s. of Eq. (3.9) as being sourced by the correlation of the noise $\delta\Phi_{\mathbf{k}}(\mathbf{J}, t)$ with $\mathrm{e}^{\mathrm{i}\mathbf{k}\cdot\boldsymbol{\theta}(t)}\varphi(\mathbf{J}, t)$, which is a functional of the noise of the generic form $R[\delta\Phi](\mathbf{J}, t)$. The technical difficulty here amounts then to computing the correlation of a stochastic noise with a functional of itself. Here, the calculation is also made more intricate because the noise $\delta\Phi_{\mathbf{k}}(\mathbf{J}, t)$ is spatially-extended as it depends both on time t, the considered resonance vector $\mathbf{k}$, and the location $\mathbf{J}$ in action space.

Fortunately, correlations of the form $\left\langle \delta\Phi_{\mathbf{k}}(\mathbf{J},t)\, R[\delta\Phi](\mathbf{J}',t')\right\rangle$ can generically be computed using Novikov's theorem (Novikov, 1965; Hänggi, 1978; Garcia-Ojalvo & Sancho, 1999). For a Gaussian noise, i.e. a noise for which only the second cumulant is non-zero, one can write

$$\boxed{\left\langle \delta\Phi_{\mathbf{k}}(\mathbf{J},t)\, R[\delta\Phi](\mathbf{J}',t')\right\rangle = \sum_{\mathbf{k}''}\int_0^{t'} \mathrm{d}t'' \int \mathrm{d}\mathbf{J}'' \left\langle \delta\Phi_{\mathbf{k}}(\mathbf{J},t)\, \delta\Phi^*_{\mathbf{k}''}(\mathbf{J}'',t'')\right\rangle \left\langle \frac{\mathcal{D}R[\delta\Phi](\mathbf{J}',t')}{\mathcal{D}\delta\Phi^*_{\mathbf{k}''}(\mathbf{J}'',t'')}\right\rangle.} \tag{3.11}$$

where the conjugate was introduced for later convenience, and $\mathcal{D}R[\delta\Phi](\mathbf{J}',t')/\mathcal{D}\delta\Phi^*_{\mathbf{k}''}(\mathbf{J}'',t'')$ stands for the functional derivative of $R[\delta\Phi](\mathbf{J}',t')$ w.r.t. the noise $\delta\Phi^*_{\mathbf{k}''}(\mathbf{J}'',t'')$. In Eq. (3.11), the r.h.s. term corresponds to the contributions arising from the noise intrinsic correlations. Let us briefly detail the physical content of that term. The l.h.s. of Eq. (3.11) aims at computing the correlation between the noise $\delta\Phi_{\mathbf{k}}(\mathbf{J},t)$, evaluated at the location $\mathbf{J}$ and time t, with a functional of the noise $R[\delta\Phi](\mathbf{J}',t')$, evaluated at the location $\mathbf{J}'$ and time t', which, because it is a functional, depends on the noise at any past time $t''\leq t'$, any location $\mathbf{J}''$, and any resonance vectori $\mathbf{k}''$. Novikov's theorem states that this correlation is given by the joint contributions from all the different noise terms $\delta\Phi^*_{\mathbf{k}''}(\mathbf{J}'',t'')$ (via the sum $\sum_{\mathbf{k}''}$) for all past values (via the integral $\int \mathrm{d}t''$) and for all the locations (via the integral $\int \mathrm{d}\mathbf{J}''$) of the correlations between $\delta\Phi_{\mathbf{k}}(\mathbf{J},t)$ and $\delta\Phi^*_{\mathbf{k}''}(\mathbf{J}'',t'')$ (via the correlation $\left\langle \delta\Phi_{\mathbf{k}}(\mathbf{J},t)\, \delta\Phi^*_{\mathbf{k}''}(\mathbf{J}'',t'')\right\rangle$) multiplied by the functional gradient $\mathcal{D}R[\delta\Phi](\mathbf{J}',t')/\mathcal{D}\delta\Phi^*_{\mathbf{k}''}(\mathbf{J}'',t'')$. This functional gradient describes how much the value of $R[\delta\Phi](\mathbf{J}',t')$ would get to vary as a result of modifying the noise $\delta\Phi^*_{\mathbf{k}''}(\mathbf{J}'',t')$ at time t'', location $\mathbf{J}''$, and resonance vector $\mathbf{k}''$. As a summary, Novikov's theorem states that the correlation between a noise and a functional of this noise scales qualitatively like the product of the correlation of the noise and the response of the functional to changes in the noise. Novikov's theorem is a therefore a very general result.

Let us now apply Novikov's theorem to the r.h.s. of Eq. (3.9). This yields terms of the form

$$\begin{aligned}\left\langle \delta\Phi_{\mathbf{k}}(\mathbf{J},t)\, \mathrm{e}^{\mathrm{i}\mathbf{k}\cdot\boldsymbol{\theta}(t)}\, \varphi(\mathbf{J},t)\right\rangle = \sum_{\mathbf{k}'}\int_0^t \mathrm{d}t' \int \mathrm{d}\mathbf{J}'\, C_{\mathbf{k}\mathbf{k}'}(\mathbf{J},\mathbf{J}',t-t') \\ \times \left\langle \mathrm{e}^{\mathrm{i}\mathbf{k}\cdot\boldsymbol{\theta}(t)}\left[\mathrm{i}\mathbf{k}\cdot\frac{\mathcal{D}\boldsymbol{\theta}(t)}{\mathcal{D}\delta\Phi^*_{\mathbf{k}'}(\mathbf{J}',t')} - \frac{\mathcal{D}\mathbf{J}(t)}{\mathcal{D}\delta\Phi^*_{\mathbf{k}'}(\mathbf{J}',t')}\cdot\frac{\partial}{\partial\mathbf{J}}\right]\varphi(\mathbf{J},t)\right\rangle,\end{aligned} \tag{3.12}$$

where we recall that $C_{\mathbf{k}\mathbf{k}'}(\mathbf{J},\mathbf{J}',t-t')$ was introduced in Eq. (3.10) as the two-point correlation function of the noise. Equation (3.12) involves the so-called response functions, $\mathcal{D}\boldsymbol{\theta}(t)/\mathcal{D}\delta\Phi^*_{\mathbf{k}'}(\mathbf{J}',t')$ and $\mathcal{D}\mathbf{J}(t)/\mathcal{D}\delta\Phi^*_{\mathbf{k}'}(\mathbf{J}',t')$, that describe how the position of the test particle at time t, $(\boldsymbol{\theta}(t),\mathbf{J}(t))$, changes as one varies the noise $\delta\Phi^*_{\mathbf{k}'}(\mathbf{J}',t')$ felt by the test particle as it arrived at $\mathbf{J}'$ at time t'.

Glancing back at the individual equations of motion from Eq. (3.4), we note that the motion of the test particle in action space between the times t and t' can formally be integrated as

$$\begin{aligned}\boldsymbol{\theta}(t) &= \boldsymbol{\theta}(t') + \int_{t'}^t \mathrm{d}s\, \boldsymbol{\Omega}(\mathbf{J}(s)) + \sum_{\mathbf{k}}\int_{t'}^t \mathrm{d}s\, \mathrm{e}^{\mathrm{i}\mathbf{k}\cdot\boldsymbol{\theta}(s)}\, \frac{\partial}{\partial\mathbf{J}}\delta\Phi_{\mathbf{k}}(\mathbf{J}(s),s), \\ \mathbf{J}(t) &= \mathbf{J}(t') - \mathrm{i}\sum_{\mathbf{k}}\mathbf{k}\int_{t'}^t \mathrm{d}s\, \mathrm{e}^{\mathrm{i}\mathbf{k}\cdot\boldsymbol{\theta}(s)}\, \delta\Phi_{\mathbf{k}}(\mathbf{J}(s),s),\end{aligned} \tag{3.13}$$

We note that these equations depend on the noise both directly through the factor $\delta\Phi_{\mathbf{k}}(\mathbf{J}(s),s)$, but also indirectly through the past history of the test particle's trajectory, $(\boldsymbol{\theta}(s),\mathbf{J}(s))$. As a consequence, if we were to compute the functional gradients of thes equations w.r.t. the noise $\delta\Phi^*_{\mathbf{k}'}(\mathbf{J}',t')$, we would not obtain closed expressions for the response functions, as their r.h.s. would involve the response functions themselves. This entices us to introduce additional assumptions to make the calculations tractable.

In Eq. (3.4), we note that at leading order, since $\delta\Phi \ll H_0$, the motion of the test particle is dominated by the background smooth mean-field potential. As a consequence, to make further progress in the calculation, when computing the test particle's response function, we will solve for the motion of the test particle at first order in the noise. Glancing back at Eq. (3.13), this implies that in its r.h.s., we substitute the occurrences of the location of the test particle, $(\boldsymbol{\theta}(s),\mathbf{J}(s))$ by its unperturbed mean-field motion between t' and t, namely $(\boldsymbol{\theta}(s),\mathbf{J}(s)) = (\boldsymbol{\theta}(t') + (s-t')\,\boldsymbol{\Omega}(\mathbf{J}(t')),\mathbf{J}(t'))$. Equation (3.13) therefore becomes

$$\begin{aligned}\boldsymbol{\theta}(t) &= \boldsymbol{\theta}(t') + \boldsymbol{\Omega}(\mathbf{J}(t'))\,(t-t') + \sum_{\mathbf{k}}\int_{t'}^t \mathrm{d}s\, \mathrm{e}^{\mathrm{i}\mathbf{k}\cdot(\boldsymbol{\theta}(t')+(s-t')\,\boldsymbol{\Omega}(\mathbf{J}(t')))}\, \frac{\partial}{\partial\mathbf{J}}\delta\Phi_{\mathbf{k}}(\mathbf{J}(t'),s), \\ \mathbf{J}(t) &= \mathbf{J}(t') - \mathrm{i}\sum_{\mathbf{k}}\mathbf{k}\int_{t'}^t \mathrm{d}s\, \mathrm{e}^{\mathrm{i}\mathbf{k}\cdot(\boldsymbol{\theta}(t')+(s-t')\,\boldsymbol{\Omega}(\mathbf{J}(t')))}\, \delta\Phi_{\mathbf{k}}(\mathbf{J}(t'),s).\end{aligned} \tag{3.14}$$

We can now compute the response functions of the test particle, as required by Eq. (3.12), by computing the functional gradient of Eq. (3.14) w.r.t. the noise $\delta\Phi_{\mathbf{k}'}(\mathbf{J}',t')$

Because it is simpler, let us start with the computation of the response function for $\mathbf{J}(t)$. We can write

$$\frac{\mathcal{D}\mathbf{J}(t)}{\mathcal{D}\delta\Phi^*_{\mathbf{k}'}(\mathbf{J}',t')} = -\mathrm{i}\sum_{\mathbf{k}}\mathbf{k}\int_{t'}^{t}\mathrm{d}s\,\mathrm{e}^{\mathrm{i}\mathbf{k}\cdot(\boldsymbol{\theta}(t')+(s-t')\boldsymbol{\Omega}(\mathbf{J}(t')))}\,\frac{\mathcal{D}\delta\Phi_{\mathbf{k}}(\mathbf{J}(t'),s)}{\mathcal{D}\delta\Phi^*_{\mathbf{k}'}(\mathbf{J}',t')}. \tag{3.15}$$

Here, we may now use the fundamental relation

$$\frac{\mathcal{D}\delta\Phi_{\mathbf{k}}(\mathbf{J},t)}{\mathcal{D}\delta\Phi^*_{\mathbf{k}'}(\mathbf{J}',t')} = \delta_{\mathrm{D}}(t-t')\,\delta_{\mathrm{D}}(\mathbf{J}-\mathbf{J}')\,\delta_{-\mathbf{k}\mathbf{k}'}, \tag{3.16}$$

that states that noises at different times, different resonance indices, or different action locations, are taken as independent from each other, when computing functional gradients.

As a consequence, we can rewrite Eq. (3.15) as

$$\begin{aligned}\frac{\mathcal{D}\mathbf{J}(t)}{\mathcal{D}\delta\Phi^*_{\mathbf{k}'}(\mathbf{J}',t')} &= \mathrm{i}\mathbf{k}'\,\mathrm{e}^{-\mathrm{i}\mathbf{k}'\cdot\boldsymbol{\theta}(t')}\,\delta_{\mathrm{D}}(\mathbf{J}'-\mathbf{J}(t'))\\ &= \mathrm{i}\mathbf{k}'\,\mathrm{e}^{-\mathrm{i}\mathbf{k}'\cdot\boldsymbol{\theta}(t)}\,\mathrm{e}^{-\mathrm{i}\mathbf{k}'\cdot\boldsymbol{\Omega}(\mathbf{J}')(t'-t)}\,\delta_{\mathrm{D}}(\mathbf{J}'-\mathbf{J}(t)),\end{aligned} \tag{3.17}$$

where to get the last line, we re-expressed $(\boldsymbol{\theta}(t'),\mathbf{J}(t'))$ in terms of $(\boldsymbol{\theta}(t),\mathbf{J}(t))$ using the unperturbed mean-field motion.

We can perform a similar computation to determine the response function of $\boldsymbol{\theta}(t)$. Starting from Eq. (3.14), we write

$$\frac{\mathcal{D}\boldsymbol{\theta}(t)}{\mathcal{D}\delta\Phi^*_{\mathbf{k}'}(\mathbf{J}',t')} = \sum_{\mathbf{k}}\int_{t'}^{t}\mathrm{d}s\,\mathrm{e}^{\mathrm{i}\mathbf{k}\cdot(\boldsymbol{\theta}(t')+(s-t')\boldsymbol{\Omega}(\mathbf{J}(t')))}\,\frac{\mathcal{D}}{\mathcal{D}\delta\Phi^*_{\mathbf{k}'}(\mathbf{J}',t)}\left[\frac{\partial}{\partial\mathbf{J}}\delta\Phi_{\mathbf{k}}(\mathbf{J}(t'),s)\right]. \tag{3.18}$$

To compute the needed functional gradient, one has to be careful. We write

$$\begin{aligned}\frac{\mathcal{D}}{\mathcal{D}\delta\Phi^*_{\mathbf{k}'}(\mathbf{J}',t')}\left[\frac{\partial}{\partial\mathbf{J}}\delta\Phi_{\mathbf{k}}(\mathbf{J}(t'),s)\right] &= \frac{\mathcal{D}}{\mathcal{D}\delta\Phi^*_{\mathbf{k}'}(\mathbf{J}',t')}\left[\int\mathrm{d}\mathbf{J}\,\delta_{\mathrm{D}}(\mathbf{J}-\mathbf{J}(t'))\,\frac{\partial\delta\Phi_{\mathbf{k}}(\mathbf{J},s)}{\partial\mathbf{J}}\right]\\ &= \int\mathrm{d}\mathbf{J}\,\delta_{\mathrm{D}}(\mathbf{J}-\mathbf{J}(t'))\,\frac{\partial}{\partial\mathbf{J}}\left[\frac{\mathcal{D}\delta\Phi_{\mathbf{k}}(\mathbf{J},s)}{\mathcal{D}\delta\Phi^*_{\mathbf{k}'}(\mathbf{J}',t')}\right]\\ &= \delta_{-\mathbf{k}\mathbf{k}'}\,\delta_{\mathrm{D}}(s-t')\int\mathrm{d}\mathbf{J}\,\delta_{\mathrm{D}}(\mathbf{J}-\mathbf{J}(t'))\,\frac{\partial}{\partial\mathbf{J}}\left[\delta_{\mathrm{D}}(\mathbf{J}'-\mathbf{J})\right]\\ &= -\delta_{-\mathbf{k}\mathbf{k}'}\,\delta_{\mathrm{D}}(s-t')\int\mathrm{d}\mathbf{J}\,\delta_{\mathrm{D}}(\mathbf{J}-\mathbf{J}(t'))\,\frac{\partial}{\partial\mathbf{J}'}\left[\delta_{\mathrm{D}}(\mathbf{J}'-\mathbf{J})\right]\\ &= -\delta_{-\mathbf{k}\mathbf{k}'}\,\delta_{\mathrm{D}}(s-t')\,\frac{\partial}{\partial\mathbf{J}'}\left[\delta_{\mathrm{D}}(\mathbf{J}'-\mathbf{J}(t'))\right],\end{aligned} \tag{3.19}$$

where, in the first line of that equation, we rewrote the partial derivative with an integral, to avoid possible confusion when computing the functional gradient. To get the second line, we noted that, because of causality, $J(t')$ does not vary when one changes the noise $\delta\Phi^*_{\mathbf{k}'}(\mathbf{J}',t')$, so that the functional gradient only acts on the partial derivative. To get the third line, we used the fundamental relation from Eq. (3.16), and to get the fourth line, we used the fact that the Dirac delta is an even function. All in all, this allows us then to rewrite the response function of $\boldsymbol{\theta}(t)$ as

$$\frac{\mathcal{D}\boldsymbol{\theta}(t)}{\mathcal{D}\delta\Phi^*_{\mathbf{k}'}(\mathbf{J}',t')} = -\mathrm{e}^{-\mathrm{i}\mathbf{k}'\cdot\boldsymbol{\theta}(t)}\,\mathrm{e}^{-\mathrm{i}\mathbf{k}'\cdot\boldsymbol{\Omega}(\mathbf{J}')(t'-t)}\,\frac{\partial}{\partial\mathbf{J}'}\left[\delta_{\mathrm{D}}(\mathbf{J}'-\mathbf{J}(t))\right], \tag{3.20}$$

where we performed a similar replacement of the unperturbed mean-field motion as in Eq. (3.17).

Having computed the system's response function at first order in the perturbations, we can now use the explicit expressions from Eqs. (3.17) and (3.20) into Eq. (3.12) to characterise the impact of the noise on the test particles' trajectories. We can rewrite the diffusion Eq. (3.9) as

$$\begin{aligned}\frac{\partial P(\mathbf{J},t)}{\partial t} = \frac{\partial}{\partial\mathbf{J}}\cdot\Bigg[\sum_{\mathbf{k},\mathbf{k}'}\mathbf{k}\int_0^t\mathrm{d}t'\int\mathrm{d}\mathbf{J}'\,C_{\mathbf{k}\mathbf{k}'}(\mathbf{J},\mathbf{J}',t-t')\,\mathrm{e}^{-\mathrm{i}\mathbf{k}'\cdot\boldsymbol{\Omega}(\mathbf{J}')(t'-t)}\\ \times\left[\mathbf{k}\cdot\frac{\partial}{\partial\mathbf{J}'}+\mathbf{k}'\cdot\frac{\partial}{\partial\mathbf{J}}\right]\left\langle\mathrm{e}^{-\mathrm{i}(\mathbf{k}'-\mathbf{k})\cdot\boldsymbol{\theta}(t)}\,\delta_{\mathrm{D}}(\mathbf{J}-\mathbf{J}(t))\,\delta_{\mathrm{D}}(\mathbf{J}'-\mathbf{J}(t))\right\rangle\Bigg].\end{aligned} \tag{3.21}$$

Here, the ensemble average implies in particular averaging over the current phase $\boldsymbol{\theta}(t)$ of the test particle. We assume that at any time t, the phase of the test particle, $\boldsymbol{\theta}(t)$, remains on average uniformly distributed in

angles, As a consequence, in Eq. (3.21), the exponential $\mathrm{e}^{-\mathrm{i}(\mathbf{k}'-\mathbf{k})\cdot\boldsymbol{\theta}(t)}$ gives the constraint $\delta_{\mathbf{k}\mathbf{k}'}$. Equation (3.21) can then be rewritten as

$$\frac{\partial P(\mathbf{J},t)}{\partial t} = \frac{\partial}{\partial \mathbf{J}}\cdot\Bigg[\sum_{\mathbf{k}}\mathbf{k}\int_0^t \mathrm{d}s \int \mathrm{d}\mathbf{J}'\, C_{\mathbf{k}}(\mathbf{J},\mathbf{J}',s)\,\mathrm{e}^{\mathrm{i}\mathbf{k}\cdot\boldsymbol{\Omega}(\mathbf{J}')s} \times\left[\mathbf{k}\cdot\frac{\partial}{\partial\mathbf{J}'}+\mathbf{k}\cdot\frac{\partial}{\partial\mathbf{J}}\right]\Big\langle\delta_{\mathrm{D}}(\mathbf{J}-\mathbf{J}(t))\,\delta_{\mathrm{D}}(\mathbf{J}'-\mathbf{J}(t))\Big\rangle\Bigg], \tag{3.22}$$

where we performed the change of variables $s = t - t'$. To simplify the last term, we write

$$\begin{aligned}\left[\mathbf{k}\cdot\frac{\partial}{\partial\mathbf{J}'}+\mathbf{k}\cdot\frac{\partial}{\partial\mathbf{J}}\right]\Big\langle\delta_{\mathrm{D}}(\mathbf{J}'-\mathbf{J}(t))\,\delta_{\mathrm{D}}(\mathbf{J}-\mathbf{J}(t))\Big\rangle &= \left[\mathbf{k}\cdot\frac{\partial}{\partial\mathbf{J}'}+\mathbf{k}\cdot\frac{\partial}{\partial\mathbf{J}}\right]\delta_{\mathrm{D}}(\mathbf{J}-\mathbf{J}')\Big\langle\delta_{\mathrm{D}}(\mathbf{J}-\mathbf{J}(t))\Big\rangle\\ &= \left[\mathbf{k}\cdot\frac{\partial}{\partial\mathbf{J}'}+\mathbf{k}\cdot\frac{\partial}{\partial\mathbf{J}}\right]\delta_{\mathrm{D}}(\mathbf{J}-\mathbf{J}')\,P(\mathbf{J},t)\\ &= \mathbf{k}\cdot\frac{\partial\delta_{\mathrm{D}}(\mathbf{J}-\mathbf{J}')}{\partial\mathbf{J}}+\mathbf{k}\cdot\frac{\partial\delta_{\mathrm{D}}(\mathbf{J}-\mathbf{J}')}{\partial\mathbf{J}'}+\delta_{\mathrm{D}}(\mathbf{J}-\mathbf{J}')\,\mathbf{k}\cdot\frac{\partial P(\mathbf{J},t)}{\partial\mathbf{J}}\\ &= \delta_{\mathrm{D}}(\mathbf{J}-\mathbf{J}')\,\mathbf{k}\cdot\frac{\partial P(\mathbf{J},t)}{\partial\mathbf{J}}.\end{aligned} \tag{3.23}$$

This allows us then to rewrite Eq. (3.22) as

$$\frac{\partial P(\mathbf{J},t)}{\partial t} = \frac{\partial}{\partial\mathbf{J}}\cdot\left[\sum_{\mathbf{k}}\mathbf{k}\int_0^t \mathrm{d}s\, C_{\mathbf{k}\mathbf{k}}(\mathbf{J},\mathbf{J},s)\,\mathrm{e}^{\mathrm{i}\mathbf{k}\cdot\boldsymbol{\Omega}(\mathbf{J})s}\,\mathbf{k}\cdot\frac{\partial P(\mathbf{J},t)}{\partial\mathbf{J}}\right]. \tag{3.24}$$

The timescale over which $P(\mathbf{J},t)$ significantly changes is the diffusion timescale, which is much larger than the dynamical time, $t_{\mathrm{d}} \simeq 1/\Omega$. The dynamical time is also the timescale over which the correlation function $C_{\mathbf{k}\mathbf{k}}(\mathbf{J},\mathbf{J},t)$ decays, as it is generated by background bath particles orbiting with that same dynamical time. As a consequence, in Eq. (3.24), we may take the limits of the time integration to $+\infty$, keeping $P(\mathbf{J},t)$ constant. That equation then takes the form of a diffusion equation of the form

$$\boxed{\frac{\partial P(\mathbf{J},t)}{\partial t} = \frac{\partial}{\partial\mathbf{J}}\cdot\left[\mathbf{D}_2(\mathbf{J})\cdot\frac{\partial P(\mathbf{J},t)}{\partial\mathbf{J}}\right],} \tag{3.25}$$

where we introduced the diffusion tensor, $\mathbf{D}_2(\mathbf{J})$ as

$$\begin{aligned}\mathbf{D}_2(\mathbf{J}) &= \sum_{\mathbf{k}}\mathbf{k}\otimes\mathbf{k}\int_0^{+\infty}\mathrm{d}t\, C_{\mathbf{k}\mathbf{k}}(\mathbf{J},\mathbf{J},t)\,\mathrm{e}^{\mathrm{i}\mathbf{k}\cdot\boldsymbol{\Omega}(\mathbf{J})t}\\ &= \frac{1}{2}\sum_{\mathbf{k}}\mathbf{k}\otimes\mathbf{k}\int_{-\infty}^{+\infty}\mathrm{d}t\, C_{\mathbf{k}\mathbf{k}}(\mathbf{J},\mathbf{J},t)\,\mathrm{e}^{\mathrm{i}\mathbf{k}\cdot\boldsymbol{\Omega}(\mathbf{J})t},\end{aligned} \tag{3.26}$$

where we used the symmetries of the correlation function. Let us finally introduce the temporal Fourier transform with the convention

$$\widehat{f}(\omega) = \int_{-\infty}^{+\infty}\mathrm{d}t\, f(t)\,\mathrm{e}^{\mathrm{i}\omega t} \quad ; \quad f(t) = \frac{1}{2\pi}\int_{-\infty}^{+\infty}\mathrm{d}\omega\,\widehat{f}(\omega)\,\mathrm{e}^{-\mathrm{i}\omega t}. \tag{3.27}$$

All in all, this allows us to rewrite the diffusion tensor as

$$\boxed{\mathbf{D}_2(\mathbf{J}) = \frac{1}{2}\sum_{\mathbf{k}}\mathbf{k}\otimes\mathbf{k}\,\widehat{C}_{\mathbf{k}\mathbf{k}}(\mathbf{J},\mathbf{J},\mathbf{k}\cdot\boldsymbol{\Omega}(\mathbf{J})),} \tag{3.28}$$

where we introduced $\widehat{C}_{\mathbf{k}\mathbf{k}}(\mathbf{J},\mathbf{J},\omega)$ as the Fourier transform of the correlation function of the fluctuations undergone by the test particle (Binney & Lacey, 1988; Weinberg, 2001).

Equations (3.25) and (3.28) are the important results of this section. It emphasises that the diffusion tensor in action space of a given test particle is driven by the power spectrum of the noise fluctuations at the location $\mathbf{J}$ and the dynamical frequency $\omega = \mathbf{k}\cdot\boldsymbol{\Omega}(\mathbf{J})$ of the test particle. Phrased differently, as a result of the presence of a dominant underlying mean-field motion, i.e. the motion $\mathrm{d}\boldsymbol{\theta}/\mathrm{d}t = \boldsymbol{\Omega}(\mathbf{J})$, the only perturbations to which a test particle can be sensitive are the perturbations in resonance with this mean-field motion. We note that Eq. (3.25) is formally identical to a heat equation. The main difference here is that the diffusion tensor, $\mathbf{D}_2(\mathbf{J})$, is strongly anisotropic, because it is a function of the considered orbital location, $\mathbf{J}$, and for a given $\mathbf{J}$, its direction

is also anisotropic, as each resonance vector $\mathbf{k}$ is associated with a different direction of diffusion in action space. We also recall that, for now, we assumed the test particle is of zero mass, i.e. it has no backreaction on the background particles. This is the reason why Eq. (3.25) only involves a diffusion coefficient and no friction component, as the noise sourcing the diffusion is completely external. In particular, we note that the amplitude of these diffusion coefficients is independent of the mass of the test particle, so that such a diffusion cannot source any mass segregation, i.e. the sinking of heavier populations within the system's centre as a result of energy equipartition. In Section 4, we will show how one can adapt the previous calculation to account for the back-reaction to the test particle perturbation, via the so-called friction force by polarisation. At that time, we will also note that the amplitude of this friction force is proportional to the mass of the test particle, so that it can drive a mass segregation between test particles of different mass.

For now, let us compute explicitly the diffusion coefficients from Eq. (3.28) for some important classes of background baths, in particular to recover the inhomogeneous Landau and Balescu-Lenard diffusion coefficients.

3.1 The Landau diffusion coefficients

The main conclusion from Eq. (3.28) was that to characterise the diffusion undergone by the test particle, one only has to characterise the correlation properties of the noise within which that test particle is embedded. As a first step, let us assume that the background bath of particles is external to the test particle (i.e. no backreaction of the test particle onto the motion of the bath particles). Furthermore, we assume that the bath itself is non-interacting, so that the dynamics of every bath particle is imposed by the specific Hamiltonian

$$H_{\rm b}(\boldsymbol{\theta}, \mathbf{J}, t) = H_0(\mathbf{J}), \tag{3.29}$$

where the mean-field Hamiltonian, $H_0(\mathbf{J})$ was already introduced in Eq. (3.2). In that limit, the bath is said to be inert, because bath particles only see the smooth averaged mean-field potential, and not its instantaneous fluctuations. At any given time, the full state of the bath is fully characterised by the discrete DF, $F_{\rm d}(\boldsymbol{\theta}, \mathbf{J}, t)$, defined as

$$F_{\rm d}(\boldsymbol{\theta}, \mathbf{J}) = \sum_{i=1}^{N} m_{\rm b}\, \delta_{\rm D}(\boldsymbol{\theta} - \boldsymbol{\theta}_i(t))\, \delta_{\rm D}(\mathbf{J} - \mathbf{J}_i(t)), \tag{3.30}$$

where the sum over i runs over the N particles of the bath, and $(\boldsymbol{\theta}_i(t), \mathbf{J}_i(t))$ stands for the location in angle-action space of the $i^{\rm th}$ particle at time t, and $m_{\rm b}$ is the individual mass of the bath particles. As already obtained in Eq. (2.13), the evolution of $F_{\rm d}$ is governed by the Klimontovich equation

$$\frac{\partial F_{\rm d}}{\partial t} + \big[F_{\rm d}, H_{\rm b}\big] = 0, \tag{3.31}$$

where $H_{\rm b}$ is the bath's one particle Hamiltonian, and $[\,\cdot\,,\,\cdot\,]$ as defined in Eq. (2.2).

Let us now assume that the bath's DF can be decomposed into two components, so that

$$F_{\rm d} = F_0 + \delta F \quad \text{with} \quad F_0 = F_0(\mathbf{J}, t); \quad \big\langle \delta F \big\rangle = 0. \tag{3.32}$$

In that equation, we introduced $F_0 = \big\langle F_{\rm d} \big\rangle$ as the underlying smooth mean-field DF of the bath particles and δF are the fluctuations around it, with $\langle\,\cdot\,\rangle$ the ensemble average over the bath realisations. As in Eq. (2.21), we also note that we assume that $F_0 = F_0(\mathbf{J}, t)$, i.e. the bath mean-field distribution is a quasi-stationary distribution (as it depends only on $\mathbf{J}$ and not on $\boldsymbol{\theta}$).

The main interest of the fluctuations δF is that they allow us to straightforwardly compute $\delta\Phi(\mathbf{x}, t)$, the instantaneous potential fluctuations present in the bath, i.e. the fluctuations that will source the diffusion of the test particle. Indeed, one has

$$\delta\Phi(\mathbf{x}, t) = \int \mathrm{d}\mathbf{x}' \mathrm{d}\mathbf{v}'\, U(\mathbf{x}, \mathbf{x}')\, \delta F(\mathbf{x}', \mathbf{v}', t). \tag{3.33}$$

We can then compute the Fourier transform in angles of the potential perturbations as

$$\begin{aligned} \delta\Phi_{\mathbf{k}}(\mathbf{J}, t) &= \int \frac{\mathrm{d}\boldsymbol{\theta}}{(2\pi)^d}\, \mathrm{e}^{-\mathrm{i}\mathbf{k}\cdot\boldsymbol{\theta}} \int \mathrm{d}\mathbf{x}' \mathrm{d}\mathbf{v}'\, U\big(\mathbf{x}[\boldsymbol{\theta}, \mathbf{J}], \mathbf{x}'\big)\, \delta F(\mathbf{x}', \mathbf{v}', t) \\ &= \int \frac{\mathrm{d}\boldsymbol{\theta}}{(2\pi)^d}\, \mathrm{e}^{-\mathrm{i}\mathbf{k}\cdot\boldsymbol{\theta}} \int \mathrm{d}\boldsymbol{\theta}' \mathrm{d}\mathbf{J}'\, U\big(\mathbf{x}[\boldsymbol{\theta}, \mathbf{J}], \mathbf{x}'[\boldsymbol{\theta}', \mathbf{J}']\big)\, \delta F(\mathbf{J}', \boldsymbol{\theta}'), \end{aligned} \tag{3.34}$$

where we relied on the fact that angle-action coordinates conserve phase space volume, so that $\mathrm{d}\mathbf{x}\mathrm{d}\mathbf{v} = \mathrm{d}\boldsymbol{\theta}\mathrm{d}\mathbf{J}$. All in all, this can be rewritten as

$$\delta\Phi_{\mathbf{k}}(\mathbf{J}, t) = (2\pi)^d \sum_{\mathbf{k}'} \int \mathrm{d}\mathbf{J}'\, \psi_{\mathbf{k}\mathbf{k}'}(\mathbf{J}, \mathbf{J}')\, \delta F_{\mathbf{k}'}(\mathbf{J}', t). \tag{3.35}$$

In that equation, we have expanded the pairwise interaction potential in angle-action space as

$$\begin{aligned} U(\boldsymbol{\theta},\mathbf{J},\boldsymbol{\theta}',\mathbf{J}') &= U\big(\mathbf{x}[\boldsymbol{\theta},\mathbf{J}],\mathbf{x}'[\boldsymbol{\theta}',\mathbf{J}']\big) \\ &= \sum_{\mathbf{k},\mathbf{k}'} \psi_{\mathbf{k}\mathbf{k}'}(\mathbf{J},\mathbf{J}')\,\mathrm{e}^{\mathrm{i}(\mathbf{k}\cdot\boldsymbol{\theta}-\mathbf{k}'\cdot\boldsymbol{\theta}')}, \end{aligned} \tag{3.36}$$

where we introduced

$$\psi_{\mathbf{k}\mathbf{k}'}(\mathbf{J},\mathbf{J}') = \int \frac{\mathrm{d}\boldsymbol{\theta}}{(2\pi)^d}\frac{\mathrm{d}\boldsymbol{\theta}'}{(2\pi)^d}\, U\big(\mathbf{x}[\boldsymbol{\theta},\mathbf{J}],\mathbf{x}'[\boldsymbol{\theta}',\mathbf{J}']\big)\,\mathrm{e}^{-\mathrm{i}(\mathbf{k}\cdot\boldsymbol{\theta}-\mathbf{k}'\cdot\boldsymbol{\theta}')}. \tag{3.37}$$

The Fourier coefficients, $\psi_{\mathbf{k}\mathbf{k}'}(\mathbf{J},\mathbf{J}')$, are called the bare susceptibility coefficients, and are defined as the Fourier transform in angles of the pairwise interaction potential. They are said to be bare, because they do not account for the bath self-gravitating amplification. They are called susceptibilities, because $\psi_{\mathbf{k}\mathbf{k}'}(\mathbf{J},\mathbf{J}')$, capture the strength of the coupling between the orbits $\mathbf{J}$ and $\mathbf{J}'$, when coupled through the pair of resonance vectors $(\mathbf{k},\mathbf{k}')$.

Using jointly the decoupled Hamiltonian from Eq. (3.29) with the decomposition from Eq. (3.32), we can write the evolution for δF. It reads

$$0 = \frac{\partial F_0}{\partial t} + \frac{\partial \delta F}{\partial t} + \big[F_0 + \delta F, H_0\big]. \tag{3.38}$$

As required by quasi-stationarity, we note that we have $\big[F_0(\mathbf{J}),H_0(\mathbf{J})\big]=0$. Recalling that $\langle\delta F\rangle = 0$ under ensemble-average, we find that $\partial F_0/\partial t = 0$, i.e. we recover the fact that the present bath is inert. As a consequence, the dynamics of the fluctuations, δF, in the bath is then governed by

$$\begin{aligned} 0 &= \frac{\partial \delta F}{\partial t} + \big[\delta F, H_0\big] \\ &= \frac{\partial \delta F}{\partial t} + \frac{\partial \delta F}{\partial \boldsymbol{\theta}}\cdot\boldsymbol{\Omega}(\mathbf{J}) \\ &= \frac{\partial \delta F_{\mathbf{k}}}{\partial t} + \mathrm{i}\mathbf{k}\cdot\boldsymbol{\Omega}(\mathbf{J})\,\delta F_{\mathbf{k}}(\mathbf{J},t), \end{aligned} \tag{3.39}$$

where we performed a Fourier transform w.r.t. the angles to get the last line. For a non-interacting bath, as described by the Hamiltonian from Eq. (3.29), particles are independent one from another and limit themselves to following the mean-field motion. Similarly to Fig. 2.4, such an inert bath is only undergoing the phase mixing in angles, imposed by the smooth mean potential. Similarly to $F_0 = F_0(\mathbf{J})$ that is taken to be constant, we can assume that the mean-field orbital frequencies, $\boldsymbol{\Omega} = \boldsymbol{\Omega}(\mathbf{J})$, are also time-independent on the dynamical timescale over which the perturbations in the bath evolve. Equation (3.39) is then straightforward to integrate in time, and one gets

$$\delta F_{\mathbf{k}}(\mathbf{J},t) = \delta F_{\mathbf{k}}(\mathbf{J},0)\,\mathrm{e}^{-\mathrm{i}\mathbf{k}\cdot\boldsymbol{\Omega}(\mathbf{J})t}, \tag{3.40}$$

where $\delta F_{\mathbf{k}}(\mathbf{J},0)$ stands to the initial fluctuations in the bath's DF at $t=0$. Having characterised the dynamics of $\delta F_{\mathbf{k}}(\mathbf{J},t)$, we can now inject it into Eq. (3.35) to explicitly determine the potential fluctuations generated by the present bath. We get

$$\boxed{\delta\Phi_{\mathbf{k}}(\mathbf{J},t) = (2\pi)^d \sum_{\mathbf{k}'}\int \mathrm{d}\mathbf{J}'\,\psi_{\mathbf{k}\mathbf{k}'}(\mathbf{J},\mathbf{J}')\,\mathrm{e}^{-\mathrm{i}\mathbf{k}'\cdot\boldsymbol{\Omega}(\mathbf{J}')t}\,\delta F_{\mathbf{k}'}(\mathbf{J}',0).} \tag{3.41}$$

In order to compute the diffusion coefficients from Eq. (3.28), we must then compute the correlation function of these potential fluctuations. Following the definition from Eq. (3.10), we can write

$$\begin{aligned} C_{\mathbf{k}\mathbf{k}}(\mathbf{J},\mathbf{J},t-t') = (2\pi)^{2d} \sum_{\mathbf{k}',\mathbf{k}''}\int \mathrm{d}\mathbf{J}'\mathrm{d}\mathbf{J}''\,\psi_{\mathbf{k}\mathbf{k}'}(\mathbf{J},\mathbf{J}')\,\psi^*_{\mathbf{k}\mathbf{k}''}(\mathbf{J},\mathbf{J}'')\,\mathrm{e}^{-\mathrm{i}\mathbf{k}'\cdot\boldsymbol{\Omega}(\mathbf{J}')t}\,\mathrm{e}^{\mathrm{i}\mathbf{k}''\cdot\boldsymbol{\Omega}(\mathbf{J}'')t'} \\ \times\big\langle\delta F_{\mathbf{k}'}(\mathbf{J}',0)\,\delta F^*_{\mathbf{k}''}(\mathbf{J}'',0)\big\rangle. \end{aligned} \tag{3.42}$$

3.2 The initial fluctuations in the bath's DF

We must now characterise the properties of the initial fluctuations in the bath's DF, as required by the remaining ensemble-averaged term in Eq. (3.42). Luckily, these are easy to characterise since they correspond to the statistics of the Poisson fluctuations in the bath at the initial time, where the bath is initially uncorrelated. As introduced in Eq. (3.32), the bath's instantaneous fluctuations are given by $\delta F = F_{\mathrm{d}} - F_0$, where F_{d} is the bath's

discrete DF as introduced in Eq. (3.30), and F_0 is the bath's smooth ensemble-averaged mean DF. To shorten the notations, we temporarily drop the time dependence $t = 0$, and write

$$\big\langle \delta F(\boldsymbol{\theta},\mathbf{J})\,\delta F(\boldsymbol{\theta}',\mathbf{J}')\big\rangle = m_{\rm b}^2 \sum_{i,j=1}^{N} \big\langle \delta_{\rm D}(\boldsymbol{\theta}-\boldsymbol{\theta}_i)\,\delta_{\rm D}(\mathbf{J}-\mathbf{J}_i)\,\delta_{\rm D}(\boldsymbol{\theta}'-\boldsymbol{\theta}_j)\,\delta_{\rm D}(\mathbf{J}'-\mathbf{J}_j)\big\rangle - F_0(\mathbf{J})\,F_0(\mathbf{J}'), \tag{3.43}$$

where we relied on the fact that the fluctuations are of zero average, i.e. $\langle \delta F\rangle = 0$. In the double sum from Eq. (3.43), there are two types of terms depending on whether $i = j$ or $i \neq j$. Dealing separately with these two components, the ensemble-averaged from Eq. (3.43) can then be written as

$$\begin{aligned} m_{\rm b}^2 \sum_{i,j=1}^{N} \big\langle \delta_{\rm D}(\boldsymbol{\theta}-\boldsymbol{\theta}_i)\,\delta_{\rm D}(\mathbf{J}-\mathbf{J}_i)\,\delta_{\rm D}(\boldsymbol{\theta}'-\boldsymbol{\theta}_j)\,\delta_{\rm D}(\mathbf{J}'-\mathbf{J}_j)\big\rangle &= m_{\rm b}^2\,\delta_{\rm D}(\boldsymbol{\theta}'-\boldsymbol{\theta}')\,\delta_{\rm D}(\mathbf{J}'-\mathbf{J}')\sum_{i=1}^{N}\big\langle \delta_{\rm D}(\boldsymbol{\theta}-\boldsymbol{\theta}_i)\,\delta_{\rm D}(\mathbf{J}-\mathbf{J}_i)\big\rangle \\ &\quad + m_{\rm b}^2\sum_{i\neq j}^{N}\big\langle \delta_{\rm D}(\boldsymbol{\theta}-\boldsymbol{\theta}_i)\,\delta_{\rm D}(\mathbf{J}-\mathbf{J}_i)\big\rangle\,\big\langle \delta_{\rm D}(\boldsymbol{\theta}'-\boldsymbol{\theta}_j)\,\delta_{\rm D}(\mathbf{J}'-\mathbf{J}_j)\big\rangle, \end{aligned} \tag{3.44}$$

where we assumed that the particles are uncorrelated one from another at the initial time. From the relation $\langle F_{\rm d}\rangle = F_0$ and the definition from Eq. (3.30), we get

$$\big\langle \delta_{\rm D}(\boldsymbol{\theta}-\boldsymbol{\theta}_i)\,\delta_{\rm D}(\mathbf{J}-\mathbf{J}_i)\big\rangle = \frac{1}{N m_{\rm b}}\,F_0(\mathbf{J}). \tag{3.45}$$

As a consequence, Eq. (3.44) becomes

$$m_{\rm b}^2 \sum_{i,j=1}^{N} \big\langle \delta_{\rm D}(\boldsymbol{\theta}-\boldsymbol{\theta}_i)\,\delta_{\rm D}(\mathbf{J}-\mathbf{J}_i)\,\delta_{\rm D}(\boldsymbol{\theta}'-\boldsymbol{\theta}_j)\,\delta_{\rm D}(\mathbf{J}'-\mathbf{J}_j)\big\rangle = m_{\rm b}\,F_0(\mathbf{J})\,\delta_{\rm D}(\boldsymbol{\theta}-\boldsymbol{\theta}')\,\delta_{\rm D}(\mathbf{J}-\mathbf{J}') + \frac{N(N-1)}{N^2}\,F_0(\mathbf{J})\,F_0(\mathbf{J}'). \tag{3.46}$$

All in all, this allows us to rewrite Eq. (3.43) as

$$\big\langle \delta F(\boldsymbol{\theta},\mathbf{J})\,\delta F(\boldsymbol{\theta}',\mathbf{J}')\big\rangle = m_{\rm b}\,F_0(\mathbf{J})\,\delta_{\rm D}(\mathbf{J}-\mathbf{J}')\,\delta_{\rm D}(\boldsymbol{\theta}-\boldsymbol{\theta}') - \frac{1}{N}\,F_0(\mathbf{J})\,F_0(\mathbf{J}'). \tag{3.47}$$

As required by Eq. (3.42), we can take the Fourier transform of that relation w.r.t. $(\boldsymbol{\theta},\boldsymbol{\theta}')$ to get

$$\big\langle \delta F_{\mathbf{k}}(\mathbf{J},0)\,\delta F^*_{\mathbf{k}'}(\mathbf{J}',0)\big\rangle = \frac{m_{\rm b}}{(2\pi)^d}\,\delta_{\mathbf{k}\mathbf{k}'}\,\delta_{\rm D}(\mathbf{J}-\mathbf{J}')\,F_0(\mathbf{J}) - \frac{1}{N}\,\delta_{\mathbf{k}\mathbf{0}}\,\delta_{\mathbf{k}'\mathbf{0}}\,F_0(\mathbf{J})\,F_0(\mathbf{J}'), \tag{3.48}$$

where we used the fact that δF is real. As can already be noted in Eq. (3.28), the harmonics $(\mathbf{k},\mathbf{k}') = (\mathbf{0},\mathbf{0})$ never contributes to the secular diffusion, so that we might already forget about the last term from Eq. (3.48). As a summary, assuming that the N particles from the bath are initially drawn independently one from another according to the smooth DF, $F_0(\mathbf{J})$, then the statistics of the initial fluctuations in the system are, as expected, governed by Poisson shot noise, and read

$$\boxed{\big\langle \delta F_{\mathbf{k}}(\mathbf{J},0)\,\delta F^*_{\mathbf{k}'}(\mathbf{J}',0)\big\rangle = \frac{m_{\rm b}}{(2\pi)^d}\,\delta_{\mathbf{k}\mathbf{k}'}\,\delta_{\rm D}(\mathbf{J}-\mathbf{J}')\,F_0(\mathbf{J}).} \tag{3.49}$$

We can now use this explicit expression in Eq. (3.42) to compute the correlation of the potential fluctuations generated by the bath. It reads

$$C_{\mathbf{k}\mathbf{k}}(\mathbf{J},\mathbf{J},t-t') = m_{\rm b}\,(2\pi)^d \sum_{\mathbf{k}'}\!\!\int \mathrm{d}\mathbf{J}'\,\big|\psi_{\mathbf{k}\mathbf{k}'}(\mathbf{J},\mathbf{J}')\big|^2\,F_0(\mathbf{J}')\,\mathrm{e}^{-\mathrm{i}\mathbf{k}'\cdot\boldsymbol{\Omega}(\mathbf{J}')(t-t')}. \tag{3.50}$$

Following Eq. (3.28), we may now compute the diffusion coefficients for the test particle, and one has

$$\boxed{\mathbf{D}_2(\mathbf{J}) = m_{\rm b}\pi(2\pi)^d \sum_{\mathbf{k},\mathbf{k}'} \mathbf{k}\otimes\mathbf{k}\!\int \mathrm{d}\mathbf{J}'\,\delta_{\rm D}(\mathbf{k}\cdot\boldsymbol{\Omega}(\mathbf{J}) - \mathbf{k}'\cdot\boldsymbol{\Omega}(\mathbf{J}'))\,\big|\psi_{\mathbf{k}\mathbf{k}'}(\mathbf{J},\mathbf{J}',\mathbf{k}\cdot\boldsymbol{\Omega}(\mathbf{J}))\big|^2\,F_0(\mathbf{J}'),} \tag{3.51}$$

where we used the relation $\int_{-\infty}^{+\infty}\mathrm{d}t\,\mathrm{e}^{\mathrm{i}\omega t} = 2\pi\delta_{\rm D}(\omega)$. Equation (3.51) is the important result of this section, and gives the so-called inhomogeneous Landau diffusion tensor. This diffusion tensor is said to be inhomogeneous, because the diffusion is described in orbital space, and it is said to be Landau, because collective effects were

not accounted for, i.e. the background bath was inert and immune to perturbations. These diffusion coefficients describe, via Eq. (3.25), the long-term orbital diffusion undergone by a test particle embedded in an inhomogeneous external background bath of N independent particles, orbiting in a smooth mean potential.

Qualitatively, the diffusion coefficients from Eq. (3.51) should be understood as follows. First, the diffusion of the test particle is sourced by the potential fluctuations from the background bath particles, as highlighted by the $m_{\rm b} = M_{\rm tot}/N$ prefactor: the larger the number of bath particles, the smoother the bath potential, and therefore the slower the diffusion. To diffuse away from its orbit $\mathbf{J}$, the test particle has to resonantly couple with the bath fluctuations. As such, the integration over $\mathrm{d}\mathbf{J}'$ should be interpreted as a scan of action space, looking for bath particles' orbits such that the resonance condition $\delta_{\rm D}(\mathbf{k}\cdot\boldsymbol{\Omega}(\mathbf{J}) - \mathbf{k}'\cdot\boldsymbol{\Omega}(\mathbf{J}'))$ is satisfied. This resonance condition is a direct consequence of the general result from Eq. (3.28), where we showed that the diffusion coefficients ask for the evaluation of the noise correlation function at the test particle's orbital frequency, $\omega = \mathbf{k}\cdot\boldsymbol{\Omega}(\mathbf{J})$, for a noise created by bath particles evolving with their own orbital frequencies, $\omega = \mathbf{k}'\cdot\boldsymbol{\Omega}(\mathbf{J}')$. We also note that each resonant coupling is parametrised by a pair of resonance vectors $(\mathbf{k},\mathbf{k}')$, which determines which linear combination of orbital frequencies is matched on resonance. As can be also seen from the factor $\mathbf{k}\otimes\mathbf{k}$ in Eq. (3.51), the resonance vector $\mathbf{k}$ also controls the direction in which the diffusion occurs in action space. Finally, we note that in the present regime where collective effects were neglected, the strength of the resonant coupling between the test particle and the background bath fluctuations is controlled by the squared bare susceptibility coefficients, $|\psi_{\mathbf{k}\mathbf{k}'}(\mathbf{J},\mathbf{J}')|^2$. As defined in Eq. (3.37), these coefficients are given by the Fourier transform in angle of the pairwise interaction potential. In essence, they describe how efficiently the orbits $\mathbf{J}$ and $\mathbf{J}'$ interact one with another.

3.3 The Balescu-Lenard diffusion coefficients

In the previous section, when computing the diffusion coefficients sourced by the background bath, we neglected collective effects, i.e. we assumed in Eq. (3.29) that the dynamics of the bath particles was only governed by the smooth mean-field potential. Of course, in practice, bath particles are not decoupled one from another, and are therefore constantly submitted to the stochastic perturbations, $\delta\Phi(\mathbf{x},t)$, that they jointly self-generate themselves. Let us now account for this contribution, by assuming that the bath is live and self-gravitating, so that the bath particles' dynamics also encompass their own self-generated perturbations. In such a regime, the specific Hamiltonian for the bath particles from Eq. (3.29) becomes

$$H_{\rm b}(\boldsymbol{\theta},\mathbf{J},t) = H_0(\mathbf{J}) + \delta\Phi\big(\mathbf{x}[\boldsymbol{\theta},\mathbf{J}],t\big), \tag{3.52}$$

where the noise $\delta\Phi(\mathbf{x},t) = \delta\Phi[\delta F]$ was already defined in Eq. (3.33) as being induced by the perturbations in the bath's DF. In order to characterise the diffusion that can be generated by such a self-gravitating background bath, we must characterise the correlation function of these potential fluctuations. This is what we now set out to do.

As previously, we start from the same decomposition of the background bath's DF as in Eq. (3.32). Similarly, the time evolution of the discrete DF, $F_{\rm d}$, is governed by the Klimontovich Eq. (2.13) that reads here

$$0 = \frac{\partial F_0}{\partial t} + \frac{\partial \delta F}{\partial t} + \big[F_0 + \delta F, H_0 + \delta\Phi[\delta F]\big], \tag{3.53}$$

where the important addition is the potential fluctuations $\delta\Phi$. We recall that $\big[F_0(\mathbf{J}), H_0(\mathbf{J})\big] = 0$, as imposed by quasi-stationarity. Assuming that under ensemble-average one has $\langle\delta F\rangle = 0$, and therefore $\langle\delta\Phi\rangle = 0$, we find that

$$\frac{\partial F_0}{\partial t} + \big\langle\big[\delta F, \delta\Phi\big]\big\rangle = 0, \tag{3.54}$$

so that the variation of the bath mean DF is second-order in the perturbations, i.e. it only takes place on secular times. Here, our goal is to characterise the dynamics of the bath's fluctuations, δF and $\delta\Phi$, that happen on the (fast) dynamical timescale. As a consequence, we will solve for this dynamics at first order in the perturbations, i.e. by keeping only terms linear in the perturbations in Eq. (3.53). Following this linear truncation, the dynamics in the fluctuations of the bath's DF is described by the linearised Klimontovich equation, that reads

$$\begin{aligned} 0 &= \frac{\partial \delta F}{\partial t} + \big[\delta F, H_0\big] + \big[F_0, \delta\Phi\big], \\ &= \frac{\partial \delta F_{\mathbf{k}}}{\partial t} + \mathrm{i}\mathbf{k}\cdot\boldsymbol{\Omega}(\mathbf{J})\,\delta F_{\mathbf{k}}(\mathbf{J},t) - \mathrm{i}\mathbf{k}\cdot\frac{\partial F_0}{\partial \mathbf{J}}\,\delta\Phi_{\mathbf{k}}(\mathbf{J},t), \end{aligned} \tag{3.55}$$

where to get the last line, we performed a Fourier transform w.r.t. the angles. Compared to the bare evolution equation obtained in Eq. (3.39), here we have to face a new difficulty, which is the fact that $\delta F_{\mathbf{k}}$ and $\delta\Phi_{\mathbf{k}}$ are directly connected one to another, as they satisfy the self-consistency requirement from Eq. (3.35). This is

exactly what we call collective effects, i.e. the fact that the dynamics of the perturbations happens in the same fluctuating potential that they create themselves.

In order to solve Eq. (3.55), we will rely on the assumption of timescale separation (Bogoliubov's ansatz). Namely, we assume that the bath's mean-field properties, $F_0(\mathbf{J})$ and $\Omega(\mathbf{J})$, can be taken to be constant on the dynamical timescales over which the amplification of the perturbations happens. As already noted in Eq. (3.54), this is a legitimate assumption as the dynamics of the bath's mean-field DF is second-order in the perturbations. As in all linear amplification mechanisms, it is a good idea to move to solve Eq. (3.55) in Laplace domain. It becomes

$$\delta\widetilde{F}_{\mathbf{k}}(\mathbf{J},\omega) = -\frac{\mathbf{k}\cdot\partial F_0/\partial\mathbf{J}}{\omega-\mathbf{k}\cdot\boldsymbol{\Omega}(\mathbf{J})}\,\delta\widetilde{\Phi}_{\mathbf{k}}(\mathbf{J},\omega) - \frac{\delta F_{\mathbf{k}}(\mathbf{J},0)}{\mathrm{i}(\omega-\mathbf{k}\cdot\boldsymbol{\Omega}(\mathbf{J}))}. \tag{3.56}$$

In Eq. (3.56), we defined the Laplace transform with the convention

$$\widetilde{f}(\omega) = \int_0^{+\infty} \mathrm{d}t\, f(t)\,\mathrm{e}^{\mathrm{i}\omega t} \quad ; \quad f(t) = \frac{1}{2\pi}\int_{\mathcal{B}} \mathrm{d}\omega\, \widetilde{f}(\omega)\,\mathrm{e}^{-\mathrm{i}\omega t}, \tag{3.57}$$

where the Bromwich contour $\mathcal{B}$ has to pass above all the poles of the integrand, i.e. $\mathrm{Im}(\omega)$ has to be large enough.

From Eq. (3.35), we can rewrite the self-consistency between δF and $\delta\Phi$ as

$$\delta\widetilde{\Phi}_{\mathbf{k}}(\mathbf{J},\omega) = (2\pi)^d \sum_{\mathbf{k}'}\int \mathrm{d}\mathbf{J}'\,\psi_{\mathbf{k}\mathbf{k}'}(\mathbf{J},\mathbf{J}')\,\delta\widetilde{F}_{\mathbf{k}'}(\mathbf{J}',\omega). \tag{3.58}$$

As a resut, in order to rewrite Eq. (3.56) only in terms of $\delta\widetilde{\Phi}_{\mathbf{k}}(\mathbf{J},\omega)$, we act on both sides of that equation with the same operator as appearing in Eq. (3.58). This gives

$$\delta\widetilde{\Phi}_{\mathbf{k}}(\mathbf{J},\omega) = -(2\pi)^d \sum_{\mathbf{k}'}\int \mathrm{d}\mathbf{J}'\,\frac{\mathbf{k}'\cdot\partial F_0/\partial\mathbf{J}'}{\omega-\mathbf{k}'\cdot\boldsymbol{\Omega}(\mathbf{J}')}\,\psi_{\mathbf{k}\mathbf{k}'}(\mathbf{J},\mathbf{J}')\,\delta\widetilde{\Phi}_{\mathbf{k}'}(\mathbf{J}',\omega) - (2\pi)^d \sum_{\mathbf{k}'}\int \mathrm{d}\mathbf{J}'\,\frac{\delta F_{\mathbf{k}'}(\mathbf{J}',0)}{\mathrm{i}(\omega-\mathbf{k}'\cdot\boldsymbol{\Omega}(\mathbf{J}'))}\,\psi_{\mathbf{k}\mathbf{k}'}(\mathbf{J},\mathbf{J}'). \tag{3.59}$$

Equation (3.59) is a complex self-consistent equation for $\delta\widetilde{\Phi}_{\mathbf{k}}(\mathbf{J},\omega)$, taking the form of a Fredholm equation with a source term.

Let us now rely on analogies with the bare case considered previously to simplify that self-consistent relation. In the absence of any collective effects, the bare solution from Eq. (3.41) reads in Laplace space

$$\big[\delta\widetilde{\Phi}_{\mathbf{k}}(\mathbf{J},\omega)\big]_{\mathrm{bare}} = -(2\pi)^d \sum_{\mathbf{k}'}\int \mathrm{d}\mathbf{J}'\,\frac{\delta F_{\mathbf{k}'}(\mathbf{J}',0)}{\mathrm{i}(\omega-\mathbf{k}'\cdot\boldsymbol{\Omega}(\mathbf{J}'))}\,\psi_{\mathbf{k}\mathbf{k}}(\mathbf{J},\mathbf{J}'). \tag{3.60}$$

Such an expression can also be recovered from Eq. (3.59), by neglecting therein the term involving $\partial F_0/\partial\mathbf{J}$. In the present dressed case, let us therefore assume that the dressed potential perturbations follow the ansatz

$$\big[\delta\widetilde{\Phi}_{\mathbf{k}}(\mathbf{J},\omega)\big]_{\mathrm{dressed}} = -(2\pi)^d \sum_{\mathbf{k}'}\int \mathrm{d}\mathbf{J}'\,\frac{\delta F_{\mathbf{k}'}(\mathbf{J}',0)}{\mathrm{i}(\omega-\mathbf{k}'\cdot\boldsymbol{\Omega}(\mathbf{J}'))}\,\psi^{\mathrm{d}}_{\mathbf{k}\mathbf{k}'}(\mathbf{J},\mathbf{J}',\omega), \tag{3.61}$$

where we introduced the (yet unknown) dressed susceptibility coefficients $\psi^{\mathrm{d}}_{\mathbf{k}\mathbf{k}'}(\mathbf{J},\mathbf{J}',\omega)$. Injecting the ansatz from Eq. (3.61) into Eq. (3.59), we immediately get the self-consistent relation satisfied by the dressed susceptibility coefficients, that reads

$$\psi^{\mathrm{d}}_{\mathbf{k}\mathbf{k}'}(\mathbf{J},\mathbf{J}',\omega) = -(2\pi)^d \sum_{\mathbf{k}''}\int \mathrm{d}\mathbf{J}''\,\frac{\mathbf{k}''\cdot\partial F_0/\partial\mathbf{J}''}{\omega-\mathbf{k}''\cdot\boldsymbol{\Omega}(\mathbf{J}'')}\,\psi_{\mathbf{k}\mathbf{k}''}(\mathbf{J},\mathbf{J}'')\,\psi^{\mathrm{d}}_{\mathbf{k}''\mathbf{k}'}(\mathbf{J}'',\mathbf{J},\omega) + \psi_{\mathbf{k}\mathbf{k}'}(\mathbf{J},\mathbf{J}'). \tag{3.62}$$

Equation (3.62) gives us a self-consistent integral relation defining the dressed susceptibility coefficients $\psi^{\mathrm{d}}_{\mathbf{k}\mathbf{k}'}(\mathbf{J},\mathbf{J}',\omega)$ as a function of the bare ones $\psi_{\mathbf{k}\mathbf{k}'}(\mathbf{J},\mathbf{J}')$. We note that the integral term from Eq. (3.62) only involves the mean-field properties from the bath, namely its smooth mean DF, $F_0(\mathbf{J})$, as well as the underlying orbital frequencies, $\boldsymbol{\Omega}(\mathbf{J})$. As such, it captures the efficiency with which the underlying collisionless system can amplify perturbations through self-gravity.

3.4 The basis method

While physically enlightening, Eq. (3.62) does not provide us with an explicit expression for the dressed susceptibility coefficients, $\psi^{\mathrm{d}}_{\mathbf{k}\mathbf{k}'}(\mathbf{J},\mathbf{J}',\omega)$. This difficulty arises here because of our need to account for inhomogeneity. Indeed, while the bath's mean potential is only a function $\mathbf{x}$, when it is expressed in angle-action coordinates, it depends on both $\boldsymbol{\theta}$ and $\mathbf{J}$. Phrased differently, while angle-action coordinates make the mean-field dynamics trivial (it simply reads $\boldsymbol{\theta}(t)=\boldsymbol{\theta}_0+\boldsymbol{\Omega}(\mathbf{J})t$ and $\mathbf{J}(t)=\mathrm{cst.}$), it makes the resolution of Poisson's

equation significantly more complicated. A traditional method to circumvent this issue is to rely on the matrix method (Kalnajs, 1976), and introduce a biorthogonal set of density and potential basis elements, on which the pairwise interaction can be decomposed.

To avoid this difficulty, we assume that we have at our disposal a complete biorthogonal set of basis elements, $(\psi^{(p)}(\mathbf{x}), \rho^{(p)}(\mathbf{x}))$ satisfying

$$\begin{cases} \psi^{(p)}(\mathbf{x}) = \displaystyle\int \mathrm{d}\mathbf{x}'\, U(\mathbf{x},\mathbf{x}')\, \rho^{(p)}(\mathbf{x}'), \\ \displaystyle\int \mathrm{d}\mathbf{x}\, \psi^{(p)*}(\mathbf{x})\, \rho^{(q)}(\mathbf{x}) = -\delta_{pq}, \end{cases} \tag{3.63}$$

where the first relation can be rewritten as Poisson's equation, $\Delta\psi^{(p)} = 4\pi G\rho^{(p)}$ for the $3D$gravitational interaction, $U(\mathbf{x},\mathbf{x}') = -G/|\mathbf{x}-\mathbf{x}'|$. By doing so, we can straightforwardly translate any decomposition of the potential fluctuations into the associated density so that

$$\delta\Phi(\mathbf{x},t) = \sum_p A_p(t)\, \psi^{(p)}(\mathbf{x}) \implies \delta\rho(\mathbf{x},t) = \sum_p A_p(t)\, \rho^{(p)}(\mathbf{x}) \text{ with } A_p(t) = -\int \mathrm{d}\mathbf{x}\, \delta\Phi(\mathbf{x},t)\, \rho^{(p)*}(\mathbf{x}). \tag{3.64}$$

There are many gains with such a basis expansion. First, Poisson's equation has been solved once and for all in Eq. (3.63) to construct the basis elements. It does not need anymore to be solved when going from densities to potentials or vice-versa. Second, one can note in the expansion of Eq. (3.64) that the spatial and temporal dependences of the potential fluctuations have been separated one from another. Indeed, the spatial part is captured by the basis elements, $\psi^{(p)}(\mathbf{x})$, while their temporal dependences are given by the coefficients $A_p(t)$.

In order to illustrate how this expansion can be used, let us first expand the pairwise interaction potential $U(\mathbf{x},\mathbf{x}')$ on these basis elements. For a fixed value of $\mathbf{x}'$, we can expand the function $\mathbf{x} \mapsto U(\mathbf{x},\mathbf{x}')$ under the form

$$U(\mathbf{x},\mathbf{x}') = \sum_p u_p(\mathbf{x}')\, \psi^{(p)}(\mathbf{x}), \tag{3.65}$$

where the coefficient $u_p(\mathbf{x}')$ follows from Eq. (3.64) and reads

$$\begin{aligned} u_p(\mathbf{x}') &= -\int \mathrm{d}\mathbf{x}\, U(\mathbf{x},\mathbf{x}')\, \rho^{(p)*}(\mathbf{x}) \\ &= -\psi^{(p)*}(\mathbf{x}'), \end{aligned} \tag{3.66}$$

where we used the fact that the interaction potential, $U(\mathbf{x},\mathbf{x}')$, is real, and we relied on the definition of the potential basis elements from Eq. (3.63). As a result, following Eq. (3.65), when expressed on the basis elements, the pairwise interaction potential reads

$$U(\mathbf{x},\mathbf{x}') = -\sum_p \psi^{(p)}(\mathbf{x})\, \psi^{(p)*}(\mathbf{x}'). \tag{3.67}$$

Finally, we can use this expression to obtain the expression of the bare susceptibilty coefficients, $\psi_{\mathbf{k}\mathbf{k}'}(\mathbf{J},\mathbf{J}')$, as defined in Eq. (3.37) as the Fourier transform in angles of the pairwise interaction potential. We immediately get

$$\boxed{\psi_{\mathbf{k}\mathbf{k}'}(\mathbf{J},\mathbf{J}') = -\sum_p \psi^{(p)}_{\mathbf{k}}(\mathbf{J})\, \psi^{(p)*}_{\mathbf{k}'}(\mathbf{J}'),} \tag{3.68}$$

where $\psi^{(p)}_{\mathbf{k}}(\mathbf{J})$ stands for the Fourier transformed basis elements naturally defined as

$$\psi^{(p)}_{\mathbf{k}}(\mathbf{J}) = \int \frac{\mathrm{d}\boldsymbol{\theta}}{(2\pi)^d}\, \psi^{(p)}\big(\mathbf{x}[\boldsymbol{\theta},\mathbf{J}]\big)\, \mathrm{e}^{-\mathrm{i}\mathbf{k}\cdot\boldsymbol{\theta}}. \tag{3.69}$$

Having obtained such a decomposition of the bare susceptibility coefficients, $\psi_{\mathbf{k}\mathbf{k}'}(\mathbf{J},\mathbf{J}')$, we can now return to the implicit definition of the dressed susceptibility coefficients, $\psi^{\mathrm{d}}_{\mathbf{k}\mathbf{k}'}(\mathbf{J},\mathbf{J}',\omega)$, from Eq. (3.62).

By analogy with Eq. (3.68), let us assume that the dressed susceptibility coefficients can be expanded under the form

$$\psi^{\mathrm{d}}_{\mathbf{k}\mathbf{k}'}(\mathbf{J},\mathbf{J}',\omega) = -\sum_{p,q} \psi^{(p)}_{\mathbf{k}}(\mathbf{J})\, \widetilde{\mathbf{E}}^{-1}_{pq}(\omega)\, \psi^{(q)*}_{\mathbf{k}'}(\mathbf{J}'), \tag{3.70}$$

where $\widetilde{\mathbf{E}}_{pq}(\omega)$ is a (yet unknown) dielectric matrix.

We may now inject this decomposition into the self-consistent relation from Eq. (3.62), and we obtain

$$\sum_{p,q} \psi^{(p)}_{\mathbf{k}}(\mathbf{J})\, \widetilde{\mathbf{E}}^{-1}_{pq}(\omega)\, \psi^{(q)*}_{\mathbf{k}'}(\mathbf{J}') = \sum_{p,q} \psi^{(p)}_{\mathbf{k}}(\mathbf{J})\, \big[\widetilde{\mathbf{M}}(\omega)\, \widetilde{\mathbf{E}}^{-1}(\omega)\big]_{pq}\, \psi^{(q)*}_{\mathbf{k}'}(\mathbf{J}') + \sum_{p,q} \psi^{(p)}_{\mathbf{k}}(\mathbf{J})\, \mathbf{I}_{pq}\, \psi^{(q)*}_{\mathbf{k}'}(\mathbf{J}'), \tag{3.71}$$

where we introduced the identity matrix $\mathbf{I}_{pq}$, as well as the system's response matrix $\widetilde{\mathbf{M}}(\omega)$ as

$$\boxed{\widetilde{\mathbf{M}}_{pq}(\omega) = (2\pi)^d \sum_{\mathbf{k}} \!\!\!\!\!\!\int \mathrm{d}\mathbf{J}\, \frac{\mathbf{k}\cdot\partial F_0/\partial\mathbf{J}}{\omega - \mathbf{k}\cdot\boldsymbol{\Omega}(\mathbf{J})}\, \psi^{(p)*}_{\mathbf{k}}(\mathbf{J})\, \psi^{(q)}_{\mathbf{k}}(\mathbf{J}).} \tag{3.72}$$

Since the basis is biorthogonal, we can identify the elements in Eq. (3.71), and we obtain the matrix relation

$$\widetilde{\mathbf{E}}^{-1}(\omega) = \widetilde{\mathbf{M}}(\omega)\, \widetilde{\mathbf{E}}^{-1}(\omega) + \mathbf{I}, \tag{3.73}$$

which immediately gives us the expression of the dielectric matrix, $\widetilde{\mathbf{E}}(\omega)$, as

$$\widetilde{\mathbf{E}}(\omega) = \mathbf{I} - \widetilde{\mathbf{M}}(\omega). \tag{3.74}$$

As a conclusion, glancing back at Eq. (3.70), the dressed susceptibility coefficients are given by

$$\boxed{\psi^{\mathrm{d}}_{\mathbf{k}\mathbf{k}'}(\mathbf{J},\mathbf{J}',\omega) = -\sum_{p,q} \psi^{(p)}_{\mathbf{k}}(\mathbf{J})\, \widetilde{\mathbf{E}}^{-1}_{pq}\, \psi^{(q)*}_{\mathbf{k}'}(\mathbf{J}').} \tag{3.75}$$

The analogy between the bare susceptibility coefficients, from Eq. (3.68), and the dressed ones, from Eq. (3.75) is striking. In that phrasing, accounting for collective effects amounts to replacing the identity matrix, $\mathbf{I}$, by the dielectric matrix, $\widetilde{\mathbf{E}}^{-1}(\omega) = [\mathbf{I} - \widetilde{\mathbf{M}}(\omega)]^{-1}$. We also note from Eq. (3.72) that for baths such that $\partial F_0/\partial\mathbf{J} = 0$, one has $\psi^{\mathrm{d}}_{\mathbf{k}\mathbf{k}'}(\mathbf{J},\mathbf{J}',\omega) = \psi_{\mathbf{k}\mathbf{k}'}(\mathbf{J},\mathbf{J}')$. The bath is unable to support any self-gravitating amplification, and collective effects can be neglected.

Equation (3.72) highlights again the importance of accouting for all the key specificities of self-gravitating systems, namely: (i) the dynamics is described in action space, $\mathbf{J}$, i.e. galaxies are *inhomogeneous*; (ii) it involves the system's mean-field DF, $F_0(\mathbf{J},t)$, i.e. galaxies are *relaxed* and are dynamically frozen on quasi-stationary states; (iii) the response matrix describes the system's linear response. i.e. galaxies are *self-gravitating*; (iv) this response matrix involves a sum over resonance vectors, $\sum_{\mathbf{k}}$, as well as a resonant denominator, $1/(\omega - \mathbf{k}\cdot\boldsymbol{\Omega}(\mathbf{J}))$, i.e. galaxies are *resonant* and support a non-trivial orbital structure; (v) finally, the response matrix describes how perturbations get dressed by self-gravity, i.e. galaxies are *perturbed*.

Let us also highlight the deep connexions existing between the present (inhomogeneous) response matrix, $\widetilde{\mathbf{M}}(\omega)$, and the dielectric function for (homogeneous) electrostatic plasmas. In the self-gravitating case, one has to deal with a few more difficulties, namely: (i) in plasmas, since the mean potential vanishes, $\mathbf{v}$ is an appropriate coordinate to describe the particles' mean-field orbital motion, while here, we needed to introduce the action coordinates $\mathbf{J}$ to describe the orbits; (ii) in plasmas, Poisson's equation is directly solved in Fourier space, by simply dividing by $1/|\mathbf{k}|^2$, while here we needed to introduce the basis elements to generically solve Poisson's equation in Eq. (3.67), as in the inhomogeneous case one has $\Phi(\mathbf{x}) = \Phi(\boldsymbol{\theta},\mathbf{J})$, i.e. this is the price to pay for the use of angle-action coordinates; (iii) in plasmas, the resonant denominator was of the form $1/(\omega - \mathbf{k}\cdot\mathbf{v})$ integrated over $\mathbf{v}$, while here it involves the resonant denominator $1/(\omega - \mathbf{k}\cdot\boldsymbol{\Omega}(\mathbf{J}))$ integrated over $\mathbf{J}$.

The response matrix, $\widetilde{\mathbf{M}}(\omega)$, from Eq. (3.72) is an essential quantity to characterise the efficiency with which the self-gravitating bath can amplify perturbations, as illustrated in Fig. 3.1. More precisely, if we were to introduce some external potential perturbations $\delta\Phi_{\mathrm{ext}}$, then the bath's instantaneous self-generated response, $\delta\Phi_{\mathrm{self}}$, would be given by the joint amplification of the external perturbation and the system's self-generated response, so that $\delta\widetilde{\Phi}_{\mathrm{self}}(\omega) \propto \widetilde{\mathbf{M}}(\omega)\cdot\big[\delta\widetilde{\Phi}_{\mathrm{self}}(\omega) + \delta\widetilde{\Phi}_{\mathrm{ext}}(\omega)\big]$. Owing to this loop of amplification, any external perturbation is said to be dressed by collective effects, as the total perturbation in the bath is given by $\big[\delta\widetilde{\Phi}_{\mathrm{self}}(\omega) + \delta\widetilde{\Phi}_{\mathrm{ext}}(\omega)\big] \propto \widetilde{\mathbf{E}}^{-1}(\omega)\cdot\delta\widetilde{\Phi}_{\mathrm{ext}}(\omega)$. As such, the matrix $\widetilde{\mathbf{E}}^{-1}(\omega) = \big[\mathbf{I} - \widetilde{\mathbf{M}}(\omega)\big]^{-1}$ plays the role of a susceptibility, that quantifies the efficiency with which perturbations are boosted. A system is then linearly unstable if there exists a complex frequency $\omega = \omega_0 + \mathrm{i}s$, with $s > 0$, such that $\widetilde{\mathbf{M}}(\omega)$ has an eigenvalue equal to 1, i.e. if there exists a frequency for which the self-gravitating dressing gets infinitely large. Similarly, a self-gravitating system will be linearly stable if there exists no such eigenmodes. From now on, we will assume that the background bath is linearly stable, so that the dielectric matrix $\widetilde{\mathbf{E}}^{-1}(\omega)$, and therefore the dressed susceptibility coefficients, $\psi^{\mathrm{d}}_{\mathbf{k}\mathbf{k}'}(\mathbf{J},\mathbf{J}',\omega)$, have no poles in the upper complex plane.

Having explicitly computed the dressed susceptibility coefficients in Eq. (3.75), we can return to Eq. (3.61) to characterise the correlation properties of the dressed noise fluctuations generated by a self-gravitating bath. We can formally take the inverse Laplace transform of Eq. (3.61) to obtain the time-dependence of the potential fluctuations in the bath. We write

$$\delta\Phi_{\mathbf{k}}(\mathbf{J},t) = -(2\pi)^d \sum_{\mathbf{k}'} \!\!\!\!\!\!\int \mathrm{d}\mathbf{J}'\, \delta F_{\mathbf{k}'}(\mathbf{J}',0)\, \frac{1}{2\pi}\int_{\mathcal{B}} \mathrm{d}\omega\, \frac{\psi^{\mathrm{d}}_{\mathbf{k}\mathbf{k}'}(\mathbf{J},\mathbf{J}',\omega)}{\mathrm{i}(\omega - \mathbf{k}'\cdot\boldsymbol{\Omega}(\mathbf{J}'))}\, \mathrm{e}^{-\mathrm{i}\omega t}, \tag{3.76}$$

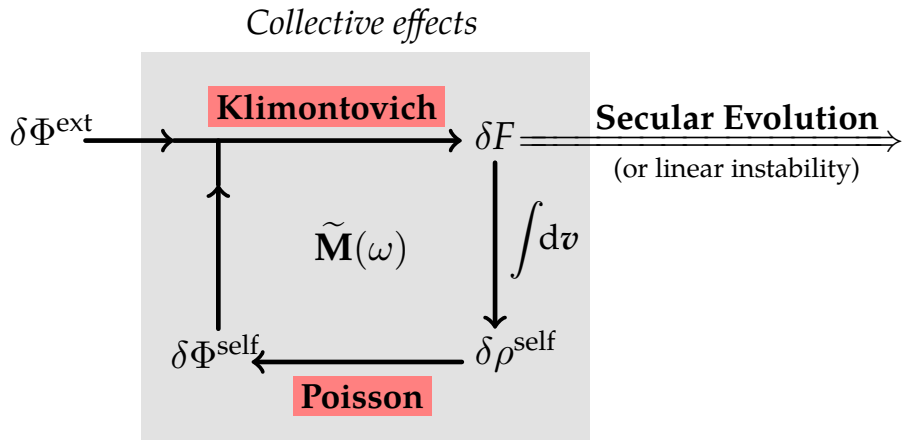

Figure 3.1: Illustration of the role of collective effects in a self-gravitating system. Any external potential perturbation, $\delta\Phi^{\rm ext}$, induces a response, δF, in the DF of a self-gravitating system, as described by the linearised Klimontovich Eq. (3.55). The system being self-gravitating, a density perturbation $\delta\rho^{\rm self}=\int \mathrm{d}\mathbf{v}\delta F$ is directly associated with this response. For the gravitational interaction, Poisson's equation then relates this density perturbation to a self-generated potential perturbation $\delta\Phi^{\rm self}$. Following this internal self-consistent amplification, the system is now submitted to the total perturbation $\delta\Phi^{\rm tot}=\delta\Phi^{\rm ext}+\delta\Phi^{\rm self}$. Accounting for the additional potential perturbation, $\delta\Phi^{\rm self}$, is accounting for collective effects.

where the Bromwich contour, $\mathcal{B}$, in the ω-plane has to pass above all the poles of the integrand. Because we have assumed that the bath is linearly stable, $\psi^{\rm d}_{\mathbf{k}\mathbf{k}'}(\mathbf{J},\mathbf{J}',\omega)$ only has poles in the lower half of the complex ω-plane, of the generic form $\omega=\omega_{\rm p}+\mathrm{i}s_{\rm p}$, with $s_{\rm p}<0$. These are called damped modes, because, once populated, their amplitude decreases exponentially in time, as we shall see. As a result, in Eq. (3.76), there is only one pole on the real axis, namely in $\omega_0=\mathbf{k}'\cdot\mathbf{\Omega}(\mathbf{J}')$. Following Fig. 3.2, we can distort the contour $\mathcal{B}$ into the contour $\mathcal{B}'$, so that the complex exponential goes to 0, and that there remains only contributions from the residues.

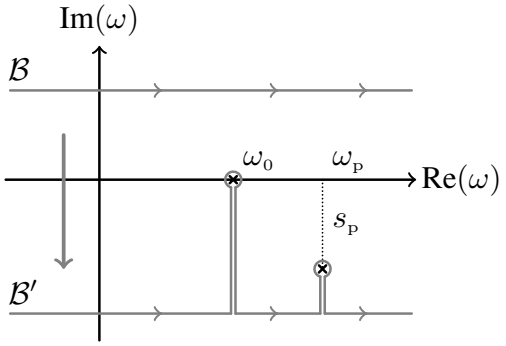

Figure 3.2: Illustration of the computation of the inverse Laplace transform from Eq.(3.76). By distorting the contour $\mathcal{B}$ into the contour $\mathcal{B}'$ with large negative complex values, only the contributions from the residues of the poles remain.

Paying a careful attention to the direction of integration, each pole contributes a $-2\pi\mathrm{i}\mathrm{Res}[...]$, and we can rewrite Eq. (3.76) as

$$\delta\Phi_{\mathbf{k}}(\mathbf{J},t)=(2\pi)^d\sum_{\mathbf{k}'}\int\mathrm{d}\mathbf{J}'\,\delta F_{\mathbf{k}'}(\mathbf{J}',0)\left[\mathrm{e}^{-\mathrm{i}\mathbf{k}'\cdot\mathbf{\Omega}(\mathbf{J}')t}\,\psi^{\rm d}_{\mathbf{k}\mathbf{k}'}(\mathbf{J},\mathbf{J}',\mathbf{k}'\cdot\mathbf{\Omega}(\mathbf{J}'))+\sum_{\rm p}\mathrm{e}^{s_{\rm p}t}\,\mathrm{e}^{-\mathrm{i}\omega_{\rm p}t}\times(...)\right],\tag{3.77}$$

where the sum over "p" runs over all the poles of $\psi^{\rm d}_{\mathbf{k}\mathbf{k}'}(\mathbf{J},\mathbf{J}',\omega)$. Since all these modes are damped, we have $s_{\rm p}<0$, so that their contributions to Eq. (3.77) vanish for $t\gtrsim 1/|s_{\rm p}|\simeq 1/|\Omega|$. This implies that after a few dynamical times, their effects can be neglected. This corresponds to the thermalisation of the bath. Indeed, a self-gravitating bath, initially uncorrelated at $t=0$, will develop dressed correlations that will settle to a steady state on a few dynamical times. Once these damped contributions have faded, Eq. (3.77) becomes

$$\boxed{\delta\Phi_{\mathbf{k}}(\mathbf{J},t)=(2\pi)^d\sum_{\mathbf{k}'}\int\mathrm{d}\mathbf{J}'\,\psi^{\rm d}_{\mathbf{k}\mathbf{k}'}(\mathbf{J},\mathbf{J}',\mathbf{k}'\cdot\mathbf{\Omega}(\mathbf{J}'))\,\delta F_{\mathbf{k}'}(\mathbf{J}',0)\,\mathrm{e}^{-\mathrm{i}\mathbf{k}'\cdot\mathbf{\Omega}(\mathbf{J}')t}.}\tag{3.78}$$

At this stage, we note that Eq. (3.78) is the direct equivalent of the bare equation (3.41). In that equation, accounting for the self-gravitating amplification only amounts to replacing the bare susceptibility coefficients,

$\psi_{\mathbf{k}\mathbf{k}'}(\mathbf{J},\mathbf{J}',\mathbf{k}\cdot\boldsymbol{\Omega}(\mathbf{J}))$, by their dressed analogs, $\psi^{\mathrm{d}}_{\mathbf{k}\mathbf{k}'}(\mathbf{J},\mathbf{J}',\mathbf{k}\cdot\boldsymbol{\Omega}(\mathbf{J}))$. As a result of these strong analogies, the statistics of the fluctuations in a dressed bath remain formally the same as the ones in an inert bare bath, except for a change in the pairwise interaction potential that is now dressed by the bath's linear response. Phrased differently, Eq. (3.78) can be interpreted as describing the potential fluctuations generated by a bath where the particles follow the mean-field orbits, $(\boldsymbol{\theta}(t),\mathbf{J}(t)) = (\boldsymbol{\theta}_0+\boldsymbol{\Omega}(\mathbf{J})t,\mathbf{J}_0)$, but interact via a different pairwise interaction potential dictated by the dressed susceptibility coefficients, $\psi^{\mathrm{d}}_{\mathbf{k}\mathbf{k}'}(\mathbf{J},\mathbf{J}',\omega)$. As such, bath's particles are said to be dressed by self-gravity, as one has to account for their associated gravitational wake. Because the bare and dressed potential fluctuations are so similar, it is therefore straightforward to characterise their correlation functions, and therefore to characterise the diffusion coefficients that it generates on a test particle.

In the present dressed case, the diffusion coefficient from Eq. (3.51) becomes

$$\boxed{\mathbf{D}_2(\mathbf{J}) = m_{\mathrm{b}}\pi(2\pi)^d\sum_{\mathbf{k},\mathbf{k}'}\mathbf{k}\otimes\mathbf{k}\int\mathrm{d}\mathbf{J}'\,\delta_{\mathrm{D}}(\mathbf{k}\cdot\boldsymbol{\Omega}(\mathbf{J})-\mathbf{k}'\cdot\boldsymbol{\Omega}(\mathbf{J}'))\left|\psi^{\mathrm{d}}_{\mathbf{k}\mathbf{k}'}(\mathbf{J},\mathbf{J}',\mathbf{k}\cdot\boldsymbol{\Omega}(\mathbf{J}))\right|^2 F_0(\mathbf{J}'),} \tag{3.79}$$

which involves the dressed susceptibility coefficients. In Eq. (3.79), we have recovered the diffusion coefficients of the inhomogeneous Balescu-Lenard equation. They describe the diffusion undergone by a test particle embedded in an external live and self-gravitating bath made of N particles interacting one with another, i.e. a bath where collective effects are accounted for. Given its deep similarities with the inhomogeneous Landau diffusion coefficients from Eq. (3.51), the previous physical discussion applies similarly. Here, once again, the big difference comes from the change in the strength of the resonant couplings, which is now controlled by the squared dressed susceptibility coefficients, $|\psi^{\mathrm{d}}_{\mathbf{k}\mathbf{k}'}(\mathbf{J},\mathbf{J}',\mathbf{k}\cdot\boldsymbol{\Omega}(\mathbf{J}))|^2$. For some classes of self-gravitating systems, this can be a very important change. This is particularly true for dynamically cold systems, such as razor-thin cold galactic discs, that can strongly amplify perturbations, leading therefore to larger diffusion coefficients, and consequently to a much faster long-term diffusion.

4 Dynamical Friction

In the previous section, we set out to characterise the diffusion undergone by a zero-mass test particle embedded in an external bath. As a result, there was no backreaction of the test particle on the bath. Relying on Novikov's theorem, we obtained in Eq. (3.25) a diffusion equation that involved only a diffusion coefficient, $\mathbf{D}_2(\mathbf{J})$, which we interpreted in Eq. (3.28) as being sourced by the correlation of the potential fluctuations generated by the bath and felt by the test particle. Then, in order to obtain explicit expressions for these diffusion coefficients, we consider the important case of a background bath composed of N particles, distributed according to a smooth mean-field DF, $F_0(\mathbf{J})$. This led us to derive in Eq. (3.51) (resp. Eq. (3.79)) the inhomogeneous Landau (resp. Balescu-Lenard) diffusion coefficients when collective effects are neglected (resp. accounted for).

However, because we neglected any backreaction of the test particle onto the background bath, we obtained in Eq. (3.25) a diffusion equation that only had a diffusion component, and no drift component that would be proportional to the mass of the test particle. Yet, if the test particle can influence the bath particles, there exists an advection term associated with the perturbations generated in the bath along the trajectory of the test particle. This component is called the friction force by polarisation, which captures in particular the process of dynamical friction. Moreover, for a closed system, such a friction component is necessary to comply with the constraint of energy conservation, as any diffusion generated in the system must be compensated elsewhere by a friction. It is this component that we now set out to characterise.

We assume therefore that the test particle now has a non-zero mass, that we denote with m_{t}. As the bath's potential fluctuations are still the ones felt by the test particle, we are interested in how the statistics of the bath's potential perturbations gets modified by the disturbances generated by the test particle. Following Eq. (3.52), the specific Hamiltonian of the bath particles becomes

$$H_{\mathrm{b}}(\boldsymbol{\theta},\mathbf{J},t) = H_0(\mathbf{J}) + \delta\Phi_{\mathrm{t}}(\boldsymbol{\theta},\mathbf{J},t) + \delta\Phi(\boldsymbol{\theta},\mathbf{J},t). \tag{4.1}$$

In that equation, we have introduced $\delta\Phi_{\mathrm{t}}(\boldsymbol{\theta},\mathbf{J},t)$ as the perturbations generated by the test particle and $\delta\Phi(\boldsymbol{\theta},\mathbf{J},t)$ as the bath's response, i.e. the fluctuations that will be felt by the test particle. This second part is made of two components, namely the response of the bath to the finite-N fluctuations associated with the discrete number of bath particles (similarly to what was already characterised in Section 3.3), as well as the self-gravitating response of the bath to the perturbation $\delta\Phi_{\mathrm{t}}(\boldsymbol{\theta},\mathbf{J},t)$ generated by the test particle. Let us now characterise these two fluctuations.

As already introduced in Eq. (3.32), we denote the instantaneous fluctuations in the bath's DF as δF. Similarly to Eq. (3.55), at first order in the perturbations, the time evolution of δF is governed by the linearised

Klimontovich equation that reads here

$$\frac{\partial \delta F}{\partial t} + \big[\delta F, H_0\big] + \big[F_0, \delta\Phi_{\rm t} + \delta\Phi\big] = 0. \tag{4.2}$$

A key point here is to note that the fluctuations of the DF, δF, is self-consistent with the bath's response, $\delta\Phi = \delta\Phi[\delta F]$, so that we have

$$\delta\Phi(\mathbf{x},t) = \int \mathrm{d}\mathbf{x}'\mathrm{d}\mathbf{v}'\, U(\mathbf{x},\mathbf{x}')\, \delta F(\mathbf{x}',\mathbf{v}'). \tag{4.3}$$

Owing to the similarity with Eq. (3.55), we can rewrite the present evolution equation in Laplace-Fourier space, to obtain a self-consistent relation satisfied by the bath's. In analogy with Eq. (3.56), we get

$$\begin{aligned}
\delta\widetilde{\Phi}_{\mathbf{k}}(\mathbf{J},\omega) = & -(2\pi)^d \sum_{\mathbf{k}'} \int \mathrm{d}\mathbf{J}'\, \frac{\mathbf{k}'\cdot\partial F_0/\partial \mathbf{J}'}{\omega - \mathbf{k}'\cdot\mathbf{\Omega}(\mathbf{J}')}\, \psi_{\mathbf{k}\mathbf{k}'}(\mathbf{J},\mathbf{J}')\, \delta\widetilde{\Phi}_{\mathbf{k}'}(\mathbf{J}',\omega) \\
& -(2\pi)^d \sum_{\mathbf{k}'} \int \mathrm{d}\mathbf{J}'\, \frac{\mathbf{k}'\cdot\partial F_0/\partial \mathbf{J}'}{\omega - \mathbf{k}'\cdot\mathbf{\Omega}(\mathbf{J}')}\, \psi_{\mathbf{k}\mathbf{k}'}(\mathbf{J},\mathbf{J}')\, \delta\widetilde{\Phi}^{\rm t}_{\mathbf{k}'}(\mathbf{J}',\omega) \\
& -(2\pi)^d \sum_{\mathbf{k}'} \int \mathrm{d}\mathbf{J}'\, \frac{\delta F_{\mathbf{k}'}(\mathbf{J}',0)}{\mathrm{i}(\omega - \mathbf{k}'\cdot\mathbf{\Omega}(\mathbf{J}'))}\, \psi_{\mathbf{k}\mathbf{k}'}(\mathbf{J},\mathbf{J}').
\end{aligned} \tag{4.4}$$

It is easy to give a physical meaning to each of the terms arising in that equation. The first term corresponds to the kernel of the integral relation satisfied by the bath's response. It captures the strength of the bath's self-gravitating amplification, i.e. the efficiency with which perturbations imposed to the bath get amplified. The bath is submitted to two types of perturbations, namely the perturbations from the massive test particle (second term), and the stochastic perturbations generated by the bath's discreteness (third term).

Our goal is to obtain an explicit expression for $\delta\widetilde{\Phi}_{\mathbf{k}}(\mathbf{J},\omega)$. To ease that inversion, we will follow the same approach as in Section 3.4, so that all the potential perturbations are projected onto the basis elements. As a consequence, we write

$$\begin{aligned}
\delta\widetilde{\Phi}_{\mathbf{k}}(\mathbf{J},\omega) &= \sum_p \widetilde{\mathbf{P}}_p(\omega)\, \psi^{(p)}_{\mathbf{k}}(\mathbf{J}), \\
\delta\widetilde{\Phi}^{\rm t}_{\mathbf{k}}(\mathbf{J},\omega) &= \sum_p \widetilde{\mathbf{T}}_p(\omega)\, \psi^{(p)}_{\mathbf{k}}(\mathbf{J}), \\
\widetilde{\mathbf{S}}_p(\omega) &= (2\pi)^d \sum_{\mathbf{k}'} \int \mathrm{d}\mathbf{J}'\, \frac{\delta F_{\mathbf{k}'}(\mathbf{J}',0)}{\mathrm{i}(\omega - \mathbf{k}'\cdot\mathbf{\Omega}(\mathbf{J}'))}\, \psi^{(p)*}_{\mathbf{k}'}(\mathbf{J}').
\end{aligned} \tag{4.5}$$

We also recall the result from Eq. (3.68) that the bare susceptibility coefficients can be decomposed on the basis elements. Injecting these decompositions into Eq. (4.4), we obtain

$$\begin{aligned}
\sum_p \widetilde{\mathbf{P}}_p(\omega)\, \psi^{(p)}_{\mathbf{k}}(\mathbf{J}) = & \sum_{p,q} \widetilde{\mathbf{M}}_{pq}(\omega)\, \widetilde{\mathbf{P}}_q(\omega)\, \psi^{(q)}_{\mathbf{k}}(\mathbf{J}) \\
& + \sum_{p,q} \widetilde{\mathbf{M}}_{pq}(\omega)\, \widetilde{\mathbf{T}}_q(\omega)\, \psi^{(p)}_{\mathbf{k}}(\mathbf{J}) \\
& + \sum_p \widetilde{\mathbf{S}}_p(\omega)\, \psi^{(p)}_{\mathbf{k}}(\mathbf{J}).
\end{aligned} \tag{4.6}$$

Recalling that the basis is biorthogonal, this self-consistency can then be rewritten under the short vectorial form

$$\widetilde{\mathbf{P}}(\omega) = \widetilde{\mathbf{M}}(\omega)\cdot\widetilde{\mathbf{P}}(\omega) + \widetilde{\mathbf{M}}(\omega)\cdot\widetilde{\mathbf{T}}(\omega) + \widetilde{\mathbf{S}}(\omega). \tag{4.7}$$

where $\widetilde{\mathbf{P}}(\omega)$ characterises the bath's response, $\widetilde{\mathbf{T}}(\omega)$ is the perturbation from the test particle, $\widetilde{\mathbf{S}}(\omega)$ is the initial finite-N fluctuations in the bath's DF. This relation also involves a self-consistent amplification by the bath's response matrix, $\widetilde{\mathbf{M}}(\omega)$, as already defined in Eq. (3.72).

If we assume that the bath is linearly stable, the dielectric matrix $\widetilde{\mathbf{E}}^{-1}(\omega) = \big[\mathbf{I} - \widetilde{\mathbf{M}}(\omega)\big]^{-1}$ is well defined, and the bath's response can then be expressed as a function of the two source terms, so that

$$\widetilde{\mathbf{P}}(\omega) = \widetilde{\mathbf{E}}^{-1}(\omega)\cdot\widetilde{\mathbf{S}}(\omega) + \big\{\widetilde{\mathbf{E}}^{-1}(\omega) - \mathbf{I}\big\}\cdot\widetilde{\mathbf{T}}(\omega), \tag{4.8}$$

where we recover that the total fluctuations generated by the bath are the result of the self-gravitating dressing of the Poisson finite-N fluctuations, as well as the dressing of the test particle's perturbation.

Before writing the time version of Eq. (4.8), we first write an explicit expression for the source term, $\widetilde{\mathbf{T}}(\omega)$, due to the test particle. We note the position of the test particle at time t, as $\mathbf{x}_{\mathrm{t}}(t)$. Then, we have

$$\delta\Phi_{\mathrm{t}}(\mathbf{x},t) = m_{\mathrm{t}}\, U(\mathbf{x},\mathbf{x}(t)). \tag{4.9}$$

When Fourier transformed in angle, this immediately gives

$$\delta\Phi^{\mathrm{t}}_{\mathbf{k}}(\mathbf{J},t) = m_{\mathrm{t}} \sum_{\mathbf{k}'} \psi_{\mathbf{k}\mathbf{k}'}(\mathbf{J},\mathbf{J}_{\mathrm{t}}(t))\, \mathrm{e}^{-\mathrm{i}\mathbf{k}'\cdot\boldsymbol{\theta}_{\mathrm{t}}(t)}, \tag{4.10}$$

where we used the definition of the bare susceptibility coefficients from Eq. (3.37), and denoted the position of the test particle in angle-action space as $(\boldsymbol{\theta}_{\mathrm{t}}(t),\mathbf{J}_{\mathrm{t}}(t))$. We now rely on our assumption of timescale separation, assuming that the orbital diffusion of the test particle takes place on a timescale much longer than the test particle's orbital motion. As a consequence, in Eq. (4.10), we replace the motion of the test particle by its mean-field limit, i.e. by $\boldsymbol{\theta}_{\mathrm{t}}(t) = \boldsymbol{\theta}^0_{\mathrm{t}} + \boldsymbol{\Omega}(\mathbf{J}_{\mathrm{t}})\, t$ and $\mathbf{J}_{\mathrm{t}}(t) = \mathbf{J}_{\mathrm{t}}$, with $\boldsymbol{\theta}^0_{\mathrm{t}}$ the initial phase of the test particle. It is then straightforward to take the Laplace transform of Eq. (4.10), and we obtain

$$\begin{aligned}
\delta\widetilde{\Phi}^{\mathrm{t}}_{\mathbf{k}}(\mathbf{J},\omega) &= m_{\mathrm{t}} \sum_{\mathbf{k}'} \psi_{\mathbf{k}\mathbf{k}'}(\mathbf{J},\mathbf{J}_{\mathrm{t}})\, \mathrm{e}^{-\mathrm{i}\mathbf{k}'\cdot\boldsymbol{\theta}^0_{\mathrm{t}}} \int_0^{+\infty} \mathrm{d}t\, \mathrm{e}^{-\mathrm{i}\mathbf{k}'\cdot\boldsymbol{\Omega}(\mathbf{J}_{\mathrm{t}})t}\, \mathrm{e}^{\mathrm{i}\omega t} \\
&= -m_{\mathrm{t}} \sum_{\mathbf{k}'} \psi_{\mathbf{k}\mathbf{k}'}(\mathbf{J},\mathbf{J}_{\mathrm{t}})\, \frac{\mathrm{e}^{-\mathrm{i}\mathbf{k}'\cdot\boldsymbol{\theta}^0_{\mathrm{t}}}}{\mathrm{i}(\omega - \mathbf{k}'\cdot\boldsymbol{\Omega}(\mathbf{J}_{\mathrm{t}}))} \\
&= \sum_p \left\{ m_{\mathrm{t}} \sum_{\mathbf{k}'} \frac{\mathrm{e}^{-\mathrm{i}\mathbf{k}'\cdot\boldsymbol{\theta}^0_{\mathrm{t}}}}{\mathrm{i}(\omega - \mathbf{k}'\cdot\boldsymbol{\Omega}(\mathbf{J}_{\mathrm{t}}))}\, \psi^{(p)*}_{\mathbf{k}'}(\mathbf{J}_{\mathrm{t}}) \right\} \psi^{(p)}_{\mathbf{k}}(\mathbf{J}).
\end{aligned} \tag{4.11}$$

All in all, glancing back at the definition from Eq. (4.5), this allows us to write the coefficients $\widetilde{\mathbf{T}}_p(\omega)$ as

$$\widetilde{\mathbf{T}}_p(\omega) = m_{\mathrm{t}} \sum_{\mathbf{k}'} \frac{\mathrm{e}^{-\mathrm{i}\mathbf{k}'\cdot\boldsymbol{\theta}^0_{\mathrm{t}}}}{\mathrm{i}(\omega - \mathbf{k}'\cdot\boldsymbol{\Omega}(\mathbf{J}_{\mathrm{t}}))}\, \psi^{(p)*}_{\mathbf{k}'}(\mathbf{J}_{\mathrm{t}}). \tag{4.12}$$

Having explicitly obtained the expression of all the terms appearing in Eq. (4.8), we can now take the inverse Laplace transform of this equation, to obtain the time dependence of the potential fluctuations within the bath. This calculation is essentially identical to the one we already performed in Eq. (3.77) when computing the Balescu-Lenard diffusion coefficients. In particular, we rely on the assumption that the bath is linearly stable, so that there are no poles from the dressed susceptibility coefficients in the upper half of the complex plane. We write

$$\begin{aligned}
\delta\Phi_{\mathbf{k}}(\mathbf{J},t) &= \sum_p \psi^{(p)}_{\mathbf{k}}(\mathbf{J}) \int_{\mathcal{B}} \frac{\mathrm{d}\omega}{2\pi}\, \mathrm{e}^{-\mathrm{i}\omega t}\, \widetilde{\mathbf{P}}_p(\omega) \\
&= (2\pi)^d \sum_{\mathbf{k}'} \!\!\int \mathrm{d}\mathbf{J}'\, \delta F_{\mathbf{k}'}(\mathbf{J}',0) \sum_{p,q} \psi^{(p)}_{\mathbf{k}}(\mathbf{J})\, \psi^{(q)*}_{\mathbf{k}'}(\mathbf{J}') \int_{\mathcal{B}} \frac{\mathrm{d}\omega}{2\pi}\, \mathrm{e}^{-\mathrm{i}\omega t}\, \frac{\widetilde{\mathbf{E}}^{-1}_{pq}(\omega)}{\mathrm{i}(\omega - \mathbf{k}'\cdot\boldsymbol{\Omega}(\mathbf{J}'))} \\
&\quad + m_{\mathrm{t}} \sum_{\mathbf{k}'} \mathrm{e}^{-\mathrm{i}\mathbf{k}'\cdot\boldsymbol{\theta}^0_{\mathrm{t}}} \sum_{p,q} \psi^{(p)}_{\mathbf{k}}(\mathbf{J})\, \psi^{(q)*}_{\mathbf{k}'}(\mathbf{J}_{\mathrm{t}}) \int_{\mathcal{B}} \frac{\mathrm{d}\omega}{2\pi}\, \mathrm{e}^{-\mathrm{i}\omega t}\, \frac{\left\{\widetilde{\mathbf{E}}^{-1}(\omega) - \mathbf{I}\right\}_{pq}}{\mathrm{i}(\omega - \mathbf{k}'\cdot\boldsymbol{\Omega}(\mathbf{J}_{\mathrm{t}}))} \\
&= -(2\pi)^d \sum_{\mathbf{k}'} \!\!\int \delta F_{\mathbf{k}'}(\mathbf{J}',0)\, \mathrm{e}^{-\mathrm{i}\mathbf{k}'\cdot\boldsymbol{\Omega}(\mathbf{J}')t} \sum_{p,q} \psi^{(p)}_{\mathbf{k}}(\mathbf{J})\, \psi^{(q)*}_{\mathbf{k}'}(\mathbf{J}')\, \widetilde{\mathbf{E}}^{-1}_{pq}(\mathbf{k}'\cdot\boldsymbol{\Omega}(\mathbf{J}')) \\
&\quad - m_{\mathrm{t}} \sum_{\mathbf{k}'} \mathrm{e}^{-\mathrm{i}\mathbf{k}'\cdot\boldsymbol{\theta}^0_{\mathrm{t}}}\, \mathrm{e}^{-\mathrm{i}\mathbf{k}'\cdot\boldsymbol{\Omega}(\mathbf{J}_{\mathrm{t}})t} \sum_{p,q} \psi^{(p)}_{\mathbf{k}}(\mathbf{J})\, \psi^{(q)*}_{\mathbf{k}'}(\mathbf{J}_{\mathrm{t}}) \left\{\widetilde{\mathbf{E}}^{-1}(\mathbf{k}'\cdot\boldsymbol{\Omega}(\mathbf{J}_{\mathrm{t}})) - \mathbf{I}\right\}_{pq}.
\end{aligned} \tag{4.13}$$

Recalling the expression of the dressed susceptibility coefficients from Eq. (3.75), we can finally write the expression of the bath's potential fluctuations as

$$\delta\Phi_{\mathbf{k}}(\mathbf{J},t) = \delta\Phi^{\mathrm{diff}}_{\mathbf{k}}(\mathbf{J},t) + \delta\Phi^{\mathrm{fric}}_{\mathbf{k}}(\mathbf{J},t) \tag{4.14}$$

In that expression, we introduced the dressed stochastic potential fluctuations, $\delta\Phi^{\mathrm{diff}}_{\mathbf{k}}(\mathbf{J},t)$, as

$$\delta\Phi^{\mathrm{diff}}_{\mathbf{k}}(\mathbf{J},t) = (2\pi)^d \sum_{\mathbf{k}'} \!\!\int \mathrm{d}\mathbf{J}'\, \psi^{\mathrm{d}}_{\mathbf{k}\mathbf{k}'}(\mathbf{J},\mathbf{J}',\mathbf{k}'\cdot\boldsymbol{\Omega}(\mathbf{J}'))\, \delta F_{\mathbf{k}}(\mathbf{J},0)\, \mathrm{e}^{-\mathrm{i}\mathbf{k}'\cdot\boldsymbol{\Omega}(\mathbf{J}')t}, \tag{4.15}$$

which were already obtained in Eq. (3.78). We also introduced the deterministic potential fluctuations, $\delta\Phi^{\rm fric}_{\mathbf{k}}(\mathbf{J},t)$, as

$$\delta\Phi^{\rm fric}_{\mathbf{k}}(\mathbf{J},t) = m_{\rm t}\sum_{\mathbf{k}'}\left\{\psi^{\rm d}_{\mathbf{k}\mathbf{k}'}(\mathbf{J},\mathbf{J}_{\rm t},\mathbf{k}'\cdot\boldsymbol{\Omega}(\mathbf{J}_{\rm t})) - \psi_{\mathbf{k}\mathbf{k}'}(\mathbf{J},\mathbf{J}_{\rm t})\right\}\mathrm{e}^{-\mathrm{i}\mathbf{k}'\cdot\boldsymbol{\theta}^0_{\rm t}}\,\mathrm{e}^{-\mathrm{i}\mathbf{k}'\cdot\boldsymbol{\Omega}(\mathbf{J}_{\rm t})t}. \tag{4.16}$$

These two potential fluctuations are associated with very different physical processes. The first component, $\delta\Phi^{\rm diff}_{\mathbf{k}}(\mathbf{J},t)$, was already obtained in Eq. (3.78), when deriving the Balescu-Lenard diffusion coefficients. It captures the dressed potential fluctuations resulting from the dressed internal finite-N fluctuations within the bath (i.e. it is sourced by $\delta F_{\mathbf{k}'}(\mathbf{J}',0)$). The second component, $\delta\Phi^{\rm fric}_{\mathbf{k}}(\mathbf{J},t)$, captures the friction force by polarisation, and describes the dressed potential perturbations present in the bath as a result of the back-reaction of the test particle. These two potential perturbations have some fundamental differences. On the one hand, $\delta\Phi^{\rm diff}_{\mathbf{k}}(\mathbf{J},t)$ is truly a stochastic perturbation, as it depends on the particular sampling of the bath's initial conditions. It is of zero mean, depends on the bath's realisations, and its amplitude is proportional to $\sqrt{m_{\rm b}}$, with $m_{\rm b}$ the mass of the bath's particles. On the other hand, because it only depends on the mean-field properties of the bath, $\delta\Phi^{\rm fric}_{\mathbf{k}}(\mathbf{J},t)$ should be interpreted as a non-stochastic, systematic perturbation. It is of non-zero mean, and its amplitude is proportional to $m_{\rm t}$, the individual mass of the test particle. As a result, the more massive the test particle, the stronger the friction force by polarisation.

In Section 3.3, we have already shown how the time correlation of $\delta\Phi^{\rm diff}_{\mathbf{k}}(\mathbf{J},t)$ leads to the inhomogeneous Balescu-Lenard diffusion tensor. More precisely, in Eq. (3.25), we obtained

$$\begin{aligned}\left(\frac{\partial P(\mathbf{J},t)}{\partial t}\right)_{\rm diff} &= \frac{\partial}{\partial\mathbf{J}}\cdot\left[\sum_{\mathbf{k}}\mathrm{i}\mathbf{k}\left\langle\delta\Phi^{\rm diff}_{\mathbf{k}}(\mathbf{J},t)\,\mathrm{e}^{\mathrm{i}\mathbf{k}\cdot\boldsymbol{\theta}(t)}\,\varphi(\mathbf{J},t)\right\rangle\right]\\ &= \frac{\partial}{\partial\mathbf{J}}\cdot\left[\mathbf{D}_2(\mathbf{J})\cdot\frac{\partial P(\mathbf{J},t)}{\partial\mathbf{J}}\right],\end{aligned} \tag{4.17}$$

where the explicit expression of the dressed diffusion tensor, $\mathbf{D}_2(\mathbf{J})$, was obtained in Eq. (3.79).

We may now focus on the long-term effects associated with $\delta\Phi^{\rm fric}_{\mathbf{k}}(\mathbf{J},t)$. We now glance back at Eq. (3.9) that describes the long-term diffusion of the test particle's PDF. Since $\delta\Phi^{\rm fric}_{\mathbf{k}}(\mathbf{J},t)$ is non-stochastic, the contribution from that component in Eq. (3.9) is easier to compute. One writes

$$\begin{aligned}\left(\frac{\partial P(\mathbf{J},t)}{\partial t}\right)_{\rm fric} &= \frac{\partial}{\partial\mathbf{J}}\cdot\left[\sum_{\mathbf{k}}\mathrm{i}\mathbf{k}\left\langle\delta\Phi^{\rm fric}_{\mathbf{k}}(\mathbf{J},t)\,\mathrm{e}^{\mathrm{i}\mathbf{k}\cdot\boldsymbol{\theta}(t)}\,\varphi(\mathbf{J},t)\right\rangle\right]\\ &= \frac{\partial}{\partial\mathbf{J}}\cdot\left[m_{\rm t}\sum_{\mathbf{k},\mathbf{k}'}\mathrm{i}\mathbf{k}\left\{\psi^{\rm d}_{\mathbf{k}\mathbf{k}'}(\mathbf{J},\mathbf{J},\mathbf{k}'\cdot\boldsymbol{\Omega}(\mathbf{J})) - \psi_{\mathbf{k}\mathbf{k}'}(\mathbf{J},\mathbf{J})\right\}\left\langle\mathrm{e}^{\mathrm{i}(\mathbf{k}-\mathbf{k}')\cdot\boldsymbol{\theta}(t)}\,\varphi(\mathbf{J},t)\right\rangle\right]\\ &= \frac{\partial}{\partial\mathbf{J}}\cdot\left[m_{\rm t}\sum_{\mathbf{k}}\mathrm{i}\mathbf{k}\,\psi^{\rm d}_{\mathbf{k}\mathbf{k}}(\mathbf{J},\mathbf{J},\mathbf{k}\cdot\boldsymbol{\Omega}(\mathbf{J}))\,P(\mathbf{J},t)\right],\end{aligned} \tag{4.18}$$

where to get the second line, we identified $\boldsymbol{\theta}(t)$ with its unperturbed mean-field motion. To get the last line of that same equation, we averaged over the phase $\boldsymbol{\theta}(t)$ of the test particle, assuming that at any time it remains on average uniformly distributed in angles, and we used the fact that $\psi_{\mathbf{k}\mathbf{k}}(\mathbf{J},\mathbf{J})$ is real. All in all, this allows us to rewrite the contribution from the friction force by polarisation as

$$\boxed{\left(\frac{\partial P(\mathbf{J},t)}{\partial t}\right)_{\rm fric} = -\frac{\partial}{\partial\mathbf{J}}\cdot\left[\mathbf{D}_1(\mathbf{J})\,P(\mathbf{J},t)\right],} \tag{4.19}$$

where we introduced the friction coefficient $\mathbf{D}_1(\mathbf{J})$ as

$$\mathbf{D}_1(\mathbf{J}) = -m_{\rm t}\sum_{\mathbf{k}}\mathrm{i}\mathbf{k}\,\psi^{\rm d}_{\mathbf{k}\mathbf{k}}(\mathbf{J},\mathbf{J},\mathbf{k}\cdot\boldsymbol{\Omega}(\mathbf{J})). \tag{4.20}$$

The last step of the present calculation is to rewrite this coefficient under a simpler form, much more similar to the associated expression of the diffusion coefficient, $\mathbf{D}_2(\mathbf{J})$, from Eq. (3.79).

4.1 Rewriting the dynamical friction

We assume that the basis elements, $\psi^{(p)}(\mathbf{x})$, are real, so that they satisfy the symmetry relation $\psi^{(p)}_{-\mathbf{k}}(\mathbf{J}) = \psi^{(p)*}_{\mathbf{k}}(\mathbf{J})$. Symmetrising Eq. (4.20) with the change $\mathbf{k}\leftrightarrow-\mathbf{k}$, and recalling the definition from Eq. (3.75), we can rewrite this equation

$$\mathbf{D}_1(\mathbf{J}) = m_{\rm t}\sum_{\mathbf{k}}\frac{\mathrm{i}\mathbf{k}}{2}\sum_{p,q}\psi^{(p)}_{\mathbf{k}}(\mathbf{J})\left\{\widetilde{\mathbf{E}}^{-1}_{pq}(\mathbf{k}\cdot\boldsymbol{\Omega}(\mathbf{J})) - \widetilde{\mathbf{E}}^{-1}_{qp}(-\mathbf{k}\cdot\boldsymbol{\Omega}(\mathbf{J}))\right\}\psi^{(q)*}_{\mathbf{k}}(\mathbf{J}). \tag{4.21}$$

Let us now explore the symmetry properties of the dielectric matrix, in particular when evaluated for a real frequency $\omega_{\rm R}$. Following Eq. (3.72), it is defined as

$$\widetilde{\mathbf{E}}_{pq}(\omega_{\rm R}) = 1 - (2\pi)^d \sum_{\mathbf{k}} \!\!\!\!\!\!\int \mathrm{d}\mathbf{J}\, \frac{\mathbf{k}\cdot\partial F_0/\partial \mathbf{J}}{\omega_{\rm R} - \mathbf{k}\cdot\mathbf{\Omega}(\mathbf{J})}\, \psi_{\mathbf{k}}^{(p)*}(\mathbf{J})\, \psi_{\mathbf{k}}^{(q)}(\mathbf{J}). \tag{4.22}$$

In that expression, the resonant denominator should be interpreted in the sense of a distribution. Given our convention for the Laplace transform in Eq. (3.57), to ensure the convergence of the Laplace transform, we must always have $\mathrm{Im}[\omega] > 0$. As a consequence, the resonant denominator should be interpreted as

$$\begin{aligned}\frac{1}{\omega_{\rm R} - \mathbf{k}\cdot\mathbf{\Omega}(\mathbf{J})} &= \frac{1}{(\omega_{\rm R} - \mathbf{k}\cdot\mathbf{\Omega}(\mathbf{J})) + \mathrm{i}0} \\ &= \mathcal{P}\left(\frac{1}{\omega_{\rm R} - \mathbf{k}\cdot\mathbf{\Omega}(\mathbf{J})}\right) - \mathrm{i}\pi\delta_{\rm D}(\omega_{\rm R} - \mathbf{k}\cdot\mathbf{\Omega}(\mathbf{J})),\end{aligned} \tag{4.23}$$

where in the first line, we added a small positive imaginary part to the frequency ω, and to get the second line, we relied on Plemelj formula. Owing to this decomposition, we therefore rewrite the dielectric matrix as

$$\widetilde{\mathbf{E}}(\omega_{\rm R}) = \widetilde{\mathbf{E}}^{\rm R}(\omega_{\rm R}) + \mathrm{i}\,\widetilde{\mathbf{E}}^{\rm I}(\omega_{\rm R}), \tag{4.24}$$

where we introduced the matrices

$$\begin{aligned}\widetilde{\mathbf{E}}^{\rm R}_{pq}(\omega_{\rm R}) &= 1 - (2\pi)^d \sum_{\mathbf{k}} \mathcal{P}\!\!\!\!\!\!\int \mathrm{d}\mathbf{J}\, \frac{\mathbf{k}\cdot\partial F_0/\partial \mathbf{J}}{\omega_{\rm R} - \mathbf{k}\cdot\mathbf{\Omega}(\mathbf{J})}\, \psi_{\mathbf{k}}^{(p)*}(\mathbf{J})\, \psi_{\mathbf{k}}^{(q)}(\mathbf{J}), \\ \widetilde{\mathbf{E}}^{\rm I}_{pq}(\omega_{\rm R}) &= \pi(2\pi)^d \sum_{\mathbf{k}} \!\!\!\!\!\!\int \mathrm{d}\mathbf{J}\, \delta_{\rm D}(\omega_{\rm R} - \mathbf{k}\cdot\mathbf{\Omega}(\mathbf{J}))\, \mathbf{k}\cdot\frac{\partial F_0}{\partial \mathbf{J}}\, \psi_{\mathbf{k}}^{(p)*}(\mathbf{J})\, \psi_{\mathbf{k}}^{(q)}(\mathbf{J}).\end{aligned} \tag{4.25}$$

Attention, we emphasise that $(\widetilde{\mathbf{E}}^{\rm R}, \widetilde{\mathbf{E}}^{\rm I})$ are not, per se, the real and imaginary parts of the dielectric matrix. Owing to the symmetry of the Fourier transformed basis elements, the two matrices satisfy the symmetries

$$\begin{aligned}\widetilde{\mathbf{E}}^{\rm R}(-\omega_{\rm R}) &= \widetilde{\mathbf{E}}^{\rm R*}(\omega_{\rm R}) \quad ; \quad \widetilde{\mathbf{E}}^{\rm I}(-\omega_{\rm R}) = -\widetilde{\mathbf{E}}^{\rm I*}(\omega_{\rm R}), \\ \widetilde{\mathbf{E}}^{\rm R\dagger}(\omega_{\rm R}) &= \widetilde{\mathbf{E}}^{\rm R}(\omega_{\rm R}) \quad ; \quad \widetilde{\mathbf{E}}^{\rm I\dagger}(\omega_{\rm R}) = \widetilde{\mathbf{E}}^{\rm I}(\omega_{\rm R}).\end{aligned} \tag{4.26}$$

As a consequence, following the definition from Eq. (4.24), we conclude that the dielectrix matrix satisfies the symmetry

$$\widetilde{\mathbf{E}}(-\omega_{\rm R}) = \widetilde{\mathbf{E}}^{*}(\omega_{\rm R}). \tag{4.27}$$

This allows us then to rewrite Eq. (4.21) as

$$\mathbf{D}_1(\mathbf{J}) = m_{\rm t} \sum_{\mathbf{k}} \frac{\mathrm{i}\mathbf{k}}{2} \sum_{p,q} \psi_{\mathbf{k}}^{(p)}(\mathbf{J}) \left\{\widetilde{\mathbf{E}}^{-1} - \widetilde{\mathbf{E}}^{-1\dagger}\right\}_{pq} \psi_{\mathbf{k}}^{(q)*}(\mathbf{J}), \tag{4.28}$$

where, to shorten the notations, we did not write explicitly that, in this expression, the dielectric matrices have to be evaluated in $\omega_{\rm R} = \mathbf{k}\cdot\mathbf{\Omega}(\mathbf{J})$.

Luckily, the matrices in bracket can be rewritten as

$$\widetilde{\mathbf{E}}^{-1} - \widetilde{\mathbf{E}}^{-1\dagger} = \widetilde{\mathbf{E}}^{-1} \left\{\widetilde{\mathbf{E}}^{\dagger} - \widetilde{\mathbf{E}}\right\} \widetilde{\mathbf{E}}^{-1\dagger}. \tag{4.29}$$

Following the symmetry relations from Eq. (4.26), the matrices within brackets can be rewritten as

$$\widetilde{\mathbf{E}}^{\dagger} - \widetilde{\mathbf{E}} = -2\mathrm{i}\,\widetilde{\mathbf{E}}^{\rm I}. \tag{4.30}$$

We can now finally reinject this result into Eq. (4.28), and we get

$$\begin{aligned}\mathbf{D}_1(\mathbf{J}) &= m_{\rm t} \sum_{\mathbf{k}} \mathbf{k} \sum_{\substack{p,q \\ r_1,r_2}} \psi_{\mathbf{k}}^{(p)}(\mathbf{J})\, \widetilde{\mathbf{E}}^{-1}_{pr_1}\, \widetilde{\mathbf{E}}^{\rm I}_{r_1r_2}\, \widetilde{\mathbf{E}}^{-1*}_{qr_2}\, \psi_{\mathbf{k}}^{(q)*}(\mathbf{J}) \\ &= m_{\rm t}\pi(2\pi)^d \sum_{\mathbf{k},\mathbf{k}'} \mathbf{k} \!\!\!\!\!\!\int \mathrm{d}\mathbf{J}'\, \delta_{\rm D}(\mathbf{k}\cdot\mathbf{\Omega}(\mathbf{J}) - \mathbf{k}'\cdot\mathbf{\Omega}(\mathbf{J}'))\, \mathbf{k}'\cdot\frac{\partial F_0}{\partial \mathbf{J}'} \\ &\quad \times \left(\sum_{p,r_1} \psi_{\mathbf{k}}^{(p)}(\mathbf{J})\, \widetilde{\mathbf{E}}^{-1}_{pr_1}(\mathbf{k}\cdot\mathbf{\Omega}(\mathbf{J}))\, \psi_{\mathbf{k}'}^{(r_1)*}(\mathbf{J}')\right) \left(\sum_{q,r_2} \psi_{\mathbf{k}}^{(q)*}(\mathbf{J})\, \widetilde{\mathbf{E}}^{-1*}_{qr_2}(\mathbf{k}\cdot\mathbf{\Omega}(\mathbf{J}))\, \psi_{\mathbf{k}'}^{(r_2)}(\mathbf{J}')\right).\end{aligned} \tag{4.31}$$

Identifying again the definition of the dressed susceptibility coefficients from Eq. (3.75) we can finally write the friction coefficient as

$$\boxed{\mathbf{D}_1(\mathbf{J}) = m_{\mathrm{t}}\pi(2\pi)^d \sum_{\mathbf{k},\mathbf{k}'} \mathbf{k} \int \mathrm{d}\mathbf{J}'\, \delta_{\mathrm{D}}(\mathbf{k}\cdot\boldsymbol{\Omega}(\mathbf{J}) - \mathbf{k}'\cdot\boldsymbol{\Omega}(\mathbf{J}'))\, \left|\psi^{\mathrm{d}}_{\mathbf{k}\mathbf{k}'}(\mathbf{J},\mathbf{J}',\mathbf{k}\cdot\boldsymbol{\Omega}(\mathbf{J}))\right|^2 \mathbf{k}'\cdot\frac{\partial F_0}{\partial \mathbf{J}'}.} \tag{4.32}$$

This is the main result of this section. It is important to note that this friction component is sourced by the gradient of the bath's DF, $\mathbf{k}'\cdot\partial F_0/\partial\mathbf{J}'$, and its amplitude is proportional to the mass, m_{t}, of the test particle. Moreover, we also note that it shares a very similar structure compared to the one of the diffusion tensor, as already obtained in Eq. (3.79). In particular, it involves the dressed susceptibility coefficients, $\psi^{\mathrm{d}}_{\mathbf{k}\mathbf{k}'}(\mathbf{J},\mathbf{J}',\omega)$, as well as the same resonance condition over orbital frequencies, $\delta_{\mathrm{D}}(\mathbf{k}\cdot\boldsymbol{\Omega}(\mathbf{J}) - \mathbf{k}'\cdot\boldsymbol{\Omega}(\mathbf{J}'))$.

5 The Balescu-Lenard equation

In the two previous sections, we successively derived the two components describing the long-term evolution of a massive test particle embedded in a discrete self-gravitating bath. In Section 3, we recovered in Eq. (3.79) the diffusion tensor, $\mathbf{D}_2(\mathbf{J})$, sourced by the temporal correlations of the finite-N dressed potential perturbations unavoidably present in the bath. Then, in Section 4, we obtained in Eq. (4.32) the expression of the friction coefficient, $\mathbf{D}_1(\mathbf{J})$, which captures the back-reaction on the test particle of the perturbations induced by that same test particle in the bath. Gathering these two components, the diffusion equation (3.9) for the test particle's PDF takes the explicit form

$$\begin{aligned}\frac{\partial P(\mathbf{J},t)}{\partial t} = -\pi(2\pi)^d \frac{\partial}{\partial\mathbf{J}}\cdot\Bigg[\sum_{\mathbf{k},\mathbf{k}'}\mathbf{k}\int\mathrm{d}\mathbf{J}'\,\left|\psi^{\mathrm{d}}_{\mathbf{k}\mathbf{k}'}(\mathbf{J},\mathbf{J}',\mathbf{k}\cdot\boldsymbol{\Omega}(\mathbf{J}))\right|^2\delta_{\mathrm{D}}(\mathbf{k}\cdot\boldsymbol{\Omega}(\mathbf{J}) - \mathbf{k}'\cdot\boldsymbol{\Omega}(\mathbf{J}'))\\ \times\left(m_{\mathrm{t}}\,\mathbf{k}'\cdot\frac{\partial}{\partial\mathbf{J}'} - m_{\mathrm{b}}\,\mathbf{k}\cdot\frac{\partial}{\partial\mathbf{J}}\right)P(\mathbf{J},t)\,F_0(\mathbf{J}',t)\Bigg].\end{aligned} \tag{5.1}$$

This is the (Fokker-Planck version of the) inhomogeneous Balescu-Lenard equation that describes the relaxation of a population of massive particle embedded within a background inhomogeneous discrete bath of N particles.

As previously discussed, this equation comprises two components. First, a diffusion component associated with the term proportional to $m_{\mathrm{b}}\mathbf{k}\cdot\partial/\partial\mathbf{J}$, and sourced by the correlations in the Poisson noise potential fluctuations in the bath. Its amplitude is proportional to the mass of the bath particles, $m_{\mathrm{b}} = M_{\mathrm{tot}}/N$, and therefore vanishes in the limit of a collisionless bath, i.e. in the limit $N\to+\infty$. Second, a friction component associated with the term proportional to $m_{\mathrm{t}}\mathbf{k}'\cdot\partial/\partial\mathbf{J}'$ and sourced by the back-reaction of the test particle onto the bath. Its amplitude is proportional to the mass, m_{t}, of the test particle, and is responsible for mass segregation. Moreover, this component does not vanish in the collisionless limit, but does vanish for a bath satisfying $\partial F_0/\partial\mathbf{J} = 0$.

Equation (5.1) describes the long-term diffusion of the statistics of a test particle (described by the PDF $P(\mathbf{J},t)$), when embedded in a bath (described by the PDF $F_0(\mathbf{J},t)$). We can now use that result to obtain the self-consistent evolution equation satisfied by the bath's DF on long timescales. This only amounts to assuming that the statistics of the test particle is given by the statistics of the bath's particles, i.e. one performs the replacements $P(\mathbf{J},t)\to F_0(\mathbf{J},t)$ and $m_{\mathrm{t}}\to m_{\mathrm{b}}$ in Eq. (5.1). One gets

$$\begin{aligned}\boxed{\frac{\partial F_0(\mathbf{J},t)}{\partial t} = -\pi(2\pi)^d \frac{\partial}{\partial\mathbf{J}}\cdot\Bigg[\sum_{\mathbf{k},\mathbf{k}'}\mathbf{k}\int\mathrm{d}\mathbf{J}'\,\left|\psi^{\mathrm{d}}_{\mathbf{k}\mathbf{k}'}(\mathbf{J},\mathbf{J}',\mathbf{k}\cdot\boldsymbol{\Omega}(\mathbf{J}))\right|^2\delta_{\mathrm{D}}(\mathbf{k}\cdot\boldsymbol{\Omega}(\mathbf{J}) - \mathbf{k}'\cdot\boldsymbol{\Omega}(\mathbf{J}'))}\\ \times\left(m_{\mathrm{b}}\,\mathbf{k}'\cdot\frac{\partial}{\partial\mathbf{J}'} - m_{\mathrm{b}}\,\mathbf{k}\cdot\frac{\partial}{\partial\mathbf{J}}\right)F_0(\mathbf{J},t)\,F_0(\mathbf{J}',t)\Bigg].\end{aligned} \tag{5.2}$$

Doing that replacement transforms the differential equation (5.1) into a self-consistent integro-differential equation for the bath's DF. This is the self-consistent inhomogeneous Balescu-Lenard equation (Heyvaerts, 2010; Chavanis, 2012), the main result of the present notes. In order to highlight the total conservation of the number of orbits, one can finally rewrite Eq. (5.2) as a continuity equation in action space, so that it reads

$$\frac{\partial F_0(\mathbf{J},t)}{\partial t} = -\frac{\partial}{\partial\mathbf{J}}\cdot\mathbf{F}(\mathbf{J},t), \tag{5.3}$$

where $\mathbf{F}(\mathbf{J},t)$ is the diffusion flux in action space, and corresponds to the direction in which particles are flowing. This flux is composed of two components, a diffusion and a friction one, and reads

$$\boxed{\mathbf{F}(\mathbf{J}) = \mathbf{D}_1(\mathbf{J})\, F_0(\mathbf{J}) - \mathbf{D}_2(\mathbf{J}) \cdot \frac{\partial F_0}{\partial \mathbf{J}},} \tag{5.4}$$

where the friction coefficient, $\mathbf{D}_1(\mathbf{J})$, and the diffusion tensor, $\mathbf{D}_2(\mathbf{J})$, follow from Eq. (5.2) and read

$$\begin{aligned}
\mathbf{D}_1(\mathbf{J}) &= m_\mathrm{b}\pi(2\pi)^d \sum_{\mathbf{k},\mathbf{k}'} \mathbf{k} \int \mathrm{d}\mathbf{J}'\, \delta_\mathrm{D}(\mathbf{k}\cdot\boldsymbol{\Omega}(\mathbf{J}) - \mathbf{k}'\cdot\boldsymbol{\Omega}(\mathbf{J}'))\, \left|\psi^\mathrm{d}_{\mathbf{k}\mathbf{k}'}(\mathbf{J},\mathbf{J}',\mathbf{k}\cdot\boldsymbol{\Omega}(\mathbf{J}))\right|^2 \mathbf{k}' \cdot \frac{\partial F_0}{\partial \mathbf{J}'}, \\
\mathbf{D}_2(\mathbf{J}) &= m_\mathrm{b}\,\pi(2\pi)^d \sum_{\mathbf{k},\mathbf{k}'} \mathbf{k}\otimes\mathbf{k} \int \mathrm{d}\mathbf{J}'\, \delta_\mathrm{D}(\mathbf{k}\cdot\boldsymbol{\Omega}(\mathbf{J}) - \mathbf{k}'\cdot\boldsymbol{\Omega}(\mathbf{J}'))\, \left|\psi^\mathrm{d}_{\mathbf{k}\mathbf{k}'}(\mathbf{J},\mathbf{J}',\mathbf{k}\cdot\boldsymbol{\Omega}(\mathbf{J}))\right|^2 F_0(\mathbf{J}').
\end{aligned} \tag{5.5}$$

Let us emphasise that all the key specificities of galaxies are accounted for in the Balescu-Lenard equation: (i) the diffusion equation takes place in action space, $\mathbf{J}$, because the galaxy is *inhomogeneous*; (ii) the dynamical quantity of interest is the system's mean DF, $F_0(\mathbf{J},t)$, because the galaxy is *relaxed* onto a quasi-stationary state; (iii) the kinetic equation involves the dressed susceptibility coefficients, $|\psi^\mathrm{d}_{\mathbf{k}\mathbf{k}'}|^2$, because the galaxy is *self-gravitating*; (iv) the collision operator involves a resonance condition over the orbital frequencies, $\delta_\mathrm{D}(\mathbf{k}\cdot\boldsymbol{\Omega}(\mathbf{J})-\mathbf{k}'\cdot\boldsymbol{\Omega}(\mathbf{J}'))$, because the galaxy is *resonant*; (v) the long-term distortions are sourced by the couplings between Poisson shot noise, as higlighted by the $1/N$ prefactor, because the galaxy is *discrete* and *perturbed*.

As detailed in the problem set, the inhomogeneous Balescu-Lenard Eq. (5.2) satisfies numerous important properties. In particular, it conserves mass, energy, and satisfies a H-theorem for Boltzmann entropy. In addition, the Balescu-Lenard diffusion flux exactly vanishes for inhomogeneous Boltzmann DFs of the form $F_0(\mathbf{J}) \propto \mathrm{e}^{-\beta H_0(\mathbf{J})}$.

It is very enlightening to compare this inhomogeneous kinetic equation, with the similar result obtained for homogeneous electrostatic plasmas, the so-called (homogeneous) Balescu-Lenard equation. Indeed, these two equations are fundamentally connected, provided that one makes the following analogies:

	(**Homogeneous**) plasmas	(**Inhomogeneous**) self-gravitating systems
Orbital coordinates	$F_0(\mathbf{v},t)$	$F_0(\mathbf{J},t)$
Basis decomposition	$U(\mathbf{x},\mathbf{x}') \sim \int \frac{\mathrm{d}\mathbf{k}}{\lvert\mathbf{k}\rvert^2}\, \mathrm{e}^{\mathrm{i}\mathbf{k}\cdot(\mathbf{x}-\mathbf{x}')}$	$U(\mathbf{x},\mathbf{x}') = -\sum_p \psi^{(p)}(\mathbf{x})\, \psi^{(p)*}(\mathbf{x}')$
Response matrix	$\sim \int \mathrm{d}\mathbf{v}\, \frac{\mathbf{k}\cdot\partial F/\partial\mathbf{v}}{(\omega - \mathbf{k}\cdot\mathbf{v})}$	$\sim \sum_{\mathbf{k}} \int \mathrm{d}\mathbf{J}\, \frac{\mathbf{k}\cdot\partial F_0/\partial\mathbf{J}}{\omega - \mathbf{k}\cdot\boldsymbol{\Omega}(\mathbf{J})}\, \psi^{(p)*}_{\mathbf{k}}(\mathbf{J})\, \psi^{(q)}_{\mathbf{k}}(\mathbf{J})$
Perturbations dressing	$\frac{1}{\left\lvert\varepsilon(\mathbf{v},\mathbf{k}\cdot\mathbf{v})\right\rvert^2}$	$\left\lvert\psi^\mathrm{d}_{\mathbf{k}\mathbf{k}'}(\mathbf{J},\mathbf{J}',\mathbf{k}\cdot\boldsymbol{\Omega}(\mathbf{J}))\right\rvert^2$
Resonance vectors	$\int \mathrm{d}\mathbf{k} \ldots$	$\sum_{\mathbf{k},\mathbf{k}'} \ldots$
Resonance condition	$\delta_\mathrm{D}(\mathbf{k}\cdot(\mathbf{v}-\mathbf{v}'))$	$\delta_\mathrm{D}(\mathbf{k}\cdot\boldsymbol{\Omega}(\mathbf{J}) - \mathbf{k}'\cdot\boldsymbol{\Omega}(\mathbf{J}'))$

(5.6)

In the limit of a dynamically hot system, i.e. a system for which collective effects can be neglected, the inhomogeneous Balescu-Lenard equation becomes the inhomogeneous Landau equation where the only change is the replacement of the dressed susceptibility coefficients $\psi^\mathrm{d}_{\mathbf{k}\mathbf{k}'}(\mathbf{J},\mathbf{J}',\mathbf{k}\cdot\boldsymbol{\Omega}(\mathbf{J}))$ by their bare analogs $\psi_{\mathbf{k}\mathbf{k}'}(\mathbf{J},\mathbf{J}')$.

It is also straightforward to generalise Eq. (5.2) to the case of a multi-mass bath. To do so, we assume that the bath is composed of multiple components of individual mass $(m_\alpha, ..., m_\beta)$, each component being described by a quasi-stationary DF of the form $F_\alpha(\mathbf{J},t)$, following the normalisation convention $\int \mathrm{d}\boldsymbol{\theta}\mathrm{d}\mathbf{J} F_\alpha = M_\alpha$, with M_α the total mass of the component α. The self-consistent evolution of the component α is then sourced by the effects from itself and all the other components. More precisely, it reads

$$\begin{aligned}
\frac{\partial F_\alpha(\mathbf{J},t)}{\partial t} = -\pi(2\pi)^d \frac{\partial}{\partial \mathbf{J}} \cdot \Bigg[\sum_{\mathbf{k},\mathbf{k}'} \mathbf{k} \int \mathrm{d}\mathbf{J}'\, \left|\psi^\mathrm{d}_{\mathbf{k}\mathbf{k}'}(\mathbf{J},\mathbf{J}',\mathbf{k}\cdot\boldsymbol{\Omega}(\mathbf{J}))\right|^2 \delta_\mathrm{D}(\mathbf{k}\cdot\boldsymbol{\Omega}(\mathbf{J}) - \mathbf{k}'\cdot\boldsymbol{\Omega}(\mathbf{J}')) \\
\times \sum_\beta \left(m_\alpha\, \mathbf{k}' \cdot \frac{\partial}{\partial \mathbf{J}'} - m_\beta\, \mathbf{k}\cdot\frac{\partial}{\partial\mathbf{J}} \right) F_\alpha(\mathbf{J},t)\, F_\beta(\mathbf{J}',t) \Bigg],
\end{aligned} \tag{5.7}$$

where the sum over β runs over all the system's components. In the multi-mass case, the dressed susceptibility coefficients now involve all the active components that drive the self-gravitating amplification, so that in the expression of the response matrix from Eq. (3.72), one has to make the replacement $F_0 \to \sum_\beta F_\beta$. We note that

it is the subtle changes in the mass prefactors in the cross term $(m_\alpha ... - m_\beta ...)$ that is the sole responsible for the mass segregation of the different components one w.r.t. another.

6 Balescu-Lenard from Klimontovich

One could be worried that in the process of "gluing" together the diffusion (Section 3) and the dynamical friction (Section 4) to obtain the self-consistent Balescu-Lenard equation (Section 5), we might have missed some subtle contributions to the system's self-consistent dynamics.

In this section, we will show how the Balescu-Lenard Eq. (5.2) can indeed be obtained directly and self-consistently from a perturbative expansion of the bath's evolution equations, more precisely by a quasi-linear expansion of the Klimontovich equation. In particular, we will emphasise how the two respective contributions from the diffusion and the friction components naturally arise. As we will note, this calculation will also be rather straightforward, as most of the technicalities have already been dealt with in the previous sections.

We recall that the bath is assumed to be composed of N particles of individual mass $m_{\rm b} = M_{\rm tot}/N$. As already introduced in Eq. (2.6), the state of the system is fully described by the discrete DF

$$F_{\rm d} = \sum_{i=1}^{N} m_{\rm b} \delta_{\rm D}(\mathbf{x} - \mathbf{x}_i(t)) \delta_{\rm D}(\mathbf{v} - \mathbf{v}_i(t)), \tag{6.1}$$

where $(\mathbf{x}_i(t), \mathbf{v}_i(t))$ stands for the location in phase space at time t of the $i^{\rm th}$ particle of the bath. The dynamics of that distribution function is exactly governed by the Klimontovich Eq. (2.13) that takes here the short form

$$\frac{\partial F_{\rm d}}{\partial t} + \big[F_{\rm d}, H_{\rm d}\big] = 0. \tag{6.2}$$

In that equation, we have introduced the (specific) discrete Hamiltonian $H_{\rm d}$ as

$$H_{\rm d}(\mathbf{x}, \mathbf{v}, t) = \frac{1}{2}|\mathbf{v}|^2 + \Phi_{\rm d}(\mathbf{x}, t). \tag{6.3}$$

Here, the crucial point is to recall that the instantaneous discrete potential, $\Phi_{\rm d} = \Phi_{\rm d}[F_{\rm d}]$, depends directly on the system's instantaneous DF, through the relation

$$\Phi_{\rm d}(\mathbf{x}, t) = \int {\rm d}\mathbf{x}' {\rm d}\mathbf{v}' \, F_{\rm d}(\mathbf{x}', \mathbf{v}', t) \, U(\mathbf{x}, \mathbf{x}'), \tag{6.4}$$

with $U(\mathbf{x}, \mathbf{x}')$ is the considered pairwise long-range interaction. In the particular case of the $3D$ gravitational interaction, for which $U(\mathbf{x}, \mathbf{x}') = -G/|\mathbf{x} - \mathbf{x}'|$, Eq. (6.4) can be rewritten as Poisson's equation, namely

$$\Delta \Phi_{\rm d} = 4\pi G \rho_{\rm d} = 4\pi G \int {\rm d}\mathbf{v} \, F_{\rm d}(\mathbf{x}, \mathbf{v}, t) = 4\pi G \sum_{i=1}^{N} m_{\rm b} \, \delta_{\rm D}(\mathbf{x} - \mathbf{x}_i(t)). \tag{6.5}$$

6.1 Quasi-linear expansion of the Klimontovich equation

Similarly to Eq. (3.32), we now assume that the system's DF can be decomposed into two components, so that

$$F_{\rm d} = F_0 + \delta F \quad \text{with} \quad F_0 = F_0(\mathbf{J}, t); \quad \big\langle \delta F \big\rangle = 0. \tag{6.6}$$

In that equation, we recall that $F_0 = \langle F_{\rm d} \rangle$ is the smooth underlying mean-field DF of the system, δF are the fluctuations around this mean distribution, with $\langle \cdot \rangle$ the ensemble average over realisations of the system. The key assumptions here are that there exist some angle-action coordinates $(\boldsymbol{\theta}, \mathbf{J})$ within which $F_0 = F_0(\mathbf{J}, t)$, i.e. for which the mean-field distribution is in a quasi-stationary state. We also assume that the system is close to that mean-field equilibrium, so that $\delta F \ll F_0$, allowing us to perform perturbative expansions w.r.t. the amplitude of the perturbations. Following Eq. (6.3), to any mean-field distribution F_0, we can associate an (integrable) mean-field Hamiltonian $H_0 = H_0(\mathbf{J}, t)$ reading

$$H_0 = \frac{1}{2}|\mathbf{v}|^2 + \Phi_0 = \frac{1}{2}|\mathbf{v}|^2 + \int {\rm d}\mathbf{x}' {\rm d}\mathbf{v}' \, F_0(\mathbf{x}', \mathbf{v}', t) \, U(\mathbf{x}, \mathbf{x}'). \tag{6.7}$$

Following Eq. (6.4), to any perturbation δF, we can also associate a perturbing potential $\delta\Phi = \delta\Phi[\delta F]$ through

$$\delta\Phi(\mathbf{x}, t) = \int {\rm d}\mathbf{x}' {\rm d}\mathbf{v}' \, U(\mathbf{x}, \mathbf{x}') \, \delta F(\mathbf{x}', \mathbf{v}', t). \tag{6.8}$$

We can now inject the decomposition from Eq. (6.6) into the evolution equation (6.2), to characterise not only the dynamics of the perturbations in the system, but also the long-term orbital reshufflings irreversibly undergone by the mean system. This reads

$$\frac{\partial F_0}{\partial t} + \frac{\partial \delta F}{\partial t} + \big[F_0 + \delta F, H_0 + \delta\Phi\big] = 0. \tag{6.9}$$

We recall that $\big[F_0(\mathbf{J},t), H_0(\mathbf{J},t)\big] = 0$ as the mean system is assumed to be in a collisionless equilibrium, and that $\langle \delta F\rangle = 0$ and $\langle \delta\Phi\rangle = 0$ as the perturbations are assumed to be of zero average. Taking the ensemble average of Eq. (6.9), we obtain

$$\frac{\partial F_0}{\partial t} + \big\langle \big[\delta F, \delta\Phi\big]\big\rangle = 0. \tag{6.10}$$

This tells us that the slow and irreversible orbital diffusion undergone by the system's averaged DF occurs at second-order in the perturbations. This is what will drive the system's secular evolution. As the mean DF is only a function of $\mathbf{J}$, we can perform an average of it w.r.t. $\boldsymbol{\theta}$, which gives us

$$\frac{\partial F_0(\mathbf{J},t)}{\partial t} = -\frac{\partial}{\partial \mathbf{J}} \cdot \mathbf{F}(\mathbf{J},t), \tag{6.11}$$

where we have introduced the diffusion flux $\mathbf{F}(\mathbf{J},t)$ as

$$\begin{aligned}
\mathbf{F}(\mathbf{J}) &= \sum_{\mathbf{k}} \mathrm{i}\mathbf{k} \big\langle \delta F_{\mathbf{k}}(\mathbf{J},t)\, \delta\Phi_{-\mathbf{k}}(\mathbf{J},t)\big\rangle, \\
&= \sum_{\mathbf{k}} \mathrm{i}\mathbf{k} \int_{\mathcal{B}} \frac{\mathrm{d}\omega}{2\pi} \int_{\mathcal{B}'} \frac{\mathrm{d}\omega'}{2\pi}\, \mathrm{e}^{-\mathrm{i}(\omega+\omega')t} \big\langle \delta\widetilde{F}_{\mathbf{k}}(\mathbf{J},\omega)\, \delta\widetilde{\Phi}_{-\mathbf{k}}(\mathbf{J},\omega')\big\rangle,
\end{aligned} \tag{6.12}$$

where our convention for the Fourier and Laplace transforms were already introduced in Eq. (3.3) and (3.57). Deriving the system's long-term kinetic equation amounts then to computing explicitly the ensemble-averaged term $\big\langle \delta F_{\mathbf{k}} \delta\Phi_{-\mathbf{k}}\big\rangle$, and express it solely as a function of the system's mean quantities such as $F_0(\mathbf{J})$ and $\boldsymbol{\Omega}(\mathbf{J})$.

We can now glance back at Eq. (6.9), and keeping only terms first order in the perturbations, we recover that the dynamics of the perturbations in the system evolves according to the linearised Klimontovich equation

$$\frac{\partial \delta F}{\partial t} + \big[\delta F, H_0\big] + \big[F_0, \delta\Phi\big] = 0. \tag{6.13}$$

In that equation, the first Poisson bracket corresponds to phase mixing, i.e. the unperturbed free streaming of perturbations as imposed by the mean-field potential (see Fig. 2.4), while the second Poisson bracket is associated with collective effects, i.e. describes the fact that the system is submitted to the perturbations that it spontaneously generates, since $\delta\Phi = \delta\Phi[\delta F]$. We have already encountered a similar equation in Eq. (3.55), when describing the dynamics of perturbations in a live self-gravitating bath. And in Eq. (3.56), we showed that in Laplace-Fourier space, the perturbations are connected through the relation

$$\delta\widetilde{F}_{\mathbf{k}}(\mathbf{J},\omega) = -\frac{\mathbf{k}\cdot\partial F_0/\partial \mathbf{J}}{\omega - \mathbf{k}\cdot\boldsymbol{\Omega}(\mathbf{J})}\, \delta\widetilde{\Phi}_{\mathbf{k}}(\mathbf{J},\omega) - \frac{\delta F_{\mathbf{k}}(\mathbf{J},0)}{\mathrm{i}(\omega - \mathbf{k}\cdot\boldsymbol{\Omega}(\mathbf{J}))}, \tag{6.14}$$

where, we recall that here we have assumed Bogoliubov's ansatz, i.e. we have assumed that the system's mean orbital structure evolves on a much longer timescale than the perturbations in the system, allowing us to treat $F_0(\mathbf{J})$ and $\boldsymbol{\Omega}(\mathbf{J})$ as time-independent on the dynamical timescale over which the perturbations evolve. In the present context, this is justified by Eq. (6.11) which shows that the orbital distortions undergone by $F_0(\mathbf{J},t)$ only occur at second order in the perturbations. Finally, following Eq. (3.61), the potential fluctuations $\delta\Phi_{\mathbf{k}}$ satisfy

$$\delta\widetilde{\Phi}_{\mathbf{k}}(\mathbf{J},\omega) = -(2\pi)^d \sum_{\mathbf{k}'} \int \mathrm{d}\mathbf{J}'\, \frac{\delta F_{\mathbf{k}'}(\mathbf{J}',0)}{\mathrm{i}(\omega - \mathbf{k}'\cdot\boldsymbol{\Omega}(\mathbf{J}'))}\, \psi^{\mathrm{d}}_{\mathbf{k}\mathbf{k}'}(\mathbf{J},\mathbf{J}',\omega). \tag{6.15}$$

In Eq. (6.15), we note that the potential perturbations present in the system are sourced by the initial Poisson fluctuations in the system, which come dressed, i.e. this expression involves the dressed susceptibility coefficients, $\psi^{\mathrm{d}}_{\mathbf{k}\mathbf{k}'}$, as defined in Eq. (3.75).

Having characterised the dynamics of the perturbations in the system, we can now set out to explicitly compute the second-order average term appearing in the diffusion flux from Eq. (6.12). Because Eq. (6.14) has two terms, the diffusion flux can similarly be separated in two components $\mathbf{F} = \mathbf{F}_1 + \mathbf{F}_2$, that respectively read

$$\begin{aligned}
\mathbf{F}_1(\mathbf{J}) &= -\sum_{\mathbf{k}} \mathbf{k} \int_{\mathcal{B}} \frac{\mathrm{d}\omega}{2\pi} \int_{\mathcal{B}'} \frac{\mathrm{d}\omega'}{2\pi}\, \frac{\mathrm{e}^{-\mathrm{i}(\omega+\omega')t}}{\omega - \mathbf{k}\cdot\boldsymbol{\Omega}(\mathbf{J})} \big\langle \delta F_{\mathbf{k}}(\mathbf{J},0)\, \delta\widetilde{\Phi}_{-\mathbf{k}}(\mathbf{J},\omega')\big\rangle, \\
\mathbf{F}_2(\mathbf{J}) &= -\sum_{\mathbf{k}} \mathrm{i}\mathbf{k}\, \mathbf{k}\cdot\frac{\partial F_0}{\partial \mathbf{J}} \int_{\mathcal{B}} \frac{\mathrm{d}\omega}{2\pi} \int_{\mathcal{B}'} \frac{\mathrm{d}\omega'}{2\pi}\, \frac{\mathrm{e}^{-\mathrm{i}(\omega+\omega')t}}{\omega - \mathbf{k}\cdot\boldsymbol{\Omega}(\mathbf{J})} \big\langle \delta\widetilde{\Phi}_{\mathbf{k}}(\mathbf{J},\omega)\, \delta\widetilde{\Phi}_{-\mathbf{k}}(\mathbf{J},\omega')\big\rangle.
\end{aligned} \tag{6.16}$$

Here, on the one hand, we note that the first diffusion component, $\mathbf{F}_1(\mathbf{J})$, is sourced by the correlations existing between one particular fluctuations in the system's DF, via the term $\delta F_{\mathbf{k}}(\mathbf{J},0)$, and the associated potential perturbations generated in the system, via the term $\delta\widetilde{\Phi}_{-\mathbf{k}}(\mathbf{J},\omega')$. As a consequence, this first flux is sourced by the correlation between one perturbation and the system's associated potential response. This corresponds exactly to the basis on which we derived the dynamical friction in Section 4, where we derived the (dressed) friction generated by the back-reaction of the bath induced by the perturbation from a test particle. As a consequence, we naturally expect that this first flux will be the one associated with the friction component of the Balescu-Lenard equation. On the other hand, we note that the second flux component, $\mathbf{F}_2(\mathbf{J})$, is sourced by the correlations between the potential fluctuations, via the term $\langle\delta\widetilde{\Phi}_{\mathbf{k}}(\mathbf{J},\omega)\,\delta\widetilde{\Phi}_{-\mathbf{k}}(\mathbf{J},\omega')\rangle$. As already discussed in detail in Section 3, we know that such potential correlations are sourcing a diffusion in the system. This is also illustrated by the fact that this component is proportional to the gradient $\mathbf{k}\cdot\partial F_0/\partial\mathbf{J}$, the same type of gradient that also appeared in the diffusion Eq. (3.25). As a consequence, we expect that this second flux will be responsible for the diffusion component of the Balescu-Lenard equation. Let us now compute explicitly the ensemble averages appearing in Eq. (6.16). The main difficulty of this calculation is to correctly perform the two inverse Laplace transforms, and correctly handle the resonant poles that appear.

6.2 Computing $\mathbf{F}_1(\mathbf{J})$

Let us first consider the flux component $\mathbf{F}_1(\mathbf{J})$, as defined in Eq. (6.16). Reinjecting the self-consistent relation from Eq. (6.15), we can rewrite $\mathbf{F}_1(\mathbf{J})$ as

$$\mathbf{F}_1(\mathbf{J}) = -\mathrm{i}(2\pi)^d \sum_{\mathbf{k}} \mathbf{k} \int_{\mathcal{B}} \frac{\mathrm{d}\omega}{2\pi} \int_{\mathcal{B}'} \frac{\mathrm{d}\omega'}{2\pi} \, \frac{\mathrm{e}^{-\mathrm{i}(\omega+\omega')t}}{\omega - \mathbf{k}\cdot\boldsymbol{\Omega}(\mathbf{J})} \sum_{\mathbf{k}'} \int \mathrm{d}\mathbf{J}' \, \frac{\psi^{\mathrm{d}}_{-\mathbf{k}\mathbf{k}'}(\mathbf{J},\mathbf{J}',\omega')}{\omega' - \mathbf{k}'\cdot\boldsymbol{\Omega}(\mathbf{J}')} \left\langle \delta F_{\mathbf{k}}(\mathbf{J},0)\, \delta F_{\mathbf{k}'}(\mathbf{J}',0) \right\rangle. \tag{6.17}$$

In Eq. (3.49), we already characterised the statistics of the fluctuations in the system's DF at the initial time. These are only sourced by the initial Poisson shot noise and gave us (for $(\mathbf{k},\mathbf{k}') \neq (0,0)$)

$$\left\langle \delta F_{\mathbf{k}}(\mathbf{J},0)\, \delta F_{\mathbf{k}'}(\mathbf{J}',0) \right\rangle = \frac{m_{\mathrm{b}}}{(2\pi)^d} \, \delta_{\mathbf{k}-\mathbf{k}'} \, \delta_{\mathrm{D}}(\mathbf{J}-\mathbf{J}') \, F_0(\mathbf{J}), \tag{6.18}$$

where we used the fact that δF is a real function, so that $\delta F_{-\mathbf{k}}(\mathbf{J}) = \delta F^*_{\mathbf{k}}(\mathbf{J})$. We can now use Eq. (6.18) to compute explicitly the initial correlations in the system's DF, and we obtain

$$\mathbf{F}_1(\mathbf{J}) = -m_{\mathrm{b}} \, F_0(\mathbf{J}) \sum_{\mathbf{k}} \mathrm{i}\mathbf{k} \int_{\mathcal{B}} \frac{\mathrm{d}\omega}{2\pi} \int_{\mathcal{B}'} \frac{\mathrm{d}\omega'}{2\pi} \, \frac{\mathrm{e}^{-\mathrm{i}(\omega+\omega')t}}{\omega - \mathbf{k}\cdot\boldsymbol{\Omega}(\mathbf{J})} \, \frac{\psi^{\mathrm{d}}_{-\mathbf{k}-\mathbf{k}}(\mathbf{J},\mathbf{J},\omega')}{\omega' + \mathbf{k}\cdot\boldsymbol{\Omega}(\mathbf{J})}. \tag{6.19}$$

We may now compute the remaining inverse Laplace transforms over ω and ω'. We have assumed that the system is linearly stable, so that $\omega' \mapsto \psi^{\mathrm{d}}_{-\mathbf{k}-\mathbf{k}}(\mathbf{J},\mathbf{J},\omega')$ has no poles in the upper half complex plane. Each of the two frequency integrals then only involve one pole, and integrals can then be carried out by lowering the integration contours to low imaginary values, where the value of $\mathrm{e}^{-\mathrm{i}(\omega+\omega')t}$ vanishes. Assuming that t is large enough for the contributions from the transients associated with the system's damped modes to be neglected (see Eq. (3.77)), only the contributions from the obvious poles in $\omega = \mathbf{k}\cdot\boldsymbol{\Omega}(\mathbf{J})$ and $\omega' = -\mathbf{k}\cdot\boldsymbol{\Omega}(\mathbf{J})$ remain, contributing each a $-2\pi\mathrm{i}$ times the associated residue. In that process, we also note that the time dependence in $\mathrm{e}^{-\mathrm{i}(\omega+\omega')t}$ exactly vanishes: this is a signature of the fact that the relaxation happens at resonance. Paying a careful attention to the signs, and making the change of variable $\mathbf{k} \mapsto -\mathbf{k}$, we can finally rewrite Eq. (6.19) as

$$\mathbf{F}_1(\mathbf{J}) = -m_{\mathrm{b}} \, F_0(\mathbf{J}) \sum_{\mathbf{k}} \mathrm{i}\mathbf{k} \, \psi^{\mathrm{d}}_{\mathbf{k}\mathbf{k}}(\mathbf{J},\mathbf{J},\mathbf{k}\cdot\boldsymbol{\Omega}(\mathbf{J})). \tag{6.20}$$

Glancing back at Eq. (4.20), we note that this expression exacly matches the diffusion coefficient $\mathbf{D}_1(\mathbf{J})$ (where one replaces m_{t} the mass of the test star with m_{b} the mass of the system's particles). As a consequence, relying on the final result from Eq. (4.32), we can rewrite the first flux as

$$\mathbf{F}_1(\mathbf{J}) = \mathbf{D}_1(\mathbf{J}) \, F_0(\mathbf{J}), \tag{6.21}$$

where the friction coefficient $\mathbf{D}_1(\mathbf{J})$ follows from Eq. (4.32) and reads

$$\mathbf{D}_1(\mathbf{J}) = m_{\mathrm{b}}\pi(2\pi)^d \sum_{\mathbf{k},\mathbf{k}'} \mathbf{k} \int \mathrm{d}\mathbf{J}' \, \delta_{\mathrm{D}}(\mathbf{k}\cdot\boldsymbol{\Omega}(\mathbf{J}) - \mathbf{k}'\cdot\boldsymbol{\Omega}(\mathbf{J}')) \left|\psi^{\mathrm{d}}_{\mathbf{k}\mathbf{k}'}(\mathbf{J},\mathbf{J}',\mathbf{k}\cdot\boldsymbol{\Omega}(\mathbf{J}))\right|^2 \mathbf{k}' \cdot \frac{\partial F_0}{\partial \mathbf{J}'}. \tag{6.22}$$

As such, we have fully recovered that, indeed, the flux $\mathbf{F}_1(\mathbf{J})$ is the contribution directly associated with the dressed dynamical friction occurring on each fluctuations in the system.

6.3 Computing $\mathbf{F}_2(\mathbf{J})$

Let us now consider the second flux $\mathbf{F}_2(\mathbf{J})$. Injecting twice Eq. (6.15) into the definition from Eq. (6.16), we can rewrite this flux as

$$\begin{aligned}\mathbf{F}_2(\mathbf{J}) = (2\pi)^{2d} \sum_{\mathbf{k}} \mathrm{i}\mathbf{k}\,\mathbf{k}\cdot\frac{\partial F_0}{\partial \mathbf{J}} \int_{\mathcal{B}}\frac{\mathrm{d}\omega}{2\pi}\int_{\mathcal{B}'}\frac{\mathrm{d}\omega'}{2\pi}\,\frac{\mathrm{e}^{-\mathrm{i}(\omega+\omega')t}}{\omega-\mathbf{k}\cdot\boldsymbol{\Omega}(\mathbf{J})} \\ \times \sum_{\mathbf{k}',\mathbf{k}''}\int\mathrm{d}\mathbf{J}'\int\mathrm{d}\mathbf{J}''\,\frac{\psi^{\mathrm{d}}_{\mathbf{k}\mathbf{k}'}(\mathbf{J},\mathbf{J}',\omega)}{\omega-\mathbf{k}'\cdot\boldsymbol{\Omega}(\mathbf{J}')}\,\frac{\psi^{\mathrm{d}}_{-\mathbf{k}\mathbf{k}''}(\mathbf{J},\mathbf{J}'',\omega')}{\omega'-\mathbf{k}''\cdot\boldsymbol{\Omega}(\mathbf{J}'')}\,\big\langle\delta F_{\mathbf{k}'}(\mathbf{J}',0)\,\delta F_{\mathbf{k}''}(\mathbf{J}'',0)\big\rangle. \end{aligned} \tag{6.23}$$

We can then use Eq. (6.18) to compute the ensemble average over the initial conditions of the DF. We get

$$\mathbf{F}_2(\mathbf{J}) = m_{\mathrm{b}}(2\pi)^d \sum_{\mathbf{k},\mathbf{k}'} \mathrm{i}\mathbf{k}\,\mathbf{k}\cdot\frac{\partial F_0}{\partial \mathbf{J}} \int_{\mathcal{B}}\frac{\mathrm{d}\omega}{2\pi}\int_{\mathcal{B}'}\frac{\mathrm{d}\omega'}{2\pi}\,\frac{\mathrm{e}^{-\mathrm{i}(\omega+\omega')t}}{\omega-\mathbf{k}\cdot\boldsymbol{\Omega}(\mathbf{J})}\int\mathrm{d}\mathbf{J}'\,\frac{\psi^{\mathrm{d}}_{\mathbf{k}\mathbf{k}'}(\mathbf{J},\mathbf{J}',\omega)}{\omega-\mathbf{k}'\cdot\boldsymbol{\Omega}(\mathbf{J}')}\,\frac{\psi^{\mathrm{d}}_{-\mathbf{k}-\mathbf{k}'}(\mathbf{J},\mathbf{J}',\omega')}{\omega'+\mathbf{k}'\cdot\boldsymbol{\Omega}(\mathbf{J}')}\,F_0(\mathbf{J}'). \tag{6.24}$$

Using the same reasoning as in Eq. (6.19), we can perform the integral over ω', noting that it involves a single pole on the real axis, in $\omega' = -\mathbf{k}'\cdot\boldsymbol{\Omega}(\mathbf{J}')$, the other poles being damped. Recalling that with our convention each pole contributes a $-2\pi\mathrm{i}$ times the residue, for t large enough so that damped modes have faded away, we can rewrite Eq. (6.24) as

$$\begin{aligned}\mathbf{F}_2(\mathbf{J}) = m_{\mathrm{b}}(2\pi)^d \sum_{\mathbf{k},\mathbf{k}'} \mathbf{k}\,\mathbf{k}\cdot\frac{\partial F_0}{\partial \mathbf{J}}\int\mathrm{d}\mathbf{J}'\,F_0(\mathbf{J}')\,\mathrm{e}^{\mathrm{i}\mathbf{k}'\cdot\boldsymbol{\Omega}(\mathbf{J}')t}\,\psi^{\mathrm{d}*}_{\mathbf{k}\mathbf{k}'}(\mathbf{J},\mathbf{J}',\mathbf{k}'\cdot\boldsymbol{\Omega}(\mathbf{J}')) \\ \times\int_{\mathcal{B}}\frac{\mathrm{d}\omega}{2\pi}\,\mathrm{e}^{-\mathrm{i}\omega t}\,\frac{\psi^{\mathrm{d}}_{\mathbf{k}\mathbf{k}'}(\mathbf{J},\mathbf{J}',\omega)}{(\omega-\mathbf{k}\cdot\boldsymbol{\Omega}(\mathbf{J}))(\omega-\mathbf{k}'\cdot\boldsymbol{\Omega}(\mathbf{J}'))}, \end{aligned} \tag{6.25}$$

where we used the relation $\psi^{\mathrm{d}}_{-\mathbf{k}-\mathbf{k}'}(\mathbf{J},\mathbf{J}',-\omega_{\mathrm{R}}) = \psi^{\mathrm{d}*}_{\mathbf{k}\mathbf{k}'}(\mathbf{J},\mathbf{J}',\omega_{\mathrm{R}})$ that is a direct consequence of the symmetry relation from Eq. (4.27). Let us now perform in Eq. (6.25) the last remaining inverse Laplace transform over ω. Paying a careful attention to the fact that there are two poles, and that each of them contributes $-2\pi\mathrm{i}$ times the associated residue, we obtain

$$\begin{aligned}\int_{\mathcal{B}}\frac{\mathrm{d}\omega}{2\pi}\,\mathrm{e}^{-\mathrm{i}\omega t}\,\frac{\psi^{\mathrm{d}}_{\mathbf{k}\mathbf{k}'}(\mathbf{J},\mathbf{J}',\omega)}{(\omega-\omega_1)(\omega-\omega_2)} &= -\mathrm{i}\left(\frac{\mathrm{e}^{-\mathrm{i}\omega_1 t}\,\psi^{\mathrm{d}}(\omega_1)}{\omega_1-\omega_2}+\frac{\mathrm{e}^{-\mathrm{i}\omega_2 t}\psi^{\mathrm{d}}(\omega_2)}{\omega_2-\omega_1}\right) \\ &= \mathrm{i}\,\mathrm{e}^{-\mathrm{i}\omega_2 t}\,\psi^{\mathrm{d}}(\omega_2)\,\frac{1}{\omega_1-\omega_2}\left(1-\mathrm{e}^{-\mathrm{i}(\omega_1-\omega_2)t}\,\frac{\psi^{\mathrm{d}}(\omega_1)}{\psi^{\mathrm{d}}(\omega_2)}\right) \end{aligned} \tag{6.26}$$

where we shortened the notations with $\omega_1 = \mathbf{k}\cdot\boldsymbol{\Omega}(\mathbf{J})$, and $\omega_2 = \mathbf{k}'\cdot\boldsymbol{\Omega}(\mathbf{J}')$, as well as $\psi^{\mathrm{d}}(\omega) = \psi_{\mathbf{k}\mathbf{k}'}(\mathbf{J},\mathbf{J}',\omega)$. When injected back in Eq. (6.25), this gives

$$\begin{aligned}\mathbf{F}_2(\mathbf{J}) = \mathrm{i}\,m_{\mathrm{b}}(2\pi)^d \sum_{\mathbf{k},\mathbf{k}'} \mathbf{k}\,\mathbf{k}\cdot\frac{\partial F_0}{\partial \mathbf{J}}\int\mathrm{d}\mathbf{J}'\,F_0(\mathbf{J}')\,\big|\psi^{\mathrm{d}}_{\mathbf{k}\mathbf{k}'}(\mathbf{J},\mathbf{J}',\mathbf{k}'\cdot\boldsymbol{\Omega}(\mathbf{J}'))\big|^2 \\ \times\lim_{t\to+\infty}\frac{1}{\omega_1-\omega_2}\left(1-\mathrm{e}^{-\mathrm{i}(\omega_1-\omega_2)t}\,\frac{\psi^{\mathrm{d}}(\omega_1)}{\psi^{\mathrm{d}}(\omega_2)}\right), \end{aligned} \tag{6.27}$$

where the limit $t\to+\infty$ stands for our assumption of the Bogoliubov's ansatz, i.e.the fact that since perturbations evolve much faster than the mean system, we may replace these perturbations with their asymptotic time behaviours, when we evaluate the long-term kinetic operator.

Luckily, that time limit can be straightforwardly computed. It is of the generic form

$$\lim_{t\to+\infty}\frac{1-\alpha\,\mathrm{e}^{-\mathrm{i}\omega_{\mathrm{R}}t}}{\omega_{\mathrm{R}}} = \lim_{t\to+\infty}\lim_{\substack{\varepsilon\to0\\\varepsilon>0}}\frac{1-\alpha\mathrm{e}^{-\mathrm{i}(\omega_{\mathrm{R}}-\mathrm{i}\varepsilon)t}}{\omega_{\mathrm{R}}-\mathrm{i}\varepsilon} = \lim_{\substack{\varepsilon\to0\\\varepsilon>0}}\frac{1}{\omega_{\mathrm{R}}-\mathrm{i}\varepsilon} = \mathcal{P}\left(\frac{1}{\omega_{\mathrm{R}}}\right)+\mathrm{i}\pi\delta_{\mathrm{D}}(\omega_{\mathrm{R}}), \tag{6.28}$$

where we used the Plemelj formula from Eq. (4.23). We can now use this result to rewrite Eq. (6.27) as

$$\mathbf{F}_2(\mathbf{J}) = -m_{\mathrm{b}}\pi(2\pi)^d \sum_{\mathbf{k},\mathbf{k}'} \mathbf{k}\,\mathbf{k}\cdot\frac{\partial F_0}{\partial \mathbf{J}}\int\mathrm{d}\mathbf{J}'\,\delta_{\mathrm{D}}(\mathbf{k}\cdot\boldsymbol{\Omega}(\mathbf{J})-\mathbf{k}'\cdot\boldsymbol{\Omega}(\mathbf{J}'))\,\big|\psi^{\mathrm{d}}_{\mathbf{k}\mathbf{k}'}(\mathbf{J},\mathbf{J}',\mathbf{k}\cdot\boldsymbol{\Omega}(\mathbf{J}))\big|^2\,F_0(\mathbf{J}'), \tag{6.29}$$

where we used the fact that the diffusion flux is real, so that the principal value does not contribute. As a consequence, we can rewrite this second contribution to the flux as

$$\mathbf{F}_2(\mathbf{J}) = -\mathbf{D}_2(\mathbf{J})\cdot\frac{\partial F_0}{\partial \mathbf{J}}, \tag{6.30}$$

where the diffusion tensor, $\mathbf{D}_2(\mathbf{J})$, was already obtained in Eq. (3.79), and reads

$$\mathbf{D}_2(\mathbf{J}) = m_\mathrm{b}\pi(2\pi)^d \sum_{\mathbf{k},\mathbf{k}'} \mathbf{k}\otimes\mathbf{k} \int \mathrm{d}\mathbf{J}'\, \delta_\mathrm{D}(\mathbf{k}\cdot\boldsymbol{\Omega}(\mathbf{J}) - \mathbf{k}'\cdot\boldsymbol{\Omega}(\mathbf{J}'))\, \big|\psi^\mathrm{d}_{\mathbf{k}\mathbf{k}'}(\mathbf{J},\mathbf{J}',\mathbf{k}\cdot\boldsymbol{\Omega}(\mathbf{J}))\big|^2\, F_0(\mathbf{J}'). \tag{6.31}$$

As such, we have fully recovered that the flux $\mathbf{F}_2(\mathbf{J})$ is associated with the diffusion component sourced by the temporal correlations in the system's self-induced and dressed potential perturbations.

Gathering the results from Eqs. (6.21) and (6.30), we have therefore been able to rewrite the total diffusion flux from Eq. (6.11) as

$$\boxed{\frac{\partial F_0(\mathbf{J},t)}{\partial t} = -\frac{\partial}{\partial \mathbf{J}}\cdot\left[\mathbf{D}_1(\mathbf{J})\, F_0(\mathbf{J}) - \mathbf{D}_2(\mathbf{J})\cdot\frac{\partial F_0}{\partial \mathbf{J}}\right],} \tag{6.32}$$

and we fully recovered the final form of the self-consistent inhomogeneous Balescu-Lenard equation already obtained in Eq. (5.2).

7 Some examples of long-term relaxation

The generic formalism developed in the previous sections can provide deep insights into the long-term dynamics of astrophysical self-gravitating systems. We will now illustrate some of these results in systems, diverse in scales and dynamical temperatures, but all governed by the same long-range gravitational interaction. We will successively consider the example of axisymmetric discs, such as the Milky Way's galactic disc, and spherical systems such as galactic nuclei, i.e. the dynamics of stars orbiting a supermassive black hole (BH).

7.1 Galactic discs

7.1.1 Angle-actions and basis for discs

A first interesting testbed for the present formalism is the case of axisymmetric galactic discs, i.e. the motion of stars constrained to a $2D$ plane. For such a system, the physical space is of dimension $d=2$, that we describe with the polar coordinates (r,ϕ). Assuming that the mean potential, $\Phi(r)$, is axisymmetric, angle-action coordinates are readily constructed (Binney & Tremaine, 2008). The two actions of the system are $(J_1,J_2)=(J_r,J_\phi)$, respectively the radial and azimuthal action, given by

$$J_1 = \frac{1}{\pi}\int_{r_\mathrm{p}}^{r_\mathrm{a}} \mathrm{d}r\, \sqrt{2(E-\Phi(r)) - L^2/r^2} \quad ; \quad J_2 = L, \tag{7.1}$$

with E and L the energy and the angular momentum of the orbit, and $(r_\mathrm{p}, r_\mathrm{a})$ its peri- and apocentre, i.e. the two roots of $v_r = \sqrt{2(E-\Phi(r)) - L^2/r^2} = 0$. To these actions are associated two orbital frequencies, defined as

$$\frac{2\pi}{\Omega_1} = 2\int_{r_\mathrm{p}}^{r_\mathrm{a}} \mathrm{d}r\, \frac{1}{\sqrt{2(E-\Phi(r)) - L^2/r^2}} \quad ; \quad \frac{\Omega_2}{\Omega_1} = \frac{L}{\pi}\int_{r_\mathrm{p}}^{r_\mathrm{a}} \mathrm{d}r\, \frac{\mathrm{d}r}{\sqrt{2(E-\Phi(r)) - L^2/r^2}}, \tag{7.2}$$

where (Ω_1,Ω_2) are respectively the radial and azimuthal frequencies. Finally, the angle-action coordinates are completed with the associated angles (θ_1,θ_2) that read

$$\theta_1 = \Omega_1 \int_{\mathcal{C}_1} \mathrm{d}r\, \frac{1}{\sqrt{2(E-\Phi(r)) - L^2/r^2}} \quad ; \quad \theta_2 = \phi + \int_{\mathcal{C}_1} \mathrm{d}r\, \frac{\Omega_2 - L/r^2}{\sqrt{2(E-\Phi(r)) - L^2/r^2}}, \tag{7.3}$$

where $\mathcal{C}_1$ is a contour starting from $r=r_\mathrm{p}$ and going up to the current position $r=r(\theta_1)$ along the radial oscillation.

Having constructed the angle-action coordinates, we must now construct some appropriate basis of densities and potentials, as defined Eq. (3.63), Owing to the azimuthal symmetry of the disc, it is natural to write the basis elements as

$$\psi^{(p)}(\mathbf{x}) = \psi^{(p)}(r,\phi) = \mathrm{e}^{\mathrm{i}\ell\phi}\, U^n_\ell(r), \tag{7.4}$$

where $U^n_\ell(r)$ are some tailored real radial functions (Kalnajs, 1976). In order to characterise the strength of the self-gravitating amplification in the system, as described by the response matrix from Eq. (3.63), we must now compute the Fourier transformed basis elements, $\psi^{(p)}_{\mathbf{k}}(\mathbf{J})$. These are given by

$$\begin{aligned}\psi^{(p)}_{\mathbf{k}}(\mathbf{J}) &= \int \frac{\mathrm{d}\boldsymbol{\theta}}{(2\pi)^2}\, \psi^{(p)}\big(\mathbf{x}[\boldsymbol{\theta},\mathbf{J}]\big)\, \mathrm{e}^{-\mathrm{i}\mathbf{k}\cdot\boldsymbol{\theta}} \\ &= \delta^\ell_{k_2}\, W^{\mathbf{k}}_{\ell n}(\mathbf{J}),\end{aligned} \tag{7.5}$$

where we introduced the coefficient $W^{\mathbf{k}}_{\ell n}(\mathbf{J})$ as

$$\begin{aligned} W^{\mathbf{k}}_{\ell n}(\mathbf{J}) &= \frac{1}{\pi}\int_0^{\pi} \mathrm{d}\theta_1\, U^n_\ell\big(r[\theta_1]\big)\, \cos\big(k_1\theta_1 + k_2(\theta_2-\phi)\big) \\ &= \frac{1}{\pi}\int_{r_\mathrm{p}}^{r_\mathrm{a}} \mathrm{d}r\, \frac{\mathrm{d}\theta_1}{\mathrm{d}r}\, U^n_\ell(r)\, \cos\big(k_1\theta_1[r] + k_2(\theta_2-\phi)[r]\big). \end{aligned} \tag{7.6}$$

Computing the Fourier transformed basis elements amounts then to computing the integral from Eq. (7.6).

7.1.2 A disc model

Let us now consider the same disc model as in Sellwood (2012). We consider a so-called Mestel disc, i.e. a disc for which the circular velocity $v_\mathrm{c}=\sqrt{r\,\partial\Phi/\partial r}$ is a constant, a disc that somewhat mimics the flat rotation curve of the MW. If the disc was fully self-gravitating and generated this potential on its own, its surface density would be $\Sigma(R)\propto 1/r$. It is more realistic to assume that the disc is not fully self-gravitating, and that the total potential is generated by three components: (i) an inert bulge that dominates the mass near the centre; (ii) an inert dark halo that dominates the mass density far from the centre; (iii) the self-gravitating disc that contributes ~ 0.5 of the radial force at intermediate radii. The bulge and the halo are said to be inert, because they only contribute to the mean-field potential, but are insensitive to perturbations. As a result of the introduction of these additional components, the Mestel disc is said to be tapered at small and large radii, as its self-gravity has been turned off in the inner and outer regions. The initial unperturbed DF of that disc is given by

$$F_0(E,L) = \xi\, C\, L^q\, \mathrm{e}^{-E/\sigma_\mathrm{r}^2}\, T_\mathrm{in}(L)\, T_\mathrm{out}(L), \tag{7.7}$$

where C is a normalisation constant for the DF so that the disc generates the full potential for $\xi=T_\mathrm{in}=T_\mathrm{out}=1$. We also introduced σ_r as the radial velocity dispersion that controls the magnitude of the stars' random motions, and the power index $q=(v_\mathrm{c}/\sigma_\mathrm{r})^2-1$ taken to be equal to 11.4. Finally, to mimic the bulge and the dark halo, we introduced the inner and outer taper function as

$$T_\mathrm{in}(L) = \frac{L^4}{(R_\mathrm{in}v_\mathrm{c})^4+L^4} \quad ; \quad T_\mathrm{out}(L) = \frac{(R_\mathrm{out}v_\mathrm{c})^5}{(R_\mathrm{out}v_\mathrm{c})^5+L^5}, \tag{7.8}$$

where R_in is the disc's scale radius, and the outer truncation is given by $R_\mathrm{out}=11.5R_\mathrm{in}$. The last important parameter in Eq. (7.7) is ξ, the active fraction between zero and unity, that controls the dynamical importance of the disc's self-gravity. In particular, for $\xi=0.5$, the disc is known to be linearly stable (Toomre, 1981), i.e. all its normal modes are damped.

We now have at our disposal a stable inhomogeneous self-gravitating system with an integrable orbital structure. As a result of the finite number of particles, we expect therefore that this system will undergo a long-term orbital relaxation, via the resonant couplings of amplified Poisson fluctuations, as described by the inhomogeneous Balescu-Lenard Eq. (5.2). Such a long-term evolution was indeed observed in the numerical simulations of Sellwood (2012), that integrated the dynamics of that disc for hundreds of dynamical times. The resulting orbital diffusion is illustrated in Fig. 7.1.

7.1.3 Diffusion flux in action space

In order to be able to compute explicitly the Balescu-Lenard Eq. (5.2) to recover the formation of the ridge, some additional difficulties have to be overcome. First, the computation of the diffusion flux requires the computation of the dressed susceptibility coefficients, $\psi^\mathrm{d}_{\mathbf{k}\mathbf{k}'}(\mathbf{J},\mathbf{J}',\omega)$, as defined in Eq. (3.75), that themselves require the computation and the inversion of the response matrix, $\widetilde{\mathbf{M}}(\omega)$, from Eq. (3.72). The second main difficulty comes from Eq. (5.2) that requires us to solve the resonance condition, $\delta_\mathrm{D}(\mathbf{k}\cdot\boldsymbol{\Omega}(\mathbf{J})-\mathbf{k}'\cdot\boldsymbol{\Omega}(\mathbf{J}'))$. We refer to Fouvry et al. (2015) for a detailed illustration of how these two numerical difficulties can be overcome.

Once these difficulties have been dealt with, one can then compute explicitly the Balescu-Lenard flux from Eq. (5.3) and compare it with measurements from numerical simulations. This is first illustrated in Fig. 7.2, where the arrows show the diffusion flux $\mathbf{F}(\mathbf{J},t)$ in action space. We note that $\mathbf{F}(\mathbf{J},t)$ is small except along a ridge that slopes leftwards up away from the $J_r=0$ axis, where most of the stars of a cool disc are concentrated.

Rather than representing $\mathbf{F}(\mathbf{J},t)$, we can represent its divergence, that, owing to the continuity Eq. (5.3) tracks the local rate of change of the system's DF. This is illustrated in Fig. 7.3, where it is also compared with the measurements from numerical simulations. In that particular figure, we recover that $\partial/\partial\mathbf{J}\cdot\mathbf{F}(\mathbf{J})$ is negligigle, except along a narrow ridge, where it is positive lower down and negative higher up, indicating that stars are diffusing from near circular orbits to more eccentric orbits, with slightly less angular momentum. Satisfactorily, we also note that the measurements from numerical simulations, and the predictions from kinetic

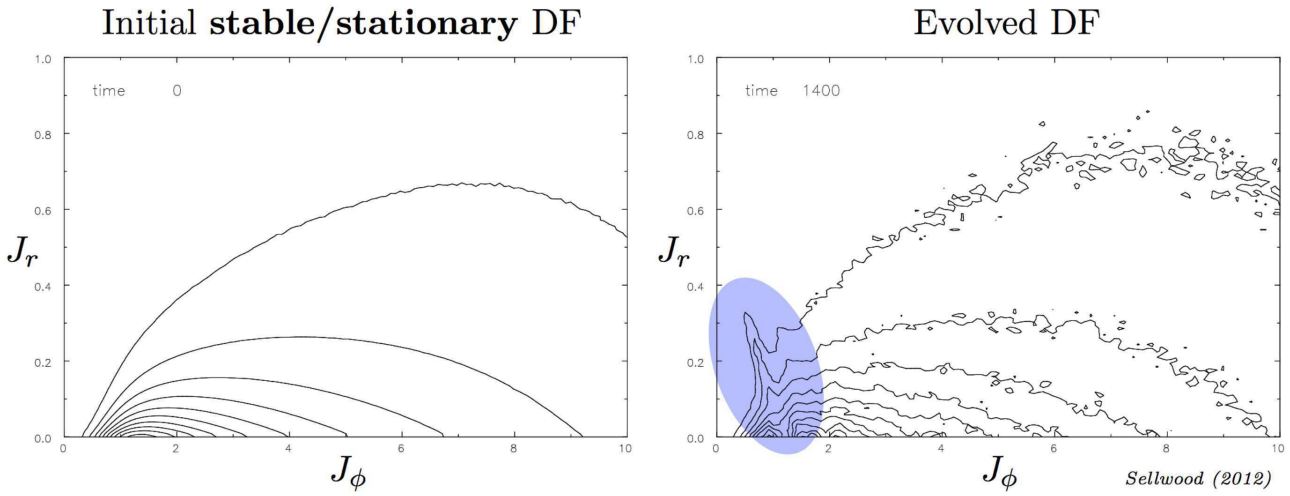

Figure 7.1: . From Sellwood (2012). Illustration of the spontaneous formation of a resonant ridge in action space observed during the numerical simulation of a discrete tapered Mestel disc. Left panel: Level lines of the DF from Eq. (7.7) at the initial time. Right panel: Level lines of that same DF after evolving the systems for hundreds of dynamical times. One can note the formation of a narrow ridge of diffusion towards more radial orbits in the central region of the disc.

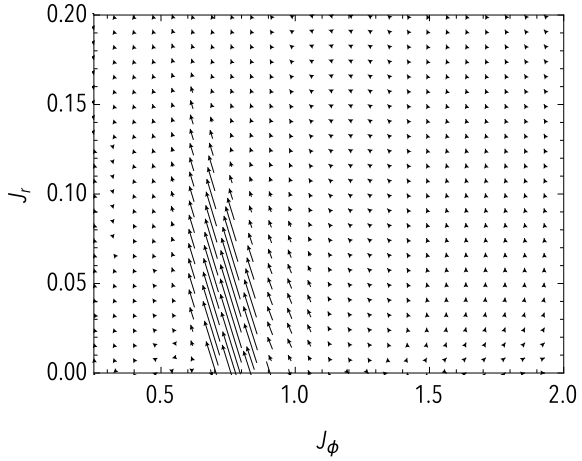

Figure 7.2: . From Fouvry et al. (2015). Illustration of the diffusion flux, $\mathbf{F}(\mathbf{J}, t=0)$, in action space for a tapered Mestel disc with active mass fraction $\xi = 0.5$. In this representation, one can clearly note that the diffusion is anisotropic, both because it only acts in a restricted region of action space, and also because it follows a very specific direction in that space.

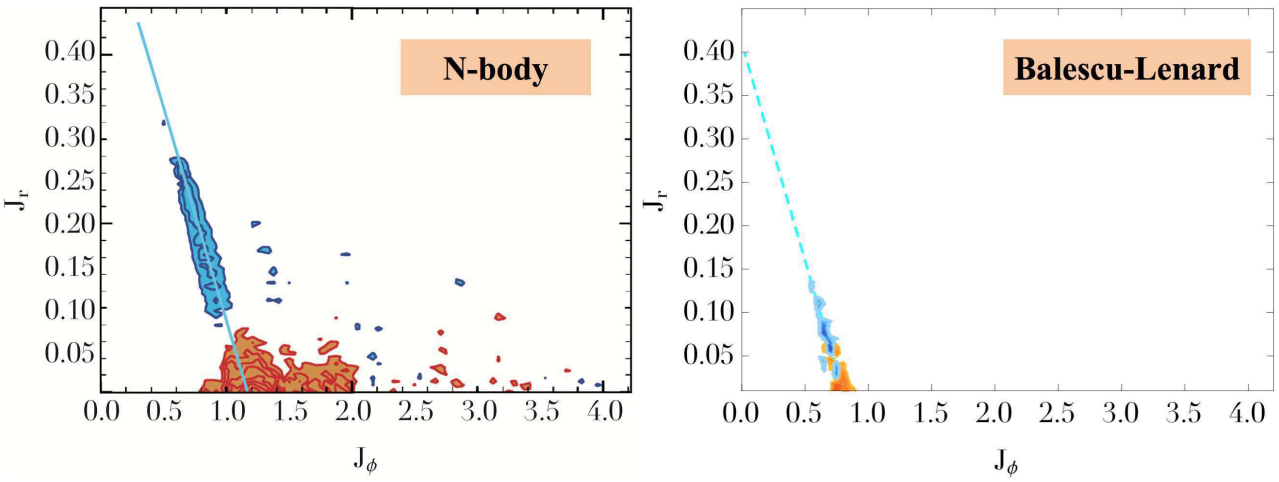

Figure 7.3: . Illustration of the contours of $\partial/\partial\mathbf{J}\cdot\mathbf{F}(\mathbf{J},t=0)$, i.e. the divergence of the diffusion flux in action space, as defined in Eq. (5.3). Blue (resp. red) contours are associated with a increment (resp. decrement) in the system's DF on secular timescales. The cyan line highlights the direction associated with the inner Lindblad resonance, $\mathbf{k}\cdot\mathbf{J}=(-2,1)\cdot(J_\phi,J_r)$, emphasising the fundamental role played by this resonance during the diffusion. Left panel: As measured in the numerical simulations of Sellwood (2012). Right panel: As predicted in Fouvry et al. (2015) using the Balescu-Lenard Eq. (5.2). Both resonant ridges are aligned with the same direction, and their overall amplitude are consistent, emphasising the key role played by collective effects to accelerate the long-term orbital diffusion.

theory are in agreement, both in the location, amplitude, and direction of the ridge. We also note that the ridge coincides with the line $\mathbf{k}\cdot\mathbf{J}=\mathrm{cst.}$, with $\mathbf{k}=(-2,1)$. Stars on this line are said to be at the inner Lindblad resonance, i.e. the resonance associated with this particular resonance $\mathbf{k}$. As can be seen from the front factor $\mathbf{k}$ in Eq. (5.2), a given resonance vector $\mathbf{k}$, only sources a diffusion along the direction of $\mathbf{k}$. As a consequence, from Fig. 7.3, we can conclude the inner Lindblad resonance is indeed the resonance dominating the disc's resonant relaxation. Following this measurement, one can perform a few additional tests of the kinetic theory.

First, from the mass prefactor in Eq. (5.2), $m_\mathrm{b}=M_\mathrm{tot}/N$, one can check the scaling of $\mathbf{F}(\mathbf{J},t)$ with the number of particle. For a fixed total mass, the larger N, the smoother the mean potential, the weaker the Poisson fluctuations, and therefore the slower the long-term relaxation. This scaling in $1/N$ can be carefully recovered from the numerical simulations.

Similarly, one can also check the dependence of the amplitude of the diffusion with ξ the disc's active fraction. The larger ξ, the stronger the self-gravitating amplification, and therefore the faster the relaxation. We must also emphasise that the dependence of $\mathbf{F}$ with ξ is far from being linear for dynamically cold systems. Indeed, following Eq. (3.72), we note that the dielectric matrix scales like $\widetilde{\mathbf{E}}=1-\xi\widetilde{\mathbf{M}}_0$, where the response matrix $\widetilde{\mathbf{M}}_0$ corresponds to the response matrix for $\xi=1$. As a consequence, the dressed susceptibility coefficients from Eq. (3.75) scale heuristically like $|\psi^\mathrm{d}|^2\propto|\psi|^2/(1-\xi)^2$. As ξ increases, the disc gets more and more self-gravitating, and gets closer and closer to being linearly unstable. As a result, the dressing of the perturbations gets larger and larger, so that the long-term diffusion get rapidly accelerated. This non-linear scaling w.r.t. ξ can also be recovered in the numerical simulations.

One of the important conclusion of these comparisons is that, indeed, the Balescu-Lenard equation predicts the action space diffusion flux that Poisson noise drives in a stable but (very) responsive disc. This evolution occurs more than 1000 times faster than naive estimates of two-particle relaxation, because the Poisson noise is dressed by self-gravity, which drastically enhance the fluctuations' amplitude, and therefore increase the efficiency of the relaxation.

7.1.4 The long-term fate of discs

The sole computation of $\mathbf{F}(t=0)$ is already a cumbersome numerical task. But, we may rely on numerical simulations to gain insight on the disc's long-term behaviour if one was able to integrate self-consistently the Balescu-Lenard Eq. (5.2) forward in time. Following the diffusion flux observed in Fig. 7.3, a resonant ridge will slowly grow in the disc's mean DF, $F_0(\mathbf{J},t)$. In particular, this ridge will locally deplete the disc from circular orbits, and move them to more radial ones. When large enough, this ridge will ultimately make the disc unstable at the collisionless level. That is, Poisson shot noise drives a disc that is initially stable towards one that is unstable, through slow reshufflings of orbits. Such a phase transition is illustrated in Fig. 7.4, where we note the change of dynamical regime between a slow collisional relaxation, described by the Balescu-Lenard, and a fast collisionless relaxation. All simulations of initially stable discs that have been integrated for long

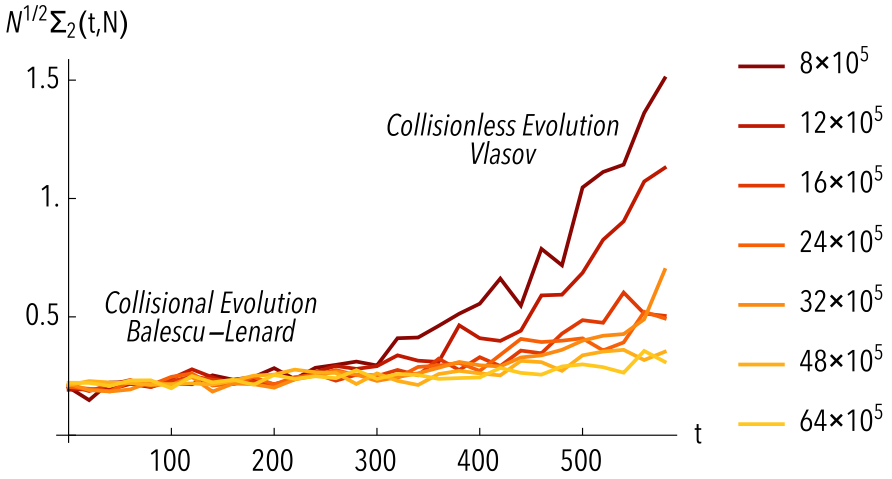

Figure 7.4: . From Fouvry et al. (2015). Illustration of the destabilisation of the disc occurring on secular timescales as a result of the slow and irreversible growth of the resonant ridge in action space, as illustrated here by the strength of non-axisymmetric perturbations in the disc as a function of time, where different colors correspond to different values of N. At some stage, the ridge gets so large that the disc becomes unstable (De Rijcke et al., 2019). The dynamics therefore drastically changes of dynamical regime, as it will undergo the (fast) growth of an unstable mode, as described by the (collisionless) Vlasov equation. The larger N, the more one has to wait for this dynamical transition to happen.

enough, developed $\mathcal{O}(1)$ non-axisymmetries that degenerated into a strong bar. The larger the number N of particles, the longer one has to wait for the bar to form, but the bar always ends up forming.

Owing to this result, we can now describe the main steps of the long-term evolution of a self-gravitating system, as summarised in Fig. 7.5.

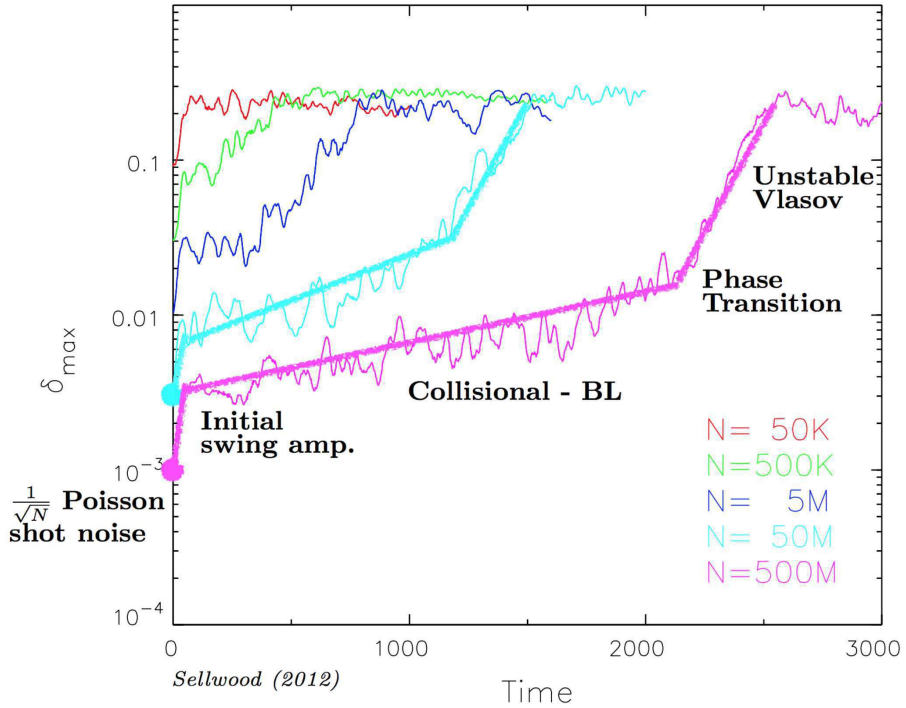

Figure 7.5: . From Sellwood (2012). Illustration of the typical fate undergone by the tapered Mestel disc, where here $\delta_{\max}$ describes the typical amplitude of non-axisymmetric fluctuations in the disc, and different colors correspond to different values of N. See the main text for a discussion of these different stages.

1. First, at the initial time, owing to the system's finite number of particles, the system unavoidably contains some Poisson shot noise fluctuations. This corresponds to the fluctuations $\delta F_{\mathbf{k}}(\mathbf{J}, 0)$, whose statistics we characterised in Eq. (3.49). The larger the number of particles, the smaller this initial value, as can be seen in Fig. 7.5.

2. Then, in the first few dynamical times, these initial Poisson fluctuations get amplified by the system's self-gravity. The disc thermalises, leading to Poisson shot noise fluctuations with amplitudes larger than at the initial time. This corresponds to the stage of thermalisation we considered in Eq. (3.78), when we characterised the amplitude of the dressed potential fluctuations, $\delta\Phi_{\mathbf{k}}(\mathbf{J},t)$, in a live self-gravitating system, and replaced the bare susceptibility coefficients, $\psi_{\mathbf{k}\mathbf{k}'}(\mathbf{J},\mathbf{J}')$ with their dressed analogs, $\psi^{\rm d}_{\mathbf{k}\mathbf{k}'}(\mathbf{J},\mathbf{J}',\omega)$.
3. Because of resonant couplings between the dressed Poisson fluctuations, the disc begins subsequently its secular evolution. This corresponds to the collisional dynamics captured by the inhomogeneous Balescu-Lenard equation, that we derived in Eq. (5.2). This dynamics is sourced by $1/N$ effects, so that the larger the number of particles, the slower the evolution. This can also be seen in Fig. 7.5, where we note that the initial slope of the magenta line is smaller than the initial slope of the cyan line. During these slow orbital distortions, a resonant ridge slowly grows in the disc's DF, as illustrated in Fig. 7.3.
4. When the resonant ridge gets too large, the disc finally becomes linearly unstable, and undergoes an out-of-equilibrium dynamical phase transition, as illustrated in Fig. 7.4. During this destabilisation, the disc's dynamics is governed by the Vlasov equation. The evolution is then collisionless, i.e. independent of the number of particles. This can also be seen in Fig. 7.5, where one can note that the final slopes of the magenta and cyan lines are the same.

7.2 Galactic nuclei

Another important example of self-gravitating system comes from the case of galactic nuclei, i.e. the long-term dynamics of stars orbiting a supermassive BH, such as SgrA*, the galactic centre of the MW, as illustrated in Fig. 7.6.

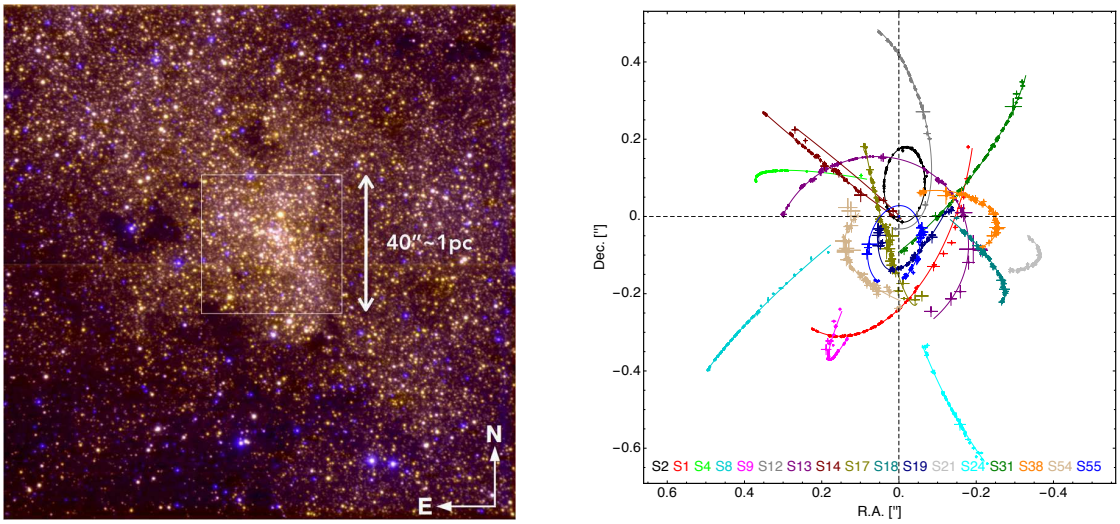

Figure 7.6: Observations of SgrA*, the galactic nucleus of the MW. The MW contains in its centre a supermassive BH of mass $M_\bullet \simeq 4\times10^6\,M_\odot$. This BH strongly dominates the stars' dynamics within its sphere influence, $r_{\rm h}\simeq 1\,{\rm pc}$, defined so that the enclosed stellar mass is $M_\star(r\leq r_{\rm h})\simeq M_\bullet$. Left panel: From Schödel et al. (2007). Observations of SgrA*'s sphere of influence. Galactic nuclei are among the densest stellar systems of the Universe, making them ideal to apply the statistical tools presented here. Right panel: From Gillessen et al. (2017). Detailed observations of the Keplerian dynamics of the S-stars in the very vicinity of SgrA* ($\sim 10\,{\rm mpc}$). We note that these stars follow very closely Keplerian ellipses, justifying the orbit-average performed in Section 7.2.2.

As we will emphasise, one of the main dynamical specificity of such a system is that it said to be dynamically degenerate, as a global resonance condition $\mathbf{k}\cdot\boldsymbol{\Omega}(\mathbf{J})=0$ is satisfied by all the orbits. Galactic nuclei are fascinating dynamical systems, because the infinite potential generated by the central BH guarantees the existence of a wide range of dynamical timescales in the system. As such, the dynamical evolution of the stellar cluster surrounding the BH comprises numerous dynamical processes acting on radically different timescales (Rauch & Tremaine, 1996; Hopman & Alexander, 2006; Alexander, 2017), as illustrated in Fig. 7.7.

1. First, the central BH being supermassive, it dominates the system's mean potential and imposes, at leading order, a Keplerian motion to each individual star. This is the system's fast dynamical timescale. Because this motion is so fast, one naturally performs an orbit-average over it, i.e. smears out the stars along their Keplerian ellipses. Following this first average, studying the long-term dynamics of a galactic nucleus amounts then to studying the long-term relaxation of a population of closed Keplerian wires.

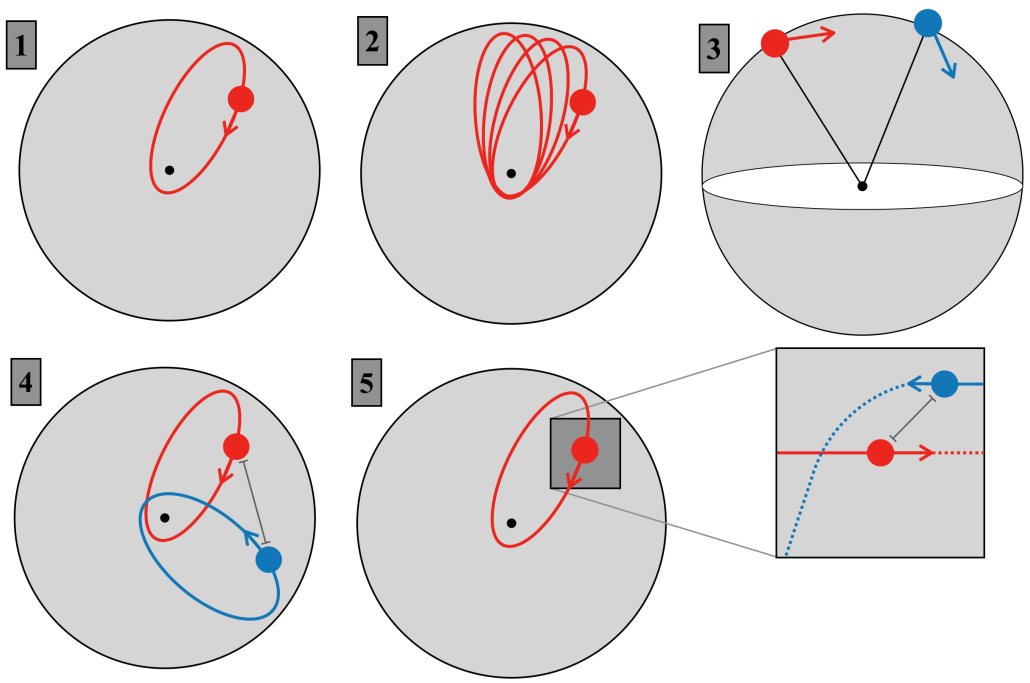

Figure 7.7: Illustration of the intricate hierarchy of timescales in a galactic nucleus. These are: (1) the dynamical time; (2) the precession time; (3) the vector resonant relaxation time; (4) the scalar resonant relaxation time; (5) the non-resonant relaxation time. Each process is briefly described in the main text.

2. Then, on longer timescales, the potential self-consistently generated by the stellar cluster, as well as the relativistic corrections from the central BH (Schwarzschild precession) cause the wires to precess in their orbital planes. This is the system's second timescale, the timescale for the precession of the Keplerian wires' pericentres.
3. Subsquently, through the non-spherical stellar fluctuations and the relativistic corrections induced by a possibly spinning BH (Lense-Thirring precession), the wires' orbital orientations get reshuffled. This process is called "vector resonant relaxation" (Kocsis & Tremaine, 2015), as wires' angular momentum change in orientation, without changing in magnitude (i.e. in eccentricity) nor in energy (i.e. in semi-major axis). This is the system's third timescale, the timescale for the redistribution of orbits' orientations.
4. On even longer timescales, resonant torques between the precessing wires lead to a diffusion of the wires' eccentricity, a process called "scalar resonant relaxation" (Rauch & Tremaine, 1996). This process is resonant because only wires that precess with matching precession frequencies couple to each other. This is the system's fourth timescale, the timescale for the eccentricity relaxation.
5. Finally, on the longest timescale, stars occasionally see each other (rather than wire seeing each other), as a result of close two-body encounters. The cumulative effects from these localised scatterings lead to a relaxation of the stars' Keplerian energy (i.e. the wires' semi-major axis), through a process called non-resonant relaxation. This is the system's last timescale, the timescale for energy relaxation.

Let us now briefly detail how the previous kinetic methods can be used to describe some of these relaxation processes.

7.2.1 The system's Hamiltonian

We consider of set of N stars of individual mass m orbiting a BH of mass $M_\bullet$. We assume that the BH is supermassive so that we have $Nm = M_\star \ll M_\bullet$. Within some given inertial frame, we denote the location of the BH with $\mathbf{X}_\bullet$ and the locations of the stars with $\mathbf{X}_i$. The total Hamiltonian of the system is then given by

$$H = \frac{\mathbf{P}_\bullet^2}{2M_\bullet} + \sum_{i=1}^{N} \frac{\mathbf{P}_i^2}{2} + \sum_{i=1}^{N} M_\bullet m U(|\mathbf{X}_i - \mathbf{X}_\bullet|) + \sum_{i=1}^{N} m\Phi_{\rm rel}^i + \sum_{i<j} m^2\, U(|\mathbf{X}_i - \mathbf{X}_j|), \tag{7.9}$$

with the usual Newtonian interaction $U(|\mathbf{X}|) = -G/|\mathbf{X}|$. In that Hamiltonian, the first two terms correspond to the kinetic energy of the BH and the stars. The third term corresponds to the Keplerian potential of the stars w.r.t. the BH, while the fourth term is associated with the relativistic corrections generated by the BH (such as the Schwarzschild and Lense-Thirring precessions). Finally, the last term corresponds to the pairwise

interactions between the stars. As we will later emphasise, this term is the only term that will involve some finite-N Poisson fluctuations, and therefore is the only term able to source some long-term relaxation in the system.

Because we know that the BH dominates the leading-order motion, we will rewrite the Hamiltonian from Eq. (7.9) as N decoupled Keplerian Hamiltonians plus perturbations. To do so, we need to perform a canonical change of coordinates towars the democratic coordinates (Duncan et al., 1998) centred on the BH. These are defined as

$$\begin{cases} \mathbf{x}_\bullet = \dfrac{M_\bullet \mathbf{X}_\bullet + \sum_{i=1}^N m\mathbf{X}_i}{M_\bullet + M_\star}, \\ \mathbf{x}_i = \mathbf{X}_i - \mathbf{X}_\bullet. \end{cases} \quad ; \quad \begin{cases} \mathbf{p}_\bullet = \mathbf{P}_\bullet + \displaystyle\sum_{i=1}^N \mathbf{P}_i, \\ \mathbf{p}_i = \mathbf{P}_i - \dfrac{m\big(\mathbf{P}_\bullet + \sum_{j=1}^N \mathbf{P}_j\big)}{M_\bullet + M_\star} \end{cases} \tag{7.10}$$

Physically, through this change of coordinate, we only keep track of the position of the system's barycentre, and the position of the stars respective to the BH. Without loss of generality, we can assume that $(\mathbf{x}_\bullet, \mathbf{p}_\bullet) = (0, 0)$, and the Hamiltonian from Eq. (7.9) becomes

$$H = \sum_{i=1}^N \left(\frac{\mathbf{p}_i^2}{2m} + M_\bullet m\, U(|\mathbf{x}_i|) + m\Phi_{\rm rel}^i \right) + \sum_{i<j}^N m^2\, U(|\mathbf{x}_i - \mathbf{x}_j|) + \frac{\big(\sum_{i=1}^N \mathbf{p}_i\big)^2}{2M_\bullet}. \tag{7.11}$$

The writing from Eq. (7.11) is satisfactory, because it consists of N independent Keplerian Hamiltonians (with relativistic corrections) describing the interaction of the stars with the central BH, plus the pairwise couplings among the stars. The last term is an additional kinetic term, that will vanish once we will perform an orbit-average over the fast Keplerian motion, i.e. over the motion imposed by the dominating BH.

7.2.2 Averaging over the fast Keplerian motion

In the Hamiltonian from Eq. (7.11), because the BH is supermassive, the dominant term comes from the interaction of the stars with the central BH. This corresponds to the 2-body Keplerian problem, which is explicitly integrable. As a consequence, in order to correctly describe this fast motion, it seems appropriate to perform a new change of canonical coordinates towards the associated angle-action coordinates, which in the context of the Keplerian motion are equivalently called orbital elements or Delaunay variables (Binney & Tremaine, 2008).

As illustrated in Fig. 7.8, we define therefore the orbital elements as

$$(\boldsymbol{\theta}, \mathbf{J}) = (M, \omega, \Omega, L_{\rm c}, L, L_z), \tag{7.12}$$

where M is the mean anomaly, i.e. the angle associated with the fast orbital motion, ω the argument of the pericentre, Ω the longitude of the ascending node. We also introduced the three actions $(L_{\rm c}, L, L_z)$ as

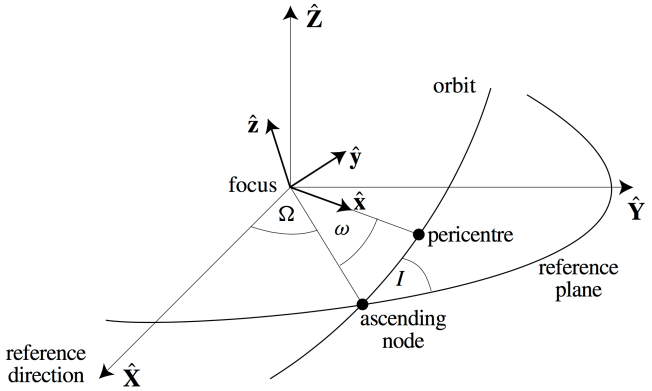

Figure 7.8: From Murray & Dermott (1999). Illustration of the Keplerian orbital elements.

$$L_{\rm c} = m\sqrt{GM_\bullet a} \quad ; \quad L = m\sqrt{GM_\bullet a(1-e^2)} \quad ; \quad L_z = L\,\cos(I), \tag{7.13}$$

with a the wire's semi-major axis, e its eccentricity, I its inclination, L the norm of the angular momentum, L_z its projection along the z-axis, and $L_{\rm c}$ the circular angular momentum.

The key property of these variables is that they allow us to express the Keplerian Hamiltonian as a simple function of the associated action variables, as one has

$$H_{\rm Kep} = \frac{\mathbf{p}_i^2}{2m} + M_\bullet m U(|\mathbf{x}_i|) = -\frac{m^3 (GM_\bullet)^2}{2L_{\rm c}^2}, \tag{7.14}$$

Here, we note that the Keplerian motion is said to be degenerate, since it depends only on one action, L_c, so that this Hamiltonian has only one non-zero orbital frequency

$$\Omega_{\rm Kep} = \frac{\partial H_{\rm Kep}}{\partial L_{\rm c}} = \dot{M} = \sqrt{\frac{GM_\bullet}{a^3}}, \tag{7.15}$$

while all the other orbital frequencies are exactly zero.

In addition to performing the change of variables to the orbital elements, relying on the fact that the BH is supermassive, we will also perform an orbit-average of the system's Hamiltonian w.r.t. the particles' fast Keplerian motion, i.e. w.r.t. the particles' mean anomaly. As a result, we will perform the replacement $H \to \int_{-\pi}^{\pi} {\rm d}M/(2\pi) H = \overline{H}$. In that process, we note that since the Hamiltonian becomes independent of the angle M, the associated action $L_{\rm c}$, whose dynamics is driven by $\dot{L}_{\rm c} = -\partial\overline{H}/\partial M = 0$ gets adiabatically conserved. Since $L_{\rm c} = L_{\rm c}(a)$, this means that the stars' semi-major axes are conserved for the orbit-averaged dynamics. Similarly, any contribution to the orbit-averaged Hamiltonian that only depends on the adiabatically conserved action $L_{\rm c}$ can also be removed; this is the case for the additional kinetic term from Eq. (7.11), that we may therefore forget about. Following the orbit-average over the mean anomalies of all the particles, particles are replaced by Keplerian wires, and the Hamiltonian from Eq. (7.11) becomes

$$\overline{H} = \sum_{i=1}^{N} m\, \overline{\Phi}^i_{\rm rel} + \sum_{i<j}^{N} m^2\, \overline{U}_{ij}, \tag{7.16}$$

where we introduced the orbit-averaged relativistic precession and the orbit-averaged wire-wire interaction as

$$\begin{aligned} \overline{\Phi}^i_{\rm rel} &= \int_{-\pi}^{\pi} \frac{{\rm d}M_i}{2\pi}\, \Phi^i_{\rm rel}, \\ \overline{U}_{ij} &= \int_{-\pi}^{\pi} \frac{{\rm d}M_i}{2\pi} \frac{{\rm d}M_j}{2\pi}\, U(|\mathbf{x}_i - \mathbf{x}_j|), \end{aligned} \tag{7.17}$$

with the usual Newtonian pairwise coupling $U(|\mathbf{x}|) = -G/|\mathbf{x}|$. We made great progress in the Hamiltonian from Eq. (7.16) as it formally ressembles the Hamiltonian considered in Eq. (3.1), i.e. it is the sum of some external potential, as well as the sum over pairwise interactions. Here, the main difference stems from the orbit-average over the fast Keplerian motion. As we have replaced particles by Keplerian wires, we effectively replaced the Newtonian particle-particle interaction by its double orbit-averaged wire-wire version (Touma et al., 2009). We can now leverage the similarity between these Hamiltonians to develop the orbit-averaged kinetic theory of galactic nuclei.

7.2.3 Mean-field orbit-averaged dynamics

Following Eq. (7.16), the specific Hamiltonian of a test wire embedded in that system is given by

$$\overline{H} = \overline{\Phi}_{\rm rel} + \sum_{i=1}^{N} m\, \overline{U}_i, \tag{7.18}$$

where $\overline{U}_i$ stands for the orbit-averaged interaction between the test wire and the background particle i, as defined in Eq. (7.17). The dominating contribution to the relativistic correction from the BH is the 1PN contribution (i.e. scaling in $1/c^2$) called the Schwarzschild precession that leads to an in-plane precession of the stars' pericentre. More precisely (see, e.g., Touma et al. (2009)), it reads

$$\Omega_{\rm rel}(a,e) = \frac{\partial\overline{\Phi}_{\rm rel}}{\partial L} = \frac{3GM_\bullet\Omega_{\rm Kep}(a)}{c^2 a(1-e^2)}. \tag{7.19}$$

We note that this precession of the pericentre is prograde, and independent of the orbital orientation of the considered test wire.

Similarly, if we assume that background distribution of wires is on average spherically symmetric, i.e. $F_0 = F_0(L_{\rm c}, L) = F(a,e)$, then it also leads to an in-plane precession of the test wire. More precisely, assuming that the background stars have the enclosed mass profile $M_\star(r)$, then it also generates a precession of the test wire's pericentre (Tremaine, 2005) governed by

$$\Omega_\star(a,e) = \frac{\partial\overline{\Phi}_\star}{\partial L} = \frac{\Omega_{\rm Kep}(a)}{\pi M_\bullet e} \int_0^\pi {\rm d}f\, M_\star\big(r[f]\big)\, \cos(f), \tag{7.20}$$

where f stands for the test particle's true anomaly. For an outward decreasing stellar density profile, this precession is retrograde, and is also independent of the particular orientation of the considered test wire.

As a result of these mean-field motions, the Hamiltonian from Eq. (7.18) takes the simple form

$$\overline{H} = \overline{\Phi}_{\rm rel}(a,e) + \overline{\Phi}_{\star}(a,e) + \delta\Phi, \tag{7.21}$$

where $\overline{\Phi}_{\rm rel}$ and $\overline{\Phi}_{\star}$ are the mean-field constructive in-plane precessions generated respectively by the relativistic corrections from the BH and the mean stellar potential, and where $\delta\Phi$ stands for the finite-N fluctuations unavoidably present in a discrete background bath. At this stage, the analogy with the generic inhomogeneous system considered in previous sections is even more obvious.

Let us now recall the main steps that led us to Eq. (7.21). First, we performed an orbit-average over the fast Keplerian motion induced by the BH. As a result, we replaced stars by their underlying Keplerian wires. As we have smeared out the stars along their mean anomaly, a Keplerian wire is then characterised by five orbital numbers. Namely, $(L_{\rm c}, L) = (a, e)$, the semi-major axis and eccentricity, describe the shape of the wire; ω, the argument of the pericentre, describes the in-plane phase of the wire's pericentre; $\widehat{\mathbf{L}} = (\Omega, L_z)$, the direction of the angular momentum vector, describes the orbital orientation of the wire. Because of adiabatic invariance, the "fast" action $L_{\rm c}$ is conserved for the orbit-averaged dynamics, i.e. a Keplerian wire cannot see its semi-major axis a change through orbit-averaged interactions. On the one hand, in the limit of a perfectly smooth background bath, the test wire's pericentre, ω, still undergoes a constructive precession, as governed by the mean-field precessiongs from Eq. (7.21). This motion is sourced by the relativistic corrections from the BH, as well as by the smooth background stellar potential. On the other hand, in the limit of a perfectly smooth background bath, the test wire's orientation, $\widehat{\mathbf{L}}$, is exactly conserved, and the test wire always remains within its initial orbital plane.

Of course, the background bath is, in practice, composed of a finite number of stars, which generates some stochastic noise in the system. As a consequence, this can source the relaxation of the test wire's orbital parameters. Yet, because the wire's pericentre undergoes a non-zero constructive precession, while its orientation does not, we expect that the statistical properties of the relaxation of the test wire's eccentricity and the test wires' orientation are going to be radically different. We therefore make the distinction between these two processes of resonant relaxation, that we respectively call "scalar resonant relaxation" for the relaxation of the norm of the test wire's angular momentum (i.e. the relaxation of eccentricity), and "vector resonant relaxation" for the relaxation of the direction of the test wires' angular momentum vector. In the sections below, we briefly sketch the physical content of these two processes.

7.2.4 Scalar Resonant Relaxation

Let us first focus on the relaxation of the test wire's L. To shorten the notations and clarify the connexions with the previous derivations, we define the shape of the wires with the in-plane actions $\mathbf{J} = (L_{\rm c}, L)$. Our goal is to describe the diffusion of the test wire's PDF, $P(\mathbf{J}, t)$. We start from the orbit-averaged Hamiltonian of Eq. (7.21). We assume that the background bath follows an isotropic angular momentum distribution, so that $F_0 = F_0(\mathbf{J}) = F_0(L_{\rm c})$. Glancing back at Eq. (3.72) where we noted that the bath's response matrix is sourced by the gradients of the bath's DF w.r.t. the actions, our assumption of an isotropic bath has the important consequence that, since $\partial F_0/\partial L = 0$, this bath cannot support any self-gravitating amplification, i.e. the bath response matrix is exactly zero. Phrased differently, the relaxation of the test wire's L is not accelerated by collective effects, so that the Landau and Balescu-Lenard diffusion coefficients, from Eq. (3.51) and (3.79), are identical. The explicit and effective calculation of these diffusion coefficients is a bit cumbersome to deal correctly with all the numerical prefactors, so that we only report the final results, following Bar-Or & Fouvry (2018). All in all, similarly to Eq. (3.25), we obtain a diffusion equation of the form

$$\frac{\partial P(\mathbf{J},t)}{\partial t} = \frac{1}{2}\frac{\partial}{\partial L}\left[L\, D_{\rm RR}(\mathbf{J})\, \frac{\partial}{\partial L}\left(\frac{P(\mathbf{J},t)}{L}\right)\right], \tag{7.22}$$

where the additional factors in L come from averages over L_z. In that equation, the diffusion coefficients, $D_{\rm RR}(L_{\rm c}, L)$ are formally similar to the ones we had already obtained in Eq. (3.51). They read

$$D_{\rm RR}(\mathbf{J}) \propto m \sum_{k,k'} k \int {\rm d}\mathbf{J}'\, \delta_{\rm D}(k\,\Omega_{\rm prec}(\mathbf{J}) - k'\,\Omega_{\rm prec}(\mathbf{J}')\, \left|\overline{\psi}_{kk'}(\mathbf{J},\mathbf{J}')\right|^2 F_0(\mathbf{J}'), \tag{7.23}$$

where we have introduced the total in-plane precession frequencies as $\Omega_{\rm prec} = \Omega_{\rm rel} + \Omega_{\star}$, and $\overline{\psi}_{kk'}(\mathbf{J},\mathbf{J}')$ are the bare in-plane orbit-averaged susceptibility coefficients, whose detailed expression can be found in Bar-Or & Fouvry (2018). Of course, the similarities between the general result from Eq. (3.51) and Eq. (7.23) are striking. There are however two subtle changes in the case of scalar resonant relaxation. First, the resonance condition,

$\delta_{\rm D}(k\,\Omega_{\rm prec}(\mathbf{J})-k'\,\Omega_{\rm prec}(\mathbf{J}'))$, involves the (slow) precession frequency rather than the (fast) orbital frequency. Second, as a result of orbit-average, diffusion only occurs in the L-direction, and no diffusion occurs in the direction of $L_{\rm c}$, the action adiabatically-conserved after orbit-average. An overall representation of the physical mechanism driving this resonant relaxation is illustrated in Fig. 7.9.

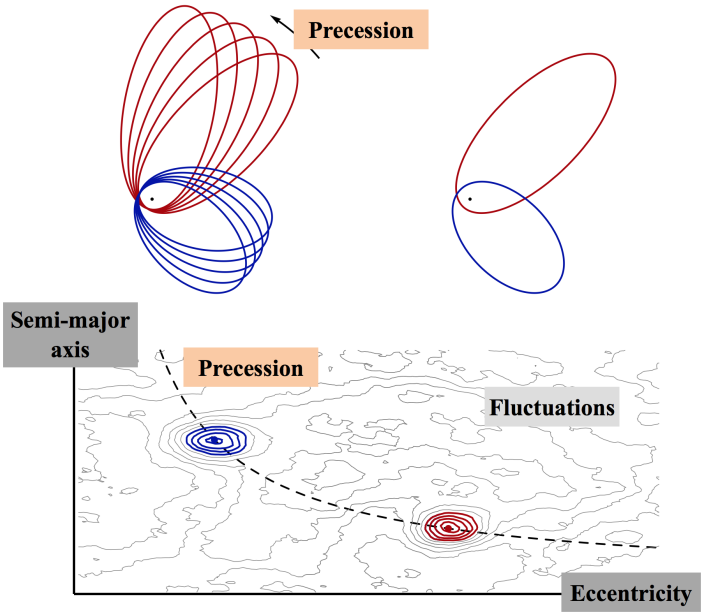

Figure 7.9: Illustration of the process of scalar resonant relaxation in a galactic nucleus, i.e. the relaxation of stellar eccentricities in the vicinity of a supermassive BH. Because the central BH dominates the system's total potential, it is natural to perform an orbit-average over this fast dynamics. Doing so, stars are replaced by Keplerian wires. Top-left panel: Illustration of two Keplerian wires in the inertial frame. As given by Eq. (7.21), as a result of the relativistic corrections from the BH and the stellar mean potential, these wires undergo an in-plane pericentre precession, as described by $\Omega_{\rm prec}(\mathbf{J})=\Omega_{\rm rel}+\Omega_\star$. Top-right panel: The same two wires, but this time in the rotating frame in which they are in resonance. As they are in resonance, these two wires are correlated and can therefore efficiently couple one to another. Bottom panel: Illustration in action space, $\mathbf{J}=(L_{\rm c},L)=(a,e)$, of the finite-$N$ fluctuations in the system, sourced by Poisson shot noise, and exhibiting overdensities for the blue and red orbits. These two wires satisfy a resonance condition, $\delta_{\rm D}(k\,\Omega_{\rm prec}(\mathbf{J})-k'\,\Omega_{\rm prec}(\mathbf{J}'))$, which permits a long-term reshuffling of the system's orbital structure, through the process of scalar resonant relaxation, as described by the diffusion coefficient from Eq. (7.23). We note that the two wires do not need to be close in position space nor in action space to diffuse, hence the name of discrete resonant encounters.

Having characterised in detail the diffusion coefficients for the relaxation of eccentricities, they can now be computed in detail. This is illustrated in Fig. 7.10 for a galactic nucleus mimicking SgrA*

7.2.5 Vector Resonant Relaxation

We also emphasised previously that as a result of the finite number of stars in the system, a test wire will also undergo some relaxation of its orbital orientation, through the process of vector resonant relaxation. Glancing back at Eq. (7.21), we note that this stochastic jitter of the orbital orientation $\widehat{\mathbf{L}}$, is sourced by the Poisson fluctuations $\delta\Phi$, and therefore will happen on a timescale longer than the precession time $t_{\rm prec}=1/|\Omega_{\rm prec}|$. Assuming that this precession of the pericentre is much faster than the timescale for the orientations reshufflings, we may therefore perform a second orbit-average of Eq. (7.21), this time over the in-plane precession of the pericentres. As a result, in Eq. (7.21), we will perform the operation $\overline{H}\to\int_{-\pi}^{\pi}{\rm d}\omega/(2\pi)\overline{H}=\overline{\overline{H}}$. As illustrated in Fig. 7.11, following this second orbit-average, Keplerian wires are replaced by Keplerian annuli, and the Hamiltonian for our test annuli becomes

$$\overline{\overline{H}}=\sum_{i=1}^{N}m\,\overline{\overline{U}}(\mathbf{J},\mathbf{J}_i,\widehat{\mathbf{L}}\cdot\widehat{\mathbf{L}}_i), \tag{7.24}$$

where $\overline{\overline{U}}(\mathbf{J},\mathbf{J}',\widehat{\mathbf{L}}\cdot\widehat{\mathbf{L}}')$ stands for the double orbit-averaged pairwise interaction between two annuli of parameters $\mathbf{J}$ and $\mathbf{J}'$, and respective orientations $\widehat{\mathbf{L}}$ and $\widehat{\mathbf{L}}'$. By symmetry, this pairwise interaction is only a function of the respective orientation of the two annuli, hence the fact that it only depends on their mutual angle, through $\widehat{\mathbf{L}}\cdot\widehat{\mathbf{L}}'$. In the Hamiltonian from Eq. (7.24), since we have performed a double orbit-average, the parameters

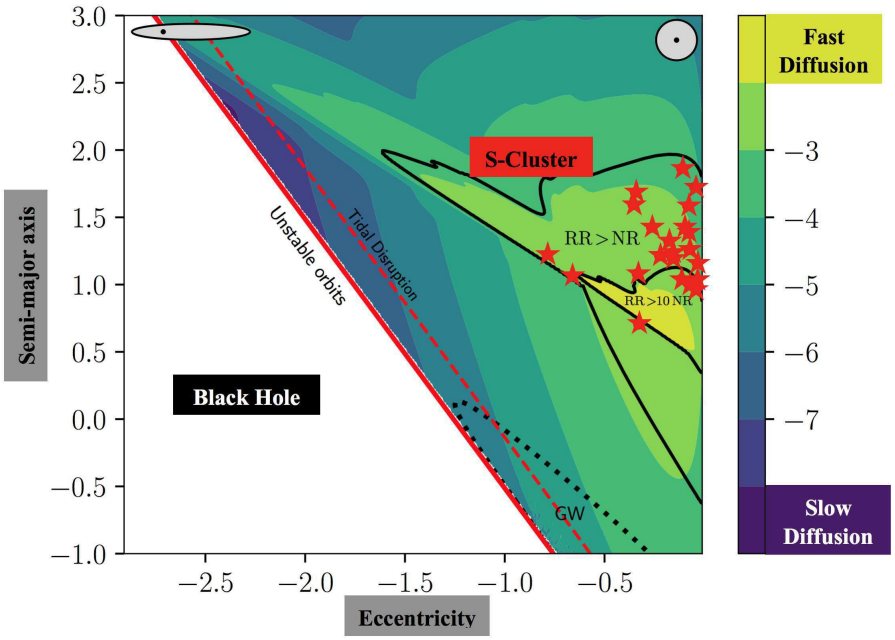

Figure 7.10: From Bar-Or & Fouvry (2018). Explicit computations of the diffusion coefficients, $D_{\rm RR}(a,e)$, from Eq. (7.23), that describe the diffusion of a star's eccentricity in a galactic nucleus similar to the one of SgrA*. Moving from the right to the left, wires get from circular to very eccentric, up to a point where they unavoidably fall on the central BH, as highlighted by the white region. Background green contours correspond the level lines of the eccentricity resonant diffusion coefficients. They dominate over the diffusion sourced by non-resonant encounters within the black region. The red stars highlight the orbital parameters of the observed S-cluster from Fig. 7.6, whose dynamics is indeed dominated by resonant processes. We also note that as a wire becomes more and more eccentric, the efficiency of its resonant relaxation rapidly drops. This is the so-called Schwarzschild barrier (Merritt et al., 2011; Bar-Or & Alexander, 2016), which is a direct consequence of the divergence of the relativistic precession frequency from Eq. (7.19) for $e \to 1$. As a wire gets more and more eccentric, it precesses faster and faster through these relativistic effects, up to a point that it precesses so fast that it cannot couple resonantly anymore to the other slowly-precessing wires, and the efficiency of the diffusion drastically drops.

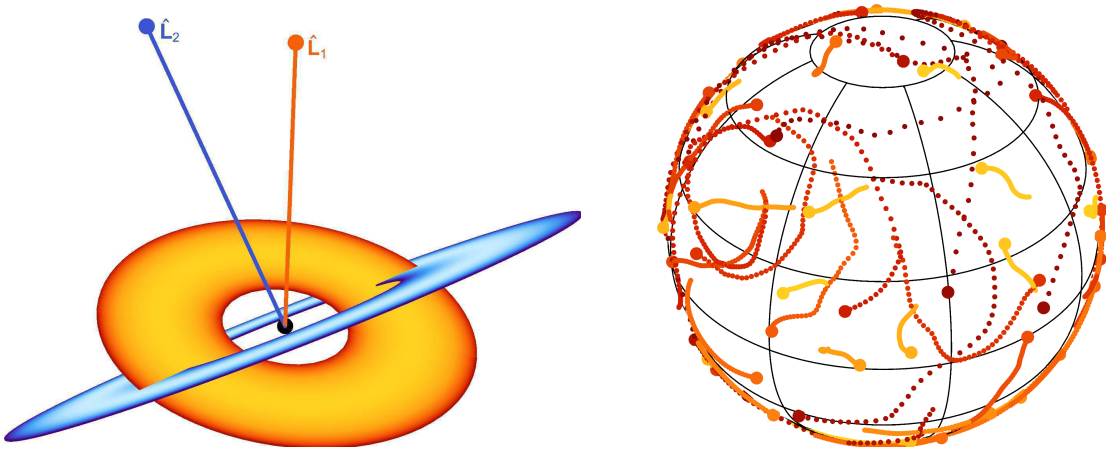

Figure 7.11: Illustration of the process of vector resonant relaxation in a galactic nucleus. Following an orbit-average over the fast Keplerian motion induced by the BH, stars are replaced by Keplerian wires. Then, following a second orbit-average over the in-plane precession induced by the relativistic corrections and the mean stellar potential, these wires are replaced by annuli, whose mutual interaction only depends on their respective orientation (left panel). To each annuli is associated a set of conserved quantities $\mathbf{J} = (L_{\rm c}, L) = (a, e)$, and a set of dynamical variables $\widehat{\mathbf{L}} = (\Omega, L_z)$. As a result of the Poisson fluctuations in the system, an annuli's orientation, $\widehat{\mathbf{L}}$, undergoes a random walk on the unit sphere (right panel, where different colors correspond to different values of a), i.e. stars see their orbital plane diffuse. This intricate stochastic dynamics is governed by the Hamiltonian from Eq. (7.24).

$\mathbf{J} = (L_c, L) = (a, e)$ of the test annuli are adiabatically-conserved, while the only dynamical variable of the test wire is $\widehat{\mathbf{L}} = (\Omega, L_z)$, i.e. the orientation of its orbital plane. Describing the vector resonant relaxation of that test annuli amounts then to describing the correlated random walk undergone by $\widehat{\mathbf{L}}$, as a result of the perturbations from the other annuli. For a spherically symmetric background distribution, one has $\overline{\overline{H}}_0 = \langle \overline{\overline{H}} \rangle = 0$, so that there are no dominant constructive background mean-field motion for the test wire's orbital orientation. This is beyond reach of the kinetic theory developed in the previous sections, where we always assumed to have at our disposal a mean-field Hamiltonian $H_0(\mathbf{J}) \gg \delta\Phi$, from which we could construct the system's mean-field orbital structure. In the case where $\overline{\overline{H}}_0 = 0$, another kinetic framework has to be developed to describe the random jitters in orientations occurring in the system, as presented for example in Kocsis & Tremaine (2015); Fouvry et al. (2019b). This is beyond the scope of the present notes.

There is still however one regime in which the present kinetic methods can be used to characterise the vector resonant relaxation of stars in galactic nuclei. For simplicity, we assume that all the annuli have the same $\mathbf{J} = (a, e)$, so that we can neglect that dependence w.r.t. $(\mathbf{J}, \mathbf{J}')$ in $\overline{\overline{U}}(\mathbf{J}, \mathbf{J}', \widehat{\mathbf{L}} \cdot \widehat{\mathbf{L}}')$. We also assume that the mean-field distribution of background stars is axisymmetric, so that we have $F_0(\widehat{\mathbf{L}}) = F_0(L_z)$. Then, the mean-field Hamiltonian associated with Eq. (7.24) is given by

$$\overline{\overline{H}}_0(\widehat{\mathbf{L}}) = \int \mathrm{d}\widehat{\mathbf{L}}' \, \overline{\overline{U}}(\widehat{\mathbf{L}} \cdot \widehat{\mathbf{L}}') \, F_0(\widehat{\mathbf{L}}') = \overline{\overline{H}}_0(L_z), \tag{7.25}$$

which naturally defines some associated out-of-plane precession frequency, $\Omega_z(L_z) = \partial \overline{\overline{H}} / \partial L_z$, that drives the precession of $\widehat{\mathbf{L}}$ around the z-axis. This also implies that we have been able to construct a mean-field quasi-stationary distribution for the system, as we have

$$\left[F_0(L_z) \, , \, \overline{\overline{H}}_0(L_z) \right] = \frac{\partial F_0}{\partial \Omega} \frac{\partial \overline{\overline{H}}}{\partial L_z} - \frac{\partial F_0}{\partial L_z} \frac{\partial \overline{\overline{H}}}{\partial \Omega} = 0, \tag{7.26}$$

where we used the fact that (Ω, L_z) are conjugate canonical variables, making the computation of the Poisson bracket obvious. As a conclusion, for an axisymmetric distribution of annuli, $F_0(L_z)$, we now have at our disposal a discrete long-range interaction N-body system, that supports a non-zero constructive mean-field motion $\widehat{\mathbf{L}}(t) = (\Omega_0 + \Omega_z(L_z^0)\, t, L_z^0)$. This is great news as this corresponds exactly to the grounds on which we derived the Balescu-Lenard equation in Eq. (5.2). As a conclusion, in analogy with Eq. (5.2), and making the identification to the angle-action coordinates $(\theta, J) = (\Omega, L_z)$, we expect that in the limit of an axisymmetric distribution of stellar orientations in a galactic nucleus, the reshuffling of the stars orientations is governed by a kinetic equation of the form

$$\begin{aligned} \frac{\partial F_0(L_z, t)}{\partial t} &\propto -m\, 2\pi^2 \frac{\partial}{\partial L_z} \left[\sum_{k,k'} k \int \mathrm{d}L_z' \left| \overline{\overline{\psi}}^{\mathrm{d}}_{kk'}(L_z, L_z', k\,\Omega_z(L_z)) \right|^2 \left(k' \, \frac{\partial}{\partial L_z'} - k \, \frac{\partial}{\partial L_z} \right) F_0(L_z) \, F_0(L_z') \right] \\ &\propto -\frac{\partial}{\partial L_z} \left[D_1(L_z) \, F_0(L_z) - D_2(L_z) \, \frac{\partial F_0(L_z)}{\partial L_z} \right], \end{aligned} \tag{7.27}$$

where $\overline{\overline{\psi}}^{\mathrm{d}}_{kk'}(L_z, L_z', \omega)$ are the dressed susceptibility coefficients between annuli. Of course, in practice, it requires some work to obtain the exact expression and prefactors for that relation, and we refer to Fouvry et al. (2019a) for precise results. An illustration of the computation of the diffusion coefficient, $D_2(L_z)$, from Eq. (7.27) is finally presented in Fig. 7.12.

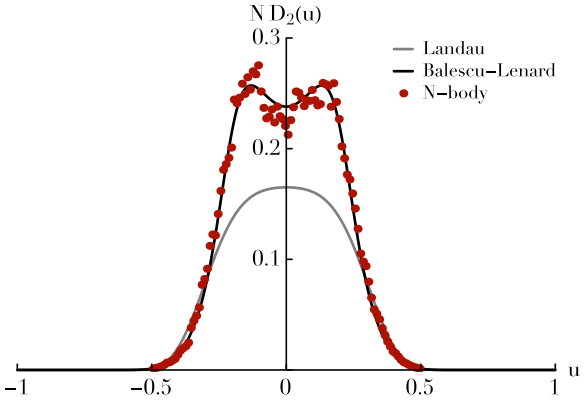

Figure 7.12: From Fouvry et al. (2019a). Illustration of the diffusion coefficient, $D_2(L_z) = D_2(L\cos(u))$ for a toy-model mimicking the double orbit-averaged Hamiltonian from Eq. (7.24) and the associated process of vector resonant relaxation in an axisymmetric galactic nucleus. Here is presented the diffusion coefficient in the absence (Landau) or presence (Balescu-Lenard) of collective effects, i.e. with or without accounting for the system's internal self-gravitating amplification, and compared with N-body measurements (that naturally include collective effects).

References

Alexander, T. 2017, ARA&A, 55, 17
Arnold, V. 1978, Mathematical methods of classical mechanics (Springer, New York)
Bar-Or, B., & Alexander, T. 2016, ApJ, 820, 129
Bar-Or, B., & Fouvry, J.-B. 2018, ApJ, 860, L23
Binney, J., & Lacey, C. 1988, MNRAS, 230, 597
Binney, J., & Tremaine, S. 2008, Galactic Dynamics: Second Edition (Princeton University Press)
Campa, A., Dauxois, T., & Ruffo, S. 2009, Phys. Rep., 480, 57
Chavanis, P.-H. 2012, Physica A, 391, 3680
De Rijcke, S., Fouvry, J.-B., & Pichon, C. 2019, MNRAS, 484, 3198
Duncan, M. J., Levison, H. F., & Lee, M. H. 1998, AJ, 116, 2067
Fouvry, J.-B., Bar-Or, B., & Chavanis, P.-H. 2019a, Phys. Rev. E, 99, 032101
—. 2019b, ApJ, 883, 161
Fouvry, J. B., Pichon, C., Magorrian, J., & Chavanis, P. H. 2015, A&A, 584, A129
Garcia-Ojalvo, J., & Sancho, J. 1999, Noise in Spatially Extended Systems (Springer New York)
Gillessen, S., Plewa, P. M., Eisenhauer, F., et al. 2017, ApJ, 837, 30
Goldstein, H. 1950, Classical mechanics (Addison-Wesley)
Hamilton, C., Fouvry, J.-B., Binney, J., & Pichon, C. 2018, MNRAS, 481, 2041
Hänggi, P. 1978, Z. Phys. B, 31, 407
Heyvaerts, J. 2010, MNRAS, 407, 355
Hopman, C., & Alexander, T. 2006, ApJ, 645, 1152
Kalnajs, A. J. 1976, ApJ, 205, 745
Klimontovich, I. 1967, The statistical theory of non-equilibrium processes in a plasma (M.I.T. Press)
Kocsis, B., & Tremaine, S. 2015, MNRAS, 448, 3265
Lynden-Bell, D. 1967, MNRAS, 136, 101
Merritt, D., Alexander, T., Mikkola, S., & Will, C. M. 2011, Phys. Rev. D, 84, 044024
Murray, C., & Dermott, S. 1999, Solar System Dynamics (Cambridge University Press)
Novikov, E. A. 1965, Sov. Phys. JETP, 20, 1290
Rauch, K. P., & Tremaine, S. 1996, New A, 1, 149
Schödel, R., Eckart, A., Alexander, T., et al. 2007, A&A, 469, 125
Sellwood, J. A. 2012, ApJ, 751, 44
Toomre, A. 1981, in Structure and Evolution of Normal Galaxies, 111–136
Touma, J. R., Tremaine, S., & Kazandjian, M. V. 2009, MNRAS, 394, 1085
Tremaine, S. 2005, ApJ, 625, 143
Weinberg, M. D. 2001, MNRAS, 328, 311